Ferredoxin and Flavodoxin as Indicators of Iron Availability in Antarctic Sea Ice Microalgal Communities

by

Andrew Henry Pankowski BSc (Hons) DipEd

Submitted in fulfilment of the requirements for the Degree of

Doctor of Philosophy

Institute for Antarctic and Southern Ocean Studies

University of Tasmania

September 2006

Statement of Originality

This is to certify that the material composing this thesis has never been accepted for any other degree or award in any other tertiary institution and, to the best of my knowledge and belief, is solely the work of the author, and contains no material previously published or written by another person, except where due reference is made in the text.

Andrew Henry Pankowski

17/09/06

Authority of Access

This thesis may be made available for loan and limited copying in accordance with the Copyright Act 1968.

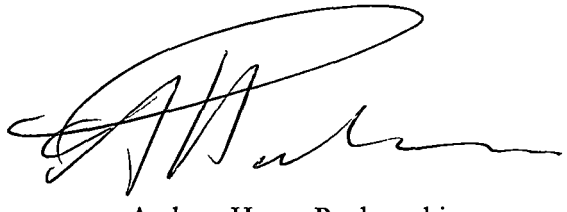

Andrew Henry Pankowski

17/09/06

Abstract

The availability of the micronutrient iron is known to exert control on phytoplankton growth and community composition in much of the Southern Ocean. The role of this trace element in regulating primary production in Antarctic pack ice is however, largely unknown.

To investigate the availability of iron to microalgae in Antarctic pack ice, immunoassays were developed for the proteins ferredoxin and flavodoxin. In pervious studies these proteins have been shown to be regulated by iron availability in many temperate marine phytoplankton and have the potential to be used as indicators of iron availability *in situ.*

Antibodies generated towards ferredoxin and flavodoxin purified from a temperate diatom were found to have good cross-reactivity with the proteins from a range of sea ice diatoms. The putative iron stress protein flavodoxin was found to be expressed constitutively in several sea ice diatoms from both the Antarctic and Arctic. Along with constitutive flavodoxin expression some sea ice diatoms were observed to never express ferredoxin suggesting that these organisms have lost the ability to produce this protein, possibly as a means to reduce cellular iron quotas.

The effects of iron availability on *Fragilariopsis curta* and *Fragilariopsis cylindrus* were determined in laboratory cultures of these organisms. Growth rates, ferredoxin and flavodoxin expression and photophysiological parameters determined by pulse amplitude modulation (PAM) fluorometry were investigated in relation to iron supply. Half saturation constants for growth were similar for both *F. cylindrus* and *F. curta* and photosynthetic parameters showed quantitatively similar reductions for

both organisms in response to reduced iron supply. Different patterns in the expression of ferredoxin and flavodoxin were observed in these two organisms. Iron replete *F. curta* only expressed flavodoxin (without ferredoxin) and cellular levels of this protein were not regulated by iron availability. In *F. cylindrus* ferredoxin was expressed under iron replete conditions and was replaced completely by flavodoxin as a very early response to iron stress, prior to reductions in growth rate or decreases in photosynthetic parameters such as Fv/Fm.

Ice cores collected from Southern Ocean pack ice north of the Adelie Land coast were analysed for both ferredoxin and flavodoxin. Flavodoxin was detected in the majority of core sections and the concentration of this protein was significantly correlated with chlorophyll concentration. Ferredoxin was less widely distributed, being detected in approximately half of all core sections examined, and flavodoxin was always detected along with this protein. These results are consistent with constitutive expression of flavodoxin in many sea ice diatoms and in combination with the culture experiments demonstrate that flavodoxin cannot be used as a stand alone marker for iron stress in this environment.

High concentrations of ferredoxin were associated with the top half of ice floes and were never observed in bottom communities which were the most highly productive. The observed distribution of this protein suggests that differences exist in the ability of these communities to access iron, however iron availability did not regulate the distribution of biomass within these floes.

Acknowledgements

Firstly I would like to thank Andrew McMinn for his support and encouragement during my candidature and for helpful comments made during the preparation of this thesis. Thanks also to John Bowman and the microbiology group of Agricultural Science for hosting me in their department and providing full access to equipment and resources. I'd also like to thank Gustaaf Hallegraeff for the use of his laboratory, my project would have been a lot more difficult without the use of your facility. Thanks also to the Aquatic Botanists, particularly Judy Marshall who got me off to a great start in the early stages of my project and to Helen Bond for doing an excellent job at keeping the lab running smoothly.

I must also thank IASOS and the University of Tasmania for financial support and I am grateful for the financial and logistical support provided by the Australian Antarctic Division

A big thanks to the captain and crew of the *Aurora Australia* for providing great advice, working tirelessly during sea ice operations and for being a great bunch of people to be confined in a small place with. The professional service provided by the pilots of Helicopter Resources was also greatly appreciated. Many people volunteered to help with sample collection I'd particularly like to thank Thommo and Clobbs who distilled some of their sea ice wisdom on my first Antarctic voyage and to Guy Abel who volunteered to be my lackey and cabin mate on the second.

Thanks also go out to David Ratkowsky for statistical advice, to Guy Williams for the production of the Mertz map and to Andy Bowie for conducting iron analyses, providing advice about trace metal clean procedures and for letting me watch him clean plastic ware. Thanks also to Loes Gerringa for taking the time to go through

my trace metal calculations. Murray and Eileen are thanked for their help at the Animal house and Roger for advice about antibody production when things weren't working very well.

Daily life in the Agricultural Science department wouldn't have been quite so much fun without the discussions and distractions provided by the Aggies and Foodies including Bisso, Claudio, Mark, Jimmy, Lydall and Julia. A special thankyou also to my IASOS buddy Abe for going through this process with me.

A big thanks to my parents for helping out along the way, including buying me a laptop which allowed me to complete this thesis in a shorter time frame, for Sunday dinners which stopped the weeks from melding into one and for always encouraging me to pursue my interests. Finnaly, I'd like to thank Ru for her constant support and for being flexible and accepting the lifestyle demands of a PhD student.

Table of Contents

Chapter 1 : Literature review

1.1 Introduction

The annual cycle of sea ice formation and degradation is a prominent process in the Antarctic marine environment. The sea ice cover is at its minimum in February covering 3.8 million square kilometres of the Southern Ocean. During the following seven months the ice cover advances north reaching its maximum extent of 19 million square kilometres in September (Comiso, 2003). Defining the northern extent of the Southern Ocean as the Polar Front (Carmack, 1990) covering an area of 38 million square kilometres (Carmack, 1990) this area equates to 50% of its surface.

Sea ice provides a habitat for a range of micro organisms (Lizotte, 2003), small metazoans (Schnack-Schiel, 2003) mammals and birds (Ainley *et al.*, 2003). Of particular note and dominance are the many species of photo-autotrophic unicellular algae that grow in brine channels and pockets within the ice, and on its exposed surfaces (Lizotte, 2003; Lizotte, 2001). There is widespread agreement that these organisms have a significant influence on higher trophic levels (Arrigo & Thomas, 2004; Brierley & Thomas, 2002). For example, the high concentration of microalgae under sea ice relative to the water column in ice covered waters provides a vital winter food source for juvenile krill, a pivotal species in the Southern Ocean (Hofmann & Lascara, 2000).

A substantial amount of research has sought to characterise the physical and chemical conditions in sea ice and how these factors influence the growth of microalgae in the ice. Light, salinity, temperature UV, dissolved gasses and macronutrients have all been investigated and much of this work is summarised in a number of reviews (Eicken, 1992; Kirst & Wiencke, 1995; Lizotte, 2003; Mock &

Thomas, 2005; Priddle *et al.*, 1996; Thomas & Dieckmann, 2002; Thomas & Papadimitriou, 2003).

In the last two decades it has become apparent that the micronutrient iron limits the growth of phytoplankton in much of the Southern Ocean (Boyd, 2002a; Boyd *et al.*, 2000). It has also been suggested that the growth of sea ice algae might be limited by this micronutrient (Thomas, 2003). Currently however, there has been no experimental confirmation of this suggestion or examination of literature in this context. This review targets this latter aspect.

1.2 The Southern Ocean

The Southern Ocean consists of a series of circumpolar water masses that differ in their physical and chemical properties (Orsi *et al.*, 1995). These relatively uniform bodies of water are separated by faster flowing frontal regions. From north to south the fronts and water masses crossed are the Subtropical Front, Subantarctic Zone, Subantarctic Front (SAF), Polar Frontal Zone, Polar Front (PF), Antarctic Zone (AZ), the Southern Antarctic Circumpolar Current Front (SACCF) and the Southern Boundary of the Antarctic Circumpolar Current (SB) (Orsi *et al.*, 1995). The water masses between the Subantarctic Front and the SB collectively comprise the Antarctic Circumpolar Current (ACC) flowing from west to east under the influence of prevailing westerly winds (Orsi *et al.*, 1995). The complete ACC is commonly subdivided into the northern ACC ranging between the SAF and the PF and the southern ACC ranging between the PF and the SB Within the southern ACC the SACCF is a relatively weak feature, not always truly circumpolar, and therefore sometimes ignored. The SB divides the southern ACC north from the Weddell Sea Gyre and the Ross Sea Gyre both situated south of the SB. Near the Antarctic continent a further feature common to all regions except the Western Antarctic Peninsula is the Antarctic Slope Front (Whitworth III *et al.*, 1998).

The SB and the fronts south of the PF are all subsurface features, occurring below the wind mixed layer, also referred to as Antarctic Surface Waters (AASW) (Orsi *et al.*, 1995; Whitworth III *et al.*, 1998). These surface waters have relatively uniform properties and extend from the PF south to the continental margins of Antarctica (Orsi *et al.*, 1995). North of the SB surface waters of the ACC overlie warmer and more saline Circumpolar Deep Water (CDW). This water mass is generally divided into Upper Circumpolar Deep Water (UCDW) with its southern most extent defining the SB (Orsi *et al*, 1995), and more dense Lower Circumpolar Deep Water (LCDW) which often extends south of the SB as far as the continental shelves (Deacon, 1982).

Compared to waters of the ACC which are relatively uniform, south of the SB water mass properties are regionally more heterogeneous (Orsi *et al.*, 1995). Near the continent prevailing winds are to the west and currents also flow westward forming an almost continuous Antarctic coastal current (Whitworth III *et al.*, 1998). In the Ross and Weddell seas the westward flowing coastal current forms the southern branch of the Ross and Weddell cyclonic gyres. In these regions the SB is located at a considerable distance from the continental margin and coincides with the northern branch of these gyre systems (Orsi *et al.*, 1995). To the east of the Ross and Weddell gyres the ACC turns south bringing CDW close to Antarctic Shelf Waters (Orsi *et al.*, 1995). In these regions the coastal currents take the form of a narrow westward flowing band (Whitworth III *et al.*, 1998).

1.3 The Seasonal Ice Zone

South of the Polar Front four major functional zones have been identified which differ in the mechanisms that control the dynamics of phytoplankton growth and nutrient concentrations (Treguer & Jacques, 1992) (Figure 1.1). These sub-systems are the Polar Front Zone (PFZ) in the immediate vicinity of the PF, the Permanently Open Ocean Zone (POOZ) occurring in the ACC and spanning the region between the Polar Front Zone and the winter ice edge, the Seasonal Ice Zone (SIZ) which is

under the influence of the annual ice cover and the highly productive Coastal and Continental Shelf Zone (CCSZ) which is also under the influence of the ice cover but confined to the southern portions of the Ross and Weddell seas and Prydz Bay (Treguer & Jacques, 1992).

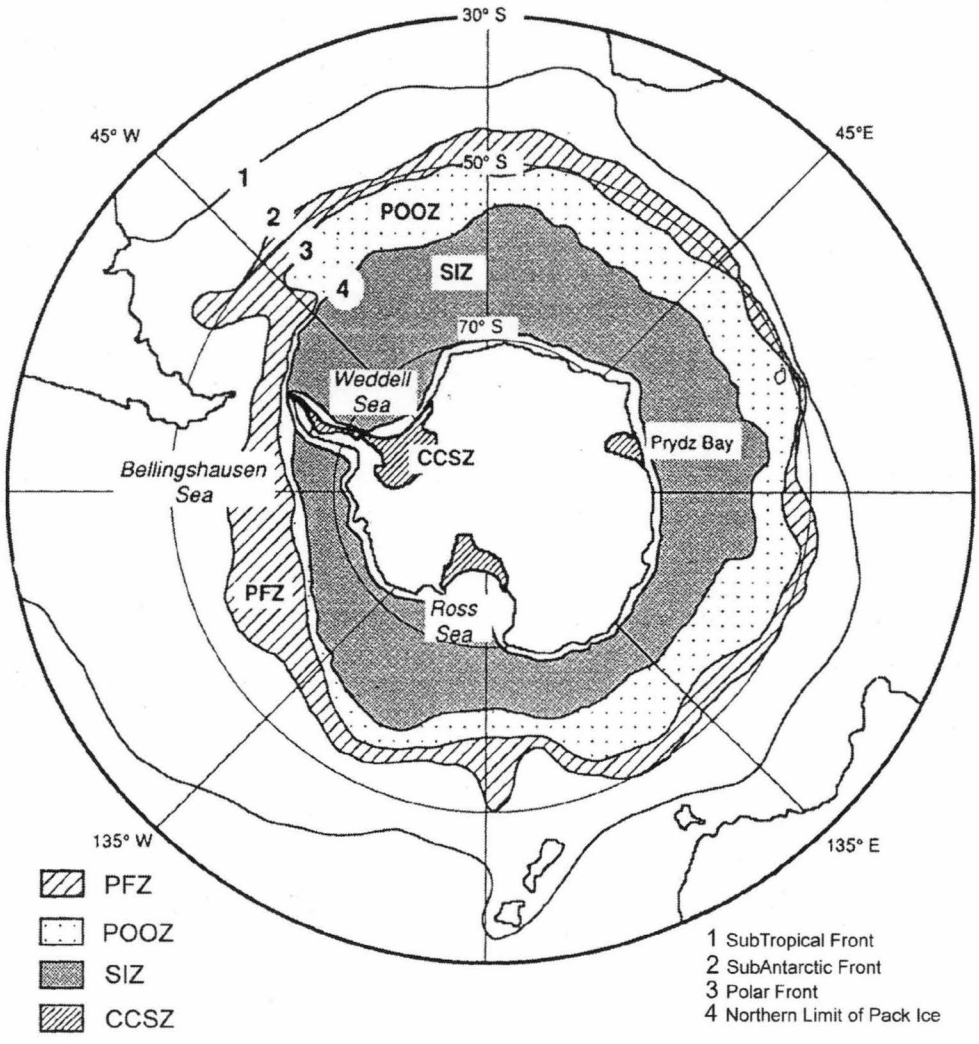

Figure 1.1 Functional Zones of the Southern Ocean (Treguer & Jacques, 1992).

Unlike the PFZ and POOZ which each occur in waters of relatively homogenous composition the seasonal ice cover extends across several water masses with different properties and which are influenced by separate hydrological processes. Examination of mean maximum winter sea ice extent (Harangozo, 2004) and the locations of the major frontal systems (Moore & Abbott, 2002; Orsi *et al.*, 1995)

(Figure 1.2) shows that in the Ross, Weddell and Southwest Pacific sectors the winter ice edge generally coincides with the location of the SB. In contrast the winter ice edge in the Indian Ocean sector as well as the Amundsen and Bellingshausen seas extends well north of this feature into waters of the ACC.

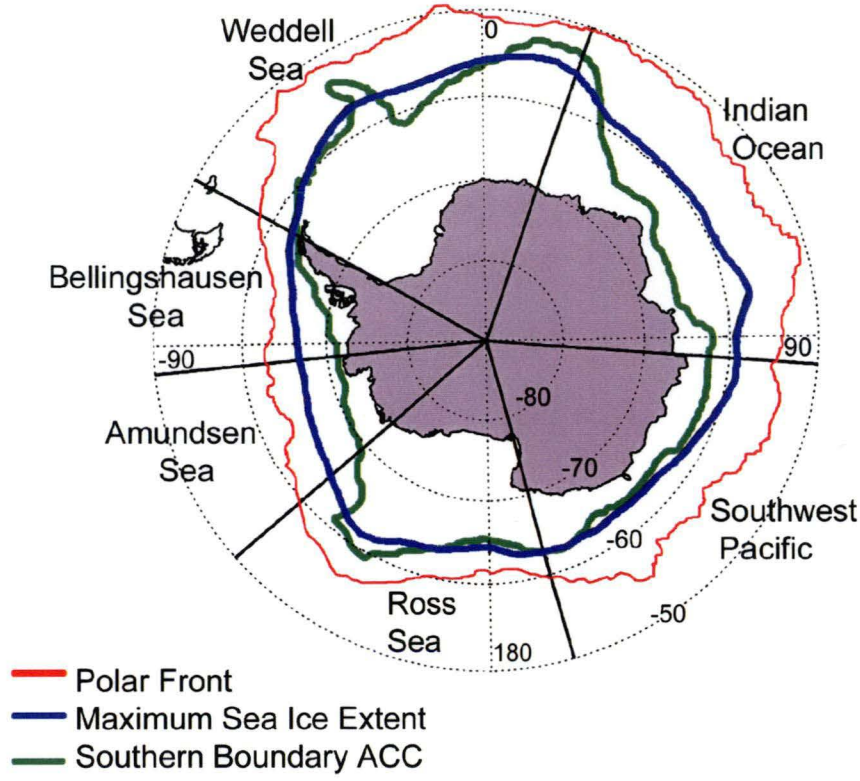

Figure 1.2 Location of the Polar Front (Moore & Abbott, 2002), the winter ice edge (Harangozo, 2004) and the Southern Boundary of the Antarctic Circumpolar Current (Orsi *et al.*, 1995).

1.4 Sea ice formation

Sea ice formation has been extensively reviewed (Eicken, 2003; Weeks, 1998; Weeks & Ackerly, 1986). A summary of the processes involved, as they relate to the Southern Ocean are outlined below. Formation of sea ice in turbulent or quiescent conditions results in ice types with vastly different properties. Congelation ice, which predominantly forms in calm coastal water consists of vertically oriented prismatic crystals which can grow several centimetres in diameter and tens of

centimetres in length (Weeks, 1998). However, under the high wind stress conditions typical of the open Southern Ocean the initial formation of an ice cover rarely takes place via this path. Rather ice formation and growth usually occurs via what has become known as the pancake cycle (Lange *et al.*, 1989; Lange & Eicken, 1991). The first step in this cycle is ice crystal nucleation and growth in the wind mixed top few meters of the water column. The frazil ice crystals which form under these turbulent conditions are generally less than a millimetre in thickness and a few to a few tens of millimetres in length (Lange *et al.*, 1989; Weeks, 1998; Weeks & Ackerly, 1986). Because of their lower density relative to seawater these needle like ice crystals float to the surface forming a soupy layer of grease ice which through further wave action agglomerates into floating pancakes which bump against each other causing characteristic upturned edges (Lange *et al.*, 1989; Weeks, 1998; Weeks & Ackerly, 1986). This bumping also causes enlargement through accretion of more frazil ice. Eventually growth of ice in the gaps between pancakes results in a continuous ice sheet (Lange *et al.*, 1989). Further thermodynamic growth of consolidated sheet ice occurs through the downward growth of congelation ice (Lange *et al*, 1989; Weeks, 1998).

If atmospheric temperatures are sufficiently low the growth of ice sheets can be quite rapid. Typically growth to 30 cm in thickness can occur in around a week (Eicken, 2003). At this point growth slows as the thickening ice slows heat flux to the atmosphere. In the Antarctic growth of ice continues until a thickness of between approximately 0.5 to 0.7 m is reached at which point the flow of heat to the atmosphere is balanced by heat flux from the ocean below (Eicken, 2003).

The accumulation of snow on sea ice further reduces the flux of heat to the atmosphere by up to 50% which results in retarded ice growth (Eicken, 2003). Although snow loading prevents the growth of ice in the downward direction it often depresses the surface of the ice below the water resulting in the formation of snow-ice through freezing of melted snow and seawater on the surface of the floe (Lange *et*

al., 1990). Like frazil ice, snow ice is of granular structure and can be distinguished from frazil ice by its oxygen isotope signal (Worby *et al.*, 1998).

First year Antarctic pack ice rarely grows thicker than 0.6 m through thermodynamic growth (Wadhams *et al.*, 1987; Worby *et al.*, 1998). However, further thickening occurs when winds and currents cause ice floes to be pushed together. This results in rafting of one floe on top of another and the formation of pressure ridges (Haas, 2003).

The combined action of thermodynamic growth and dynamic thickening results in a heterogenous ice cover. In any particular area a spectrum of ice types often co-exist ranging from grease ice, nilas (thin consolidated sheets), pancakes, level first year floes through to floes which have been deformed to different degrees by ridging and rafting. A further ice type which forms through degradation of other ice types is brash ice (Weeks, 1998).

1.5 Microstructure of sea ice

Unlike ice formed from freshwater, which consists primary of solid water, sea ice is a semisolid composed of solid water permeated by a network of brine filled channels (Weeks & Ackerly, 1986). The space occupied by these brine channels varies with temperature. As ice temperature decreases more water freezes out of the brine resulting in smaller brine volume, higher salinity brines and lower connectivity of pore spaces (Eicken, 1992). At –6° C brine salinity is 100 ‰, at –10° C it increases to 145 ‰ and at –21° C is 216 ‰ (Mock & Thomas, 2005) On a snow free ice floe the temperature at the surface of the ice will be close to that of the atmosphere. The underside of the ice will be at the freezing point of seawater. Between these extremes exists a gradient of temperature, salinity, brine volume and brine channel connectivity (Eicken, 1992). Such gradients are not fixed but fluctuate with changing air temperature. A layer of overlying snow serves to insulate the ice from the atmosphere further modifying these gradients.

1.6 Sea ice microalgal communities

All sea ice contains some microalgae. Even freshly formed frazil ice harbours a higher density of algal cells than the water from which it forms. This is thought to result from a physical scavenging process where phytoplankton cells adhere to frazil ice crystals as they form and rise up through the water column (Garrison *et al.*, 1983). This enrichment effect results in a species composition similar to that occurring in the water column. But as ice grows and ages there appears to be selection for certain organisms which are thought to be better adapted to the conditions within sea ice (Gleitz & Thomas, 1993).

Within consolidated sheet ice four dominant communities can be recognized from the position they occupy within the ice (Horner, 1985). Bottom communities grow on the under surface of floes in contact with the underlying seawater. Freeboard communities form at the level of the sea surface where water erodes a layer between the snow ice on the surface and the sea ice below. Brine communities inhabit highly branched network of microscopic brine pockets within the ice. Infiltration communities are those found in the layer between the top of the ice and the overlying snow. These latter communities usually form after snow loading depresses the top of the ice below water causing flooding of the surface, which provides a suitable habitat for growth (Horner *et al.*, 1992).

1.7 Productivity of sea ice microalgae

Several attempts have been made to quantify the contribution of these organisms to Antarctic marine primary production. The two most recent estimates of total sea ice based production are those by Legendre *et al.* (1992) and Arrigo *et al.* (1997). The first based on algal standing stock data calculated a contribution of ice based production of 63-70 x 10^{12} g C yr^{-1} (Tg C yr^{-1}). Using a numerical model Arrigo *et al.* (1997) calculated a slightly lower figure of 36 Tg C yr^{-1}. In comparison latest estimates of water column based production in the seasonal ice zone are 1300 Tg C

yr^{-1} with approximately 400 Tg of this being due to ice edge blooms that occur as the sea ice retreats (Arrigo *et al.*, 1998; Arrigo *et al.*, 1997). The above estimates suggest that ice based production accounts for around 3% to 5% of total primary production in the sea ice zone, however these are likely to be underestimates. A significant oversight of both estimates is that the contribution of pack ice bottom communities was not included. At the time that both estimates were carried out there was a widespread belief that bottom communities were rare in Antarctic pack ice (Arrigo *et al.*, 2003b). More recent observations suggest that these communities are dominant in some regions. Grose & McMinn (2003) used ship based observations and ice core chlorophyll analysis to calculate a contribution of 8.51 Tg C yr^{-1} in Eastern Antarctica with 76% of this occurring in bottom communities. In contrast total ice based production based on the model by Arrigo suggests significantly lower production of 1.93 Tg yr^{-1} for this sector. Similarly, recent observations in the Ross Sea suggests that bottom communities may also dominate in this region (Arrigo *et al.*, 2003a). Inclusion of these communities in current estimates may significantly increase the contribution of sea ice primary production to total Southern Ocean primary production.

Arrigo (2003) has compiled data for standing stocks, photosynthetic rate and primary production for sea ice communities. From this data some important generalisations can be made. Peak biomass accumulation in Antarctic pack ice is consistently less than 100 mg chl *a* m^2 while levels in Antarctic fast ice regularly exceeded 200 mg chl *a* m^2. Furthermore, bottom ice communities are more productive than surface communities which in turn are more productive than brine communities. Finally, maximum photosynthetic rates of pack ice algae far exceed those of communities from the fast ice . This latter observation is at variance with the higher standing stocks in the fast ice and suggests that significant losses occur in the pack ice, possibly through grazing.

1.8 Physicochemical factors and growth of sea ice microalgae

Each particular sea ice community experiences different physical and chemical conditions. It is therefore necessary to examine the various communities separately when considering which factors provide the dominant forcing for growth. Considerable research effort has been undertaken to establish the physico-chemical conditions within sea ice and the effects of these parameters on ice algae. Generally these studies have sought to identify if and how sea ice microalgae are able to adapt to these conditions. Factors that have been studied include light, nutrient availability, salinity and temperature effects and dissolved gas concentrations. Few studies have attempted to elucidate the relative influence of each factor on algal processes. Much work is still required to define which are of greatest importance.

1.8.1 Light

Because of their spatially fixed position sea ice microalgal communities experience a relatively stable light regime compared to the fluctuating light field experienced by phytoplankton in the mixed euphotic zone (Eicken, 1992). The dominant process influencing the light field is the progression of the seasons which regulates overall light intensity and photoperiod (Sakshaug & Slagstad, 1991). There is also significant latitudinal variation in the timing of this progression (Sakshaug & Slagstad, 1991). Regions at latitudes greater than 66.5° S experience complete darkness during winter and a 24 hour photoperiod during summer. During summer midday summer surface irradiances have been reported to be as high as 2000 μmol photons m^{-2} s^{-1} (Cota & Sullivan, 1990; Kristiansen *et al.*, 1998; Robinson *et al.*, 1997). These high light intensities and long day lengths result in daily incident irradiances that can be higher than in equatorial regions (Sakshaug & Slagstad, 1991).

On a more localised scale, the light field experienced by sea ice microalgal communities is modulated by absorption and reflection of light by ice, snow and particles within the ice, including microalgae. These attenuation processes result in large vertical gradients of light within a floe (Eicken, 1992). Brine communities living towards the top of a snow free floe will experience irradiances close to those of full sunlight. Snow cover strongly attenuates light. Maximum irradiance in the range 450-850 μmol photons m^{-2} s^{-1} were reported for surface communities in summer under half a metre of snow (Kristiansen *et al.*, 1998). At the other extreme bottom communities in ice greater than one meter thick receive 1% or less of surface irradiance (McMinn & Ashworth, 1998; Palmisano *et al.*, 1987).

Much of the research into the role of light in the sea ice microalgal community has focussed on determining relationships between photosynthesis (P) and irradiance (E). The P vs E response curves obtained from such methodologies has given insight into how these communities adapt to, and function in, their light environments. Many of these studies have concentrated on communities growing in the very low light environment under thick fast ice near the continent. These communities show characteristics of extreme shade adaptation with photosynthesis saturating at low irradiance (E_k values around 10 μmol photons m^{-2} s^{-1}), low assimilation numbers (0.2 mg C (mg chl *a*) $^{-1}$ hr^{-1}) and a photoinhibition response that occurs at relatively low light levels (Kirst & Wiencke, 1995; McMinn *et al.*, 2000; Trenerry *et al.*, 2002). Growth under these low light conditions is achieved through high light harvesting efficiency (a*) and low maximum photosynthetic rates (P^*_m) such that these organisms are able to attain quantum yields of photosynthesis which approach theoretically maximum limits (Arrigo, 2003). Species which grow on the underside of fast ice may be genetically constrained to growth at low photon flux density (Palmisano *et al.*, 1987).

Although fewer studies have been conducted on pack ice communities it appears that these are more like open ocean phytoplankton in their response to light. Light

saturated photosynthetic rates between 0.3 to 3.6 mg C (mg chl *a*)$^{-1}$ h^{-1} were reported for algae in a range of pack ice types (grease, nilas, pancake, consolidated floes) in the Weddell Sea (Lizotte & Sullivan, 1992a). These values are typical of those collated from a range of studies in different pack ice communities in various locations (Arrigo, 2003). The similarity between photosynthetic rates in pack ice communities and phytoplankton in adjacent leads has also been noted on a number of occasions (Arrigo *et al.*, 2003a; Lizotte & Sullivan, 1992b). The ability of algae from pack ice to utilise higher photon flux densities compared to organisms from fast ice is also demonstrated by higher E_k values which range between 30 and 150 µmol photons m^{-2} s^{-1} (Kirst & Wiencke, 1995). Along with greater capacity to utilise higher irradiances an ability to resist photoinhibition at light intensities of up to 500 µmol photons m^{-2} s^{-1} has also been observed (Kristiansen *et al.*, 1998).

In summary the ability of these organisms to acclimate to both the high light environment near the surface of a floe and low light bottom ice environment is well demonstrated.

The timing of sea ice production is not well constrained by current sampling efforts. Furthermore, few studies have sought to identify when light ceases to be a limiting resource for the various communities. Some attempts have been made to model the effects of light on algal processes. The most comprehensive examination of the role of light as an environmental forcing was conducted during modelling of primary production in pack ice infiltration and freeboard communities (Arrigo *et al.*, 1997). It was found that surface communities were not limited by light from October when ice extent is maximal through to February. Timing of the release from light limitation occurred about one month later for algae inhabiting the freeboard layer. The model did not examine bottom communities or algae inhabiting the brine channel microhabitat. As expected from latitudinal variation in seasonal light availability there was approximately a one month difference in the timing of peak productivity from north to south. For the two communities examined the model

predicts that the majority of production occurs during November and December when light is not a limiting resource (Arrigo *et al.*, 1997).

Further information about the role of light has been gained from observations made during autumn, winter and spring when light intensity is potentially limiting. Active growth of algae during the months leading into winter has been observed (Garrison *et al.*, 2003; Melnikov, 1998). In the latter study the light history of a floe had a significant effect of on biomass accumulation. Younger floes in the south of the Ross Sea were found to contain low biomass because they formed late in the season (May) when light was limiting at these high latitudes. Further to the north, sea ice was thicker, having started its growth in the south earlier in the season and continuing to grow as it travelled north. These floes experienced a more favourable light regime and contained higher levels of biomass, predominantly as internal assemblages (Garrison *et al.*, 2003). The lack of bottom communities was thought to reflect lower light availability in this habitat. In agreement with this photosynthetic rates measured *in situ* during autumn in the Weddell Sea were higher for interior (brine) communities than bottom communities from the same core (0.7-1.17 mg C (mg chl *a*)$^{-1}$ h^{-1} compared to 0.02 to 0.056 mg C (mg chl *a*)$^{-1}$ h^{-1}) (Mock, 2002). The authors suggested that light limited productivity in the bottom of the ice but that temperature, which was as low as -7° C limited growth closer to the ice surface.

1.8.2 Nutrients

In the Antarctic Seasonal Ice Zone surface water concentrations of nitrate, phosphate and silicate remain high all year round (Trull *et al.*, 2001). Algal communities that are in direct contact with the water column therefore have access to replete levels of macronutrients (Thomas & Papadimitriou, 2003). During sea ice formation seawater salts, including the major nutrient ions, are rejected from the growing ice and concentrated in brines (Thomas & Papadimitriou, 2003). This results in brine

macronutrient concentrations substantially higher than the levels found in seawater from which the ice formed, and which are proportional to bulk salinity.

During evolution of an ice floe the concentrations of macronutrients in brines can be changed by biological uptake, remineralisation and exchange with the water column. This latter process is predominantly regulated by ice porosity, which is dependent on temperature (Eicken, 1992). For example, when ice with a bulk salinity of 5‰ is cooled from -2° C to -20° C its porosity decreases from 122% to 17% (Eicken *et al.*, 2000).

Depletion of one or more nutrients has been observed in sea ice (Arrigo *et al.*, 2003a; Kennedy *et al.*, 2002). However Arrigo *et al.* (2003a) observed that in combination with depleted nitrate, high levels of ammonia were found. Hence, nitrogen was unlikely to be limiting to these communities. Moderate to slight nutrient depletion appears to be more common in Antarctic pack ice brines (Arrigo *et al.*, 2003a; Clarke & Ackerly, 1984; Dieckmann *et al.*, 1991; Garrison *et al.*, 2003; Gleitz & Thomas, 1993; Trevena *et al.*, 2000).

Despite the common occurrence of nutrient concentrations in sea ice brines, which are above those thought to be limiting to algal growth, other evidence suggests that nutrient supply may often control biomass accumulation in these communities. Highest concentrations of biomass are often associated with those regions of a floe which are in direct contact with the water column (Arrigo, 2003; Kennedy *et al.*, 2002). Communities at even 5-10 cm from the ice water interface have carbon isotope ratios indicative of nutrient stress (McMinn *et al.*, 1999). Similarly, Kennedy *et al.* (2002) observed that brine communities distant from the ice water interface consistently contained biomass levels which were below the amount expected from the observed nitrate drawdown. In the same floes communities in close proximity to the ice water interface contained higher levels of biomass than expected from the observed nitrate drawdown. They suggested that a gradient of

nutrient supply existed from the ice water interface to the most distantly removed communities with the latter essentially growing in a fully closed system. However complete exhaustion of nitrate was realised in only a fraction of the samples.

Clearly within brine communities rates of macronutrient utilisation, resupply and regeneration will determine nutrient availability, however, the large scale importance of these processes during the seasonal development of the sea ice microalgal communities are currently poorly understood.

Processes that deliver nutrients to surface communities are better understood. In these communities nutrients are supplied when snow loading depresses the surface of the ice beneath the water. Such flooding occurs in 15-30% of the pack ice in Antarctica (Wadhams *et al.*, 1987) and has been reported to be responsible for a significant proportion of Antarctic sea ice primary production (Arrigo *et al.*, 1997). Commonly observed is a pattern of decreasing nutrient concentrations with distance from the edge of a floe, with nitrate exhaustion evident at the centre of floes (Kristiansen & Farbrot, 1991; Syvertsen & Kristiansen, 1993). Algal biomass levels are similarly highest at the edges of floes and lowest near the centre.

1.8.3 Inorganic carbon

Few studies have directly measured CO_2 concentrations in ice. The study by Gleitz *et al.* (1995) conducted on pack ice in the Weddell Sea perhaps best demonstrates the situation in sea ice brines. They found that in winter, CO_2 concentrations were primarily determined by changes due to freezing and concentration. In summer, brine chemistry was strongly influenced by biological activity with depletion of total inorganic carbon associated with complete exhaustion of CO_2, and elevated pH and dissolved oxygen concentrations. Stoichiometry of inorganic carbon depletion and O_2 increases suggest that these chemical changes result from photosynthesis within enclosed brine inclusions (Thomas & Dieckmann, 2002).

Evidence for depletion of CO_2 in sea ice brines has been gained mostly from carbon isotope ratios in brines and particulate organic carbon (POC) extracted from sea ice (Thomas & Papadimitriou, 2003). Delta ^{13}C ($\delta\ ^{13}C$) of sea ice POC from a number of studies (reviewed by Thomas & Papadimitriou, 2003) are as low as –8 ‰ compared to -21‰ to -30‰ for polar phytoplankton. The highest enrichments occurred in habitats with the minimum potential for CO_2 exchange with the external seawater. For example Dunbar & Leventer (1992) observed maximum $\delta\ ^{13}C$ of –23‰ to –26‰ in winter for fast ice bottom communities in McMurdo Sound which were lowered to –11‰ to –17‰ in late November early December when biomass levels were highest, suggestive of decreased CO_2. The work of Kennedy *et al.* (2002) discussed above in the context of macronutrient limitation observed similar trends for CO_2 availability based on $\delta\ ^{13}C$ values of particulate organic carbon in the ice.

Despite this evidence for observed decreases in CO_2 availability inorganic carbon is unlikely to be liming to all organisms in sea ice. Carbon concentrating mechanisms which allow utilisation of bicarbonate have been identified in sea ice microalgae (Mitchell & Beardall, 1996). Evidence has also been gained which suggests that those organisms that can utilise bicarbonate have a competitive advantage in a closed system such as within brine channels (Gleitz *et al.*, 1996).

1.8.4 Salinity/Temperature

Sea ice microhabitats such as bottom communities, that are in direct contact with the water column, experience extremely stable temperatures (-1.8 ° C), as the ice water boundary must be in equilibrium with the freezing point of seawater. However, in other microhabitats, particularly within brine channels, the temperature can be considerably lower. Within such habitats temperature and salinity cannot be considered independently as decreases in temperature will result in further

crystallization of water out of brines and the concomitant increase in brine salinity (Eicken, 2003).

Adaptation to low temperatures can be considered from two perspectives. The first is for growth at the ice water boundary where temperature is constant at –1.8° C and salinity is close to that of seawater (35 ‰). The second is for communities that exist higher in the ice where temperatures can be considerably lower and will fluctuate somewhat with air temperatures causing brine salinity to also vary. In such an environment the ability to maintain metabolic activity at low temperature and the capacity to adapt to fluctuating salinity and temperature are both important.

Sea ice algae are well adapted to low temperatures. Four Antarctic diatoms were found to have optimum growth temperatures between 3° C and 5 ° C with temperature above 6° C to 8° C being lethal (Fiala & Oriol, 1990). In general it appears that most species are capable of growth at salinities of 100 ‰ and temperatures as low as –6° C (Gleitz and Thomas, 1993 and references therein; Mock, 2002).

Growth at low temperatures has been shown to saturate at very low light levels (Aletsee & Jahnke, 1992). Davison (1991) suggests that at cold temperatures growth at irradiances above 200 μmols photons m^{-2} sec^{-1} becomes sub optimal because of uncoupling between processes that produce electrons and process that consume them such as CO_2 fixation and nitrate uptake. Recent studies on Antarctic microalgae inhabiting brines with a salinity of 85 ‰ suggest that photosynthesis operates normally at temperatures as low as -5° C but that the organisms are susceptible to photoinhibition when the temperature falls to -10° C (Ralph *et al.*, 2005) . Mock & Valentin (2004) showed that during acclimation to low temperatures by a sea ice diatom, genes encoding photosystem two (PSII) units and carbon fixation were down-regulated while chaperones and genes for plastid protein synthesis and

turnover were up-regulated. It was proposed that induction of these latter genes were necessary to avoid cold shock photoinhibition.

Changes in salinity alone have also been shown to significantly alter rates of photosynthesis. Gleitz & Kirst (1991) observed a 55% decrease in short term photosynthetic rate when salinity of field samples was increased from 34‰ to 110‰. In longer term laboratory studies increases in salinity initially decreased rates of photosynthesis but complete recovery was evident within two weeks (Grossmann & Gleitz, 1993). Salinity downshifts can also suppress photosynthetic capacity (Pm) and efficiency (α value) as well as the quantum yield of PSII charge separation. These changes suggest that both primary charge separation and electron flow downstream of PSII are effected by lowered salinity (Bates & Cota, 1986). Similar to the observations on increasing salinity, sea ice organisms are able to adapt to falling salinity within a the time frame of weeks (Ryan *et al.*, 2004).

Although much is known about the tolerance of various sea ice organisms to temperature and salinity there is little understanding of how significant these factors are *in situ*. Few observations have been made of photosynthesis under *in situ* temperature and salinity conditions of upper pack ice. During autumn, rates of photosynthesis in the upper brine community at –7° C and salinities of 110 ‰ were an order of magnitude higher than in bottom communities at the same location (Mock, 2002). These rates (0.7 to 1.2 mg C (mg chl*a*)$^{-1}$ h^{-1}) are comparable to those observed for a range of pack ice communities incubated closer to the freezing point of seawater (Arrigo, 2003), suggesting that these communities were well adapted to their low temperature.

1.9 Iron limitation of phytoplankton in the Southern Ocean

Martin *et al* (1990b) were the first to provide evidence that low iron concentrations may limit growth of phytoplankton in Antarctic waters, through accurate (uncontaminated) dissolved iron measurements in the vicinity of the Antarctic

Peninsula. Iron concentrations were low (0.16 nM) in low productivity oceanic waters of Drake Passage but elevated (7.6 nM) in higher productivity waters near the neritic Gerlache Strait. More direct evidence for limitation by this micronutrient was obtained by plankton experiments in austal summer 1988/1989 in the Weddell sea region (Buma *et al.*, 1991; Debaar *et al.*, 1990) and in austral summer 1989/1990 in the Ross Sea. (Martin *et al.*, 1990a) as well as during the 1990/1991 season in the Drake Passage region (Helbling *et al.*, 1991). Considerable research effort has since focussed on the role of iron in controlling primary production in Antarctic waters. This has taken the form of precise measurement of iron concentrations (e.g. de Baar *et al.*, 1999; Sedwick *et al.*, 2000) deck-board bottle iron enrichment studies (e.g. Boyd *et al.*, 1996; Timmermans *et al.*, 1998) and mesoscale iron enrichment experiments (Boyd *et al.*, 2000; Coale *et al.*, 2004; Gervais *et al.*, 2002). It is now well established that iron availability in the Southern Ocean significantly contributes to controlling phytoplankton productivity and community structure.

For waters south of the polar front evidence suggests that iron controls primary production during austral summer but that light is the dominant forcing in winter (Boyd, 2002a). The more favourable light climate in summer results from both warming and shallowing of the mixed layer and increased insolation. During austral spring and summer iron and light can co-limit growth (Boyd, 2002a; Lancelot *et al.*, 2000; van Oijen *et al.*, 2004b). Co-limitation occurs when the average mixed layer irradiance (which is determined by mixed layer depth and down-welling irradiance) limits growth rates, but iron concentrations are simultaneously low, such that an increase in irradiance will not lead to increased growth rates (Boyd *et al.*, 2000). This leads to a situation where blooms are most likely in early spring when there is still some iron around and the mixed layer begins to shallow (de Baar *et al.*, 1999). Despite the significant effect of iron on phytoplankton in the Southern Ocean there has been no work on the role of iron in controlling primary production in the sea ice. Some insight into this question can be gained through relating spatial and temporal

distribution of iron in the Southern Ocean to processes responsible for the evolution of the seasonal sea ice cover.

1.10 Distribution of iron in the Southern Ocean

1.10.1 The Antarctic circumpolar current

Waters of the Southern Ocean south of the Polar Front are characterised by year round high levels of silicate, nitrate and phosphate (Coale *et al.*, 2004; Trull *et al.*, 2001). The concentration of iron in the Southern Ocean varies both spatially and temporally. The most extensively studied region with respect to iron is the ACC and Ross Sea along 170°W. For this region there is a relatively complete picture with studies conducted from spring (October) to autumn (March) (Coale *et al.*, 2005; Fitzwater *et al.*, 2000, Measures & Vink, 2001; Sedwick & DiTullio, 1997; Sedwick *et al.*, 2000).

In the ACC along 170°W dissolved iron concentrations are uniformly low and temporal changes are small. In spring when mixed layer depth is maximal for the year at around 100 m dissolved iron concentrations are between 0.15 to 0.33 nM (Measures & Vink, 2001). Analyses conducted by the same research group in mid summer suggest slightly lower concentrations (0.08 to 0.21 nM) throughout the region from the northern Ross Sea gyre to the Polar Front. The highest concentrations observed during this time of the year were in the vicinity of the Southern Antarctic Circumpolar Current Front. Using a different analytical technique Coale *et al.* (2005) found that dissolved iron level remained low and relatively constant (<0.05 nM) throughout the year in this region of the ACC. Both studies observed similar slightly elevated iron concentrations at depth (0.3 nM) and identified poor supply from below and seasonal export of iron from the mixed layer as dominant factors controlling the iron content of surface waters.

Primary productivity, quantum yield of fluorescence (Fv/Fm) and the response of the phytoplankton community to added iron were determined in conjunction with the

iron analyses of Measures & Vink (2001) in the ACC (Hiscock *et al.*, 2003). In the region between the PF and SB in early spring the community was dominated by diatoms, whose growth was regulated by iron availability. Later in the season when iron levels and silicate decreased, photosynthetic performance increased as the community switched to one dominated by picoplankton. This community was not limited by iron due to their better adaptation to low iron conditions.

The concentrations of iron measured in other regions of the ACC are similar to those in the Ross Sea sector. For example, west of the Antarctic Peninsula (de Baar *et al.*, 1999) and in the Southwest Pacific sector (140° E) (Sohrin *et al.*, 2000) iron concentrations were around 0.2 nM. In the former study low concentrations of algal biomass were observed (de Baar *et al.*, 1999) and iron limitation was confirmed by bottle enrichment experiments (Timmermans *et al.*, 1998). Low iron concentrations in Upper Circumpolar Deep Water (UCDW) throughout much of the ACC appear to be responsible for the consistently low concentrations of this micronutrient in surface waters (de Baar *et al.*, 1999; Martin *et al.*, 1990b; Sohrin *et al*, 2000). These low deepwater iron concentrations set a limit on the concentration of iron in surface waters (Hoppema *et al.*, 2003) . Although upwelling of UCDW occurs all year round, the process that supplies iron into surface water is entrainment during deepening of the mixed layer, which occurs in autumn and winter when wind speeds are highest and convection most prevalent (Hoppema *et al.*, 2003). Therefore highest iron concentrations occur at the end of winter. In the ACC this results in concentrations slightly lower than those in UCDW due to mixing with iron depleted surface waters (Hoppema *et al.*, 2003).

In regions of the ACC downwind from continental margins, such as east of the Antarctic Peninsula (Weddell Sea sector) higher iron concentrations have been reported in both surface waters and UCDW (Croot *et al.*, 2004; Loscher *et al.*, 1997). Elevated iron concentrations in such regions have been attributed to entrainment of sediments resulting when frontal systems interact with continental shelves (de Baar

et al., 1999; Loscher *et al.*, 1997). The study of satellite ocean colour data has provided evidence for the importance of this entrainment process on a larger scale (Moore & Abbott, 2002). This study suggests that phytoplankton blooms are unevenly distributed in the Polar Front region, being most frequently observed where the current interacts with large topographic features.

1.10.2 The continental margin

In contrast to the low levels measured in the ACC the concentration of iron in water masses associated with the continental margin can be significantly higher. Concentrations reported for several regions range from 0.6 to 2.3 nM (Coale *et al.*, 2005; de Baar *et al.*, 1999; Fitzwater *et al.*, 2000; Measures & Vink, 2001; Sedwick & DiTullio, 1997; Sedwick *et al.*, 2000; Sohrin *et al.*, 2000).

Studies conducted on waters above the continental shelf in the Ross Sea have observed highest iron concentrations in early spring which are depleted by phytoplankton growth during summer (Sedwick *et al* , 2000; Watson *et al.*, 1994). Iron addition bioassay experiments conducted in this region suggest that dissolved iron concentrations which averaged 1.0 nM in spring were not limiting to phytoplankton (Sedwick *et al.*, 2000). In the same region during summer iron concentrations were around 0.23 nM and phytoplankton showed a significant response to iron addition, and macronutrient levels were still high (Sedwick *et al.*, 2000).

Winter mixing on the continental shelf often results in deep mixed layers. In some areas winter convection overturns the whole water column and the mixed layer occupies the entire water column which may be up to 1000 m deep (Whitworth III *et al.*, 1998; Wong *et al.*, 1998). High iron levels in these waters appear to result from the formation of these deep mixed layer and input of particulate iron from the re-suspension of sediments (Coale *et al.*, 2005; Fitzwater *et al.*, 2000; Sedwick *et al.*, 2000).

1.10.3 Between the southern boundary of the Antarctic circumpolar current and the continental margin

This region of the Southern Ocean has received less attention than the two regions which border it. Waters of these regions contain a significant amount of the seasonal ice cover (Figure 1.2). In the previously mentioned studies conducted in the Ross Sea sector of the Southern Ocean Measures & Vink (2001) observed lowest iron concentrations south of the SB. Furthermore, the resident phytoplankton population was found to be limited by iron throughout the period of the survey (September-March)(Hiscock *et al.*, 2003). Similarly Coale *et al.* (2003) observed iron responsive communities in this region of the ACC during both spring and summer. This region between the SB and the continental margin is south of and spatially isolated from UCDW. Hence it was suggested that entrainment of deepwater during winter mixing result in only a slight elevation in surface water iron concentrations (Hiscock *et al.*, 2003).

1.11 Sea ice formation in relation to oceanic iron concentration

Monthly sea ice coverage data for 22 years shows that minimum sea ice extent occurs in February and expands over the following seven months to reach maximum cover in September (Comiso, 2003). During the period of active sea ice expansion mixed layers are at their deepest and iron concentrations are likely to be at seasonally highest levels.

The iron content of newly forming sea ice will reflect the iron content of the water from which it forms. As is evident from the discussion above, ice forming in waters of the ACC and in waters between the SB and continental margin would be expected to contain lower concentrations of iron than ice forming in waters near continental margins. However, ice floes drift under the influence of winds and ocean currents and as such iron content of floes will reflect their drift history. Mean Southern Ocean sea ice motion has been computed from satellite data (Emery *et al.*, 1997).

Several broad generalisations about sea ice drift can be made. Close to the coast, the ice movement follows the prevailing westward wind and current direction. This results in an almost continuous flow of ice along the coast. In the ACC the flow is to the east. In the Weddell Sea the westward coastal flow in the south turns north in the south west Weddell Sea then eastward and becomes part of the ACC. Cyclonic ice circulation also occurs in the western Ross Sea. Additional northward transport of ice from the coastal zone is concentrated in an area that spans approximately 30 degrees of longitude in the vicinity of Prydz Bay in Eastern Antarctica

Substantial northward advection of ice occurs in several regions. This has been well documented in the Ross Sea where ice begins formation in coastal waters near the Ross Sea polynya and is transported offshore (Arrigo *et al* , 2003a; Emery *et al.*, 1997; Garrison *et al.*, 2003). In this region a generally northward pattern of drift would result in the upper layers of a flow having relatively high iron content compared to ice forming later in the season in offshore waters of the ACC. However this simplistic pattern of iron content is unlikely even in the Ross Sea sector where ice drift is reasonably uniform to the north. The opening and re-freezing of leads as floes travel north will result in increased heterogeneity of iron in sea ice from any one area.

1.12 Iron speciation in sea ice

In oxygenated seawater iron exists predominantly in the +3 oxidation state At the pH of oceanic seawater inorganic iron speciation is dominated by the formation of oxy-hydroxides which have low solubility (Liu & Millero, 2002). The solubility of iron in seawater is greatly increased by the presence of natural organic ligands. Over 99% of iron in seawater is believed to be bound to such ligands (Ussher *et al.*, 2004). The exact chemical nature of these ligands is largely unknown, however the stability constants and molecular weight of these compounds are similar to those of iron binding siderophores produced by various microorganisms (Macrellis *et al.*, 2001;

Witter *et al.*, 2000). Furthermore, marine bacteria and certain phytoplankton are known to excrete such molecules (Granger & Price, 1999; Soria-Dengg *et al.*, 2001; Wilhelm & Trick, 1994). Iron speciation is further modified by redox reactions. These occur as a result of photoreduction of organic iron complexes (Barbeau *et al.*, 2001; Gerringa *et al.*, 2000) and potentially via reductants produced by microorganisms (Maldonado & Price, 2001; Rose *et al.*, 2005). These processes ultimately result in elevated concentrations of inorganic Fe^{+2} and Fe^{+3} complexes which are thought to be highly bioavailable (Hudson & Morel, 1990; Shaked *et al.*, 2005; Sunda & Huntsman, 1995).

The chemical, physical and biological processes operating during ice formation and aging will further influence the speciation and availability of iron in sea ice. During ice formation the exclusion of ions from the ice crystal lattice will likely cause concentration of dissolved iron in sea ice brines, as occurs with macronutrients (Thomas & Papadimitriou, 2003). The solubility of iron hydroxides (the dominant inorganic iron species in seawater) in sodium chloride at pH 8.0 changes very little in response to ionic strength between 0.1 and 5 M (Liu & Millero, 1999). This suggests that ionic strength changes accompanying brine formation are unlikely to result in significant effects on inorganic iron solubility. Increases in pH accompanying biological activity within the ice (Gleitz *et al.*, 1995) and low temperatures within sea ice brines may, however, substantially increase the solubility of inorganic iron species (Liu & Millero, 1999). The effects of such changes on the organically bound iron fraction are largely unknown However production of iron binding ligands by organisms inhabiting brine channels have the potential to greatly affect iron speciation as these molecules will be retained within the brine channel system. Redox reactions are also likely to play an important part in the speciation of iron in sea ice particularly in the upper portion of floes where light intensity is highest. Brine channels in the upper sea ice have also been reported to contain high concentrations of photo-produced hydrogen peroxide (Mock & Thomas, 2005 and

references therein) which has the potential to increase the rate of oxidation of photochemically produced Fe^{+2} (Gonzalez-Davila *et al.*, 2005; Rose & Waite, 2002).

1.13 Additional sources of iron in sea ice

Several studies have indicated that sea ice may contain significant amounts of iron. Indirect evidence for this has been gained from observations of elevated dissolved iron in the presence of melting sea ice in the Ross Sea (Fitzwater *et al.*, 2000; Sedwick & DiTullio, 1997; Sedwick *et al.*, 2000) It was suggested by these authors that sea ice in this region may incorporate resuspended sediments and/or that the overlying snow cover may contain high concentrations of iron. Sedwick *et al.* (2000) measured iron in snow on sea ice from the Ross Sea and found concentrations as high as 20 nM. Edwards & Sedwick (2001) reported values from 0.36 to 53 nM in Antarctic snow from several regions and provided evidence that much of this iron was readily soluble. Loscher *et al.* (1997) reported 30 nM as typical concentration of iron in snow and sea ice based on six samples. Martin *et al.* (1990b) reported similar concentrations of iron in ice of unknown age near Gerlach Strait. A further potential source of iron is the biological material that become concentrated in sea ice during its formation (Garrison *et al.*, 1983) which may be regenerated by heterotrophic processes (Lizotte, 2003).

Sea ice drift, incorporation of sediments, accumulation of snow, and various physical chemical and biological processes occurring within sea ice have been proposed as factors which may lead to significant heterogeneity in sea ice iron content and biological availability. The heterogeneity of iron in sea ice is likely to be much greater than for the distribution of iron in Antarctic waters. Data on the iron content of Antarctic sea ice is severely lacking, being restricted to a few analyses (Loscher *et al.*, 1997; Martin *et al.*, 1990b). There is currently no information on the biological availability of iron in sea ice. The lack of research into the distribution and availability of iron in Antarctic sea ice no doubt stems from the logistical

difficulties in working with Antarctic sea ice and the lack of analytical techniques suitable to address these questions. The research that I conducted in this dissertation sought to address the question of iron availability in the Antarctic sea ice microalgal community. This was done through the development, validation and trialling on field samples of immunoassays for two algal proteins which were known to be regulated by the availability of iron.

Chapter 2 : Development of immunoassays for the iron regulated proteins ferredoxin and flavodoxin

2.1 Introduction

It has now been widely shown that primary production in many regions of the worlds oceans, including much of the Southern Ocean, is limited by the availability of iron (Boyd, 2002a, b; Coale *et al.*, 2004). Limitation by this micronutrient has generally been demonstrated using nutrient addition bioassays, where a water sample containing the resident phytoplankton population is enriched with iron and the response observed is compared to that of a control sample. These experiments have been undertaken in both *in vitro* mesocosm (Eldridge *et al.*, 2004; Timmermans *et al.*, 1998; van Leeuwe *et al.*, 1997) and *in situ* mesoscale formats (Boyd *et al.*, 2000; Coale *et al.*, 2004; Gervais *et al.*, 2002). In both formats the response of the community is monitored using biomass indicators (chlorophyll, cells, carbon), nutrient uptake kinetics and/or biophysical indicators of nutrient stress such as Fv/Fm. All of these bioassay approaches rely on observing differences between control and enriched treatments with the response of the control treatment representing the situation *in situ* In mesoscale enrichments the assumption of controls representing the community *in situ* is valid. However, iron enrichment mesocosm experiments have been criticised because of confounding effects which result from enclosing the community in a vessel, such as exclusion of grazers (Coale *et al* , 1996)

The role of iron in the Antarctic sea ice microalgal community has not been examined. Iron addition bioassays, the dominant method used to examine iron

availability to phytoplankton, have not been attempted with sea ice. Application of this method to the sea ice environment is problematic for a number or reasons. The first is that there are currently no well tested methods available to take trace metal clean sea ice cores. Bowie and Sedwick (personal communication) conducted trials with a trace metal clean sea ice corer consisting of an all plastic barrel with two high purity titanium blades but had limited success. Sampling was very slow with less than the top 30 cm of a core taken during an hour of coring.

Even if equipment and methods could be developed to sample sea ice "cleanly" there are still numerous uncertainties with conducting iron enrichment bioassays on sea ice.

To ensure that the sea ice biota has access to the added iron, additions would have to be made to samples of brine, melted sea ice or to thin slices of ice cores. Analogous methods have been employed to measure primary productivity in various sea ice algal communities, where C^{14} bicarbonate is added to brine (Stoecker *et al.*, 2000), melted sections of ice cores (Lizotte & Sullivan, 1992a) or thin slices of sea ice cores (Mock & Gradinger, 1999) Used in the context of an iron addition bioassay all three methods are problematic.

Melting of ice cores causes extreme alterations to environmental conditions (Ryan *et al.*, 2004). To reduce osmotic shock, salinity changes are minimised by adding large volumes of seawater to the melting ice (Arrigo, 2003). This act alone would alter iron availability, thus invalidating controls

Using an approach where either brine samples or thin sections are incubated with iron would avoid the problems described above. However, both approaches would remove organisms from the strong gradients of light temperature and salinity within the ice (Eicken, 1992) and destroy nutrient supply regimes within the ice (Thomas & Papadimitriou, 2003) including those that control iron availability. Thus once again control incubations would not accurately represent the situation *in situ.*

It is thus clear that these approaches are problematic. To determine whether iron is limiting to sea ice algae other methods must be examined.

Iron limited growth of phytoplankton affects many chemical, biochemical, biophysical and physiological parameters but few of these can be used as stand alone markers for low iron stress. Chlorophyll per cell (Greene *et al.*, 1991; McKay *et al.*, 1997), nitrate and nitrite reductase activity (Kudo *et al.*, 2000; Milligan & Harrison, 2000; Timmermans *et al.*, 1994), silicate:nitrate and silicate:phospate consumption ratios (Hutchins & Bruland, 1998; Takeda, 1998) and photophysiological parameters such as Fv/Fm (Boyd & Abraham, 2001; Davey & Geider, 2001) all vary with iron nutritional status, but none of these are exclusive markers for low iron stress. To be indicative of iron limitation these parameters need to be measured in the context of an iron addition bioassay to show relative differences before and after iron resupply to the resident phytoplankton population.

An approach which may provide a way to investigate the iron nutritional status of sea ice algae is the use of specific protein markers for iron stress. Ferredoxin and flavodoxin are two such candidate proteins which are emerging as potential iron stress markers (Doucette *et al.*, 1996; Erdner *et al.*, 1999; La Roche *et al.*, 1996; La Roche *et al.*, 1995).

Both proteins transfer high potential electrons from photosystem one (PSI) to other key biochemical pathways including to nitrite reductase and to ferredoxin-NADP reductase which produces the ubiquitous redox catalyst NADPH (La Roche *et al.*, 1993; Raven *et al.*, 1999). Ferredoxin is an iron sulphur protein whereas flavodoxin contains a flavin mononucleotide (FMN) prosthetic group, but the proteins are functionally equivalent. La Roche *et al.* (1993; 1995) were the first to show that flavodoxin expression was massively up regulated in many diatom species when stressed by a lack of iron. They suggested that it could be used as an *in situ* marker for iron stress. Using an HPLC technique Erdner *et al.* (1999) measured both

ferredoxin and flavodoxin levels in a number of marine algae and showed that suppression of ferredoxin expression and induction of flavodoxin is a common response to low iron stress. Both proteins have also been used as markers for iron nutritional status in field samples (Boyd *et al.*, 1999; Boyd *et al.*, 2000; Erdner & Anderson, 1999, La Roche *et al.*, 1996; McKay *et al.*, 2000, Timmermans *et al.*, 1998). Measurement of these proteins in sea ice provides a way to potentially assess the iron nutritional status of sea ice algae.

Two methods have been used to measure or detect ferredoxin and flavodoxin. Doucette *et al.* (1996) developed a quantitative HPLC method with a limit of detection of 1 μg mL^{-1}. The main drawback of this method being its lack of sensitivity During the IronEx-II mesoscale ocean fertilisation experiment flavodoxin was the sole protein detected (Erdner & Anderson, 1999) and only after biomass levels has risen to approximately 2 μg chl *a* L^{-1} (Coale *et al.*, 1996). The exact amount of water filtered on this day is not given in their publication but they routinely filtered 100-600 L of water for each sampling during the experiment. This translates to requiring 200-1200 μg of chlorophyll to detect these proteins using the HPLC method. In pack ice in the Ross Sea where bottom communities dominated, mean algal standing stocks of 2.53 mg m^{-2} were reported (Arrigo *et al.*, 2003a). Compiled standing crop data from 13 cruises suggests that a range of one order of magnitude above and below this value are typical (Dieckmann *et al.*, 1998). At these levels a sample taken with a 13 cm diameter ice corer would sample approximately 3-300 μg of chlorophyll *a*, if the algae contained within a whole ice core could be concentrated into a single sample. From these simple calculations it is clear that the HPLC approach is not a feasible method to detect these proteins in ice cores.

An alternative to the HPLC approach was developed by La Roche *et al.* (1995) who developed a qualitative western blot immunoassay for flavodoxin. A similar immunoassay for ferredoxin was developed for diatom ferredoxin by McKay *et al* (1999) using proteins isolated from *Thalassiosira weissflogii*. The western blot

immunoassay techniques are several orders of magnitude more sensitive than the HPLC method. The immunoassay approach would therefore probably only require 2-12 μg of chlorophyll. This amount of chlorophyll corresponds to a fraction of an ice core based on the above estimates of pack ice standing stocks. This may allow for some vertical profiling of the proteins in sea ice which may provide insights into processes effecting iron availability in sea ice. One drawback of the immunoassay as it is currently used is its semi quantitative format where, comparison of the amounts of these proteins can only be made for samples run on the same gel (usually 10 samples).

The relationships between ferredoxin and flavodoxin expression and iron availability are poorly understood. Although in culture experiments the majority of organisms express flavodoxin under iron limited growth and ferredoxin when iron supply is in excess of cellular requirements (Erdner *et al.*, 1999; La Roche *et al.*, 1995), field studies have often shown persistent expression of flavodoxin in communities which have been released from iron limitation through iron enrichment (Erdner & Anderson, 1999; La Roche *et al.*, 1996; Timmermans *et al.*, 1998). Furthermore, there is some evidence to suggest that certain organisms have constitutive flavodoxin expression. For example, *Cylindrotheca closterium* was observed to produce small amounts of flavodoxin under iron replete conditions (La Roche *et al.*, 1995). Clones of a *Rhizosolenia* species were also observed to sustain expression of this protein under high iron conditions (McKay *et al*, 2000). No studies to date have examined the expression of these proteins in Antarctic diatoms which have evolved in an environment with chronic low iron concentrations. A quantitative assay would be critical for determining the relationships between iron supply and ferredoxin and flavodoxin expression in cultures of Antarctic isolates and field samples.

Here I describe the development of a quantitative immunoassay for both ferredoxin and flavodoxin. The chapter outlines methods used to grow the marine algae *Cylindrotheca closterium* such that it expresses ferredoxin or flavodoxin, and the

procedures for purification of both proteins to high purity, enabling their use as standards in the assay. The generation of antibodies to the proteins and the development, refinement and initial validation of the assay are also described.

2.2 Methods

2.2.1 Seawater collection

Seawater for both iron replete and iron limited culturing was collected at Tessellated Pavement, Eaglehawke Neck, Tasmania with an electric powered diaphragm pump into a 1000 L polyethylene cube. No attempt was made to prevent contamination of the seawater by iron. The water was stored at ambient temperature in the dark. Prior to use for culturing the water was filtered from a 20 L stainless steel pressure vessel (Millipore) through a filter set housed in a 90 mm stainless steel filter holder. The pre-filter was type A/E glass (PALL) and final filter 0.2 μm Supor® 200 (PALL). The filter set was sterilized by autoclaving for 20 min at 121° C.

2.2.2 Culture media

Media used to grow both iron replete and iron limited cultures were based on f/2 media (Guillard & Ryther, 1962). For iron replete cultures the media contained standard f/2 levels of macro-nutrients, vitamins, trace metals, iron and EDTA. Iron limited media contained similar enrichments except that iron was added at either 10 or 20 nM and the amount of EDTA reduced to equal that of total trace metals.

Nutrient stock solutions were prepared in sterile 50 mL polypropylene screw cap centrifuge tubes (Greiner) To maintain trace metals in solution trace metal and iron stocks were prepared in 0.01 M H Cl. Other stocks were prepared with >18 MΩ Milli Q water (Milli Q water). Individual stock solutions were filtered through 0.2 μm Supor® (PALL) membrane syringe filters prior to use.

2.2.3 Growth of *Cylindrotheca closterium* for protein purification

The neritic diatom *Cylindrotheca closterium* (strain CS5, CSIRO, Australia) was used as a source of both ferredoxin and flavodoxin. Cultures were grown at 20° C at an irradiance of 130 μmols photons m^{-2} sec^{-1} provided by cool white fluorescent lights on a 12/12 light dark cycle.

Inoculum used to grow the bulk cultures was maintained in autoclave sterilised 250 mL polycarbonate jars with polypropylene caps containing 100 mL of media. Prior to use these were soaked overnight in 0.01 % Triton X 100 in Milli Q water followed by 5 rinses with Milli Q water then soaked in 1 M HCl overnight followed again with five Milli Q rinses. No special attempt was made to prevent contamination by airborne particles during cleaning (i.e. handling of culture ware was not performed in a trace metal clean environment) but all culture manipulations were performed in a laminar flow hood.

Media used to maintain inoculum for the iron replete cultures contained normal f/2 levels of iron (11.7 μM) and for iron limited cultures contained 250 nM iron. Prior to growing iron limited cultures the inoculum was acclimated for at least two transfers in the 250 nM iron media. These were transferred every 5 days to maintain exponential growth.

To generate the biomass required for protein purification 4 x 15 L iron replete and iron limited cultures were grown in autoclave sterilised 19 L polycarbonate carboys bubbled continuously with filtered (0.2μm Supor®, PALL) air. Carboys for iron limited culturing were cleaned as described above for the 250 mL jars. Iron concentration in the replete media was 11.7 μM whereas iron was added to a concentration of 10 or 20 nM in iron limiting media.

Carboys were inoculated with 200 mL of starter culture which had been grown to late exponential phase. Growth of cultures was monitored by extracted chlorophyll

analysis and prior to harvest cell counts were performed on duplicate 1 mL samples using a Sedwick-Rafter cell At least four hundred cells were counted for each replicate count. Cultures were allowed to grow for five days to late exponential phase then harvested by concentrating onto 5 μm polycarbonate filters (Osmonics) and centrifuging the concentrate at 2000 x g for 10 min. Cell material was frozen at –20 ° C for no more than one month.

2.2.4 Chlorophyll analysis

For extracted chlorophyll analysis aliquots were removed daily and filtered onto 13mm GFF filters and extracted into 10 mL of methanol at -20° C for 24 hours. Fluorescence was measured on a Turner designs 10AU model fluorometer both before and after acidification and the values used to calculate chlorophyll concentrations corrected for phaeophytin (Arar, 1997).

2.2.5 Purification of flavodoxin

The flavodoxin purification scheme was similar to that used by La Roche *et al.* (1995) the main difference being that elution of proteins from the ion exchange column was effected with a salt gradient rather than in batch mode. To the frozen cell pellet from two carboys (9 g wet weight) was added 20 mL of ice cold 100 mM Tris-HCl buffer pH 7.6 containing 4 mM DL-Dithiothreitol (DTT) and 200 μM Phenylmethanesulfonyl fluoride (PMSF). Cell lysis was achieved by sonication in 60 second bursts with intermittent cooling in an ice/water bath. The mixture was made to 0.1% protamine sulphate then centrifuged at 20000 x g for 30 minutes and the supernatant transferred to a clean 50 mL screw cap centrifuge tube and placed on ice. Solid ammonium sulphate was added to 50% saturation and the mixture left to stand on ice for a further 30 minutes. The resultant precipitate was removed by centrifugation at 20000 x g for 20 minutes and the supernatant taken to 70% saturation with ammonium sulphate. After another 30 minutes on ice the precipitate was removed by centrifugation and the straw yellow supernatant enriched in

flavodoxin was made to 100% saturation with ammonium sulphate. After centrifugation at 20000 x g for 20 minutes the protein pellet was dissolved in a small volume of 50 mM Tris-HCl buffer pH 7.6 and desalted on a 10 mL column of Sephadex® G-25 (Amersham) equilibrated with the same buffer. The protein fraction from the desalting column was loaded onto a 5 mL column of Diethylaminoethyl (DEAE) Sephacel® (Sigma-Aldrich) and washed with 10 mL of 50 mM Tris-HCl buffer pH 7.6 followed by 10 mL of the same buffer made to 0.2 M NaCl. The column was then developed with a 30 mL gradient (0.2 M to 0.7 M) of NaCl in 50 mM Tris-HCl buffer pH 7.6. The main protein peak enriched in flavodoxin eluted between 0.4- 0.5 M NaCl. Fractions containing flavodoxin were pooled and concentrated with Centricon® (3000 MW cut-off, Millipore) ultrafiltration spin column and a visible absorbance spectrum taken to determine concentration and purity. The concentrate was dispensed into microcentrifuge tubes and stored frozen at -80° C.

2.2.6 Purification of ferredoxin

The procedure for ferredoxin purification was similar to the one used to purify flavodoxin but with slightly different conditions and an additional hydroxyapatite chromatography "polishing" step. The first steps used in the purification scheme were also similar to those used by McKay *et al.* (1999) to purify ferredoxin and by La Roche *et al.* (1995) to purify flavodoxin.

Cell material (19.8 g wet weight) from iron replete cultures was suspended in 90 mL of 100 mM Tris-HCl buffer pH 7.6, 1 mM EDTA, 4 mM DTT and 200 µM PMSF. Cell lysis was achieved by sonication on ice. Soluble proteins were recovered by centrifugation at 20000 x g for 30 minutes. The solution was made to 0.1% protamine sulphate (Sigma-Aldrich) to precipitate nucleic acids and was centrifuged at 20000 x g for 20 minutes. The supernatant was made to 45% saturation with ammonium sulphate on ice, the protein pellet removed by centrifugation then made

to 65% saturation. After stirring on ice for 30 minutes the precipitated protein was removed by centrifugation and the supernatant transferred to a dialysis bag (Sigma-Aldrich, high retention) and dialysed twice against 2 L of 50 mM Tris-HCl pH 7 6. The solution was clarified by filtration through a 0.45 μM syringe filter (Acrodisc® Supor®, PALL) and loaded onto a 5 mL column of DEAE Sephacel®. The column was washed with 20 mL of 50 mM Tris-HCl pH 7.6, then with a further 25 mL of the same buffer made to 0.2 M with NaCL. The column was developed with 40 mL of a linear gradient of 0.2 M NaCl to 0.7 M NaCl. Fractions containing ferredoxin (determined by a high absorbance at 460 nm) were pooled and exchanged into 15 mM phosphate buffer pH 7.0 with a Centricon® (3000 MW cut-off, Millipore) ultrafiltration spin column and loaded onto a 1.5 mL column of Bio-Gel HTP hydroxyapatite (Biorad). The column was developed with 10 mL of a gradient from 15 mM phosphate buffer to 150 mM phosphate buffer. Fractions containing ferredoxin were reloaded onto another 1.5 mL hydroxyapatite column, washed with 10 mL of 35 mM phosphate buffer and eluted with 10 mL of 50 mM phosphate buffer. Purity and concentration were determined in a similar way to that of flavodoxin.

2.2.7 Antibody production

Antibodies towards ferredoxin and flavodoxin were raised in rabbits. Proteins were exchanged into 500 μL phosphate buffered saline pH 7.2 (PBS) using a Centricon® (3000 MW cut-off, Millipore) ultrafiltration spin column and thoroughly emulsified with an equal volume of Freund's Incomplete Adjuvant (Sigma-Aldrich) by repeated drawing and expressing of the mixture through a syringe. All injections were given via the intramuscular route in the thigh muscle. Initial injections contained 100 μg of protein and boosters of 50 μg were given at 14 day intervals until sufficiently high antibody titres were obtained. Decisions on whether to boost or not were made on the basis of antibody titre which was measured by double antibody capture Enzyme-Linked Immunosorbent Assay (ELISA) on blood taken 12 days after each booster.

2.2.8 Antibody capture ELISA for determining antibody titre

To measure antibody titre, polystyrene multiwell plates (high binding, Greiner Bio-One) were coated by incubating overnight with 75 µL of 5 µg mL^{-1} ferredoxin or flavodoxin in PBS. Wells were washed 3 times with 200 µL per well PBS then blocked for 1 hr with 300 µL of 3% skim milk in PBS. Wells were then washed 3 times with 300 µL per well PBS-T (0.05% Tween 20) then incubated with 100 µL of serially diluted (1:1) serum from 1/100 to 1/51200 made in PBS-T. After an incubation period of 1.5 hr wells were washed three times with 300 µL of PBS-T and then incubated for 1 hr with 1/2500 anti rabbit HRP conjugate (Promega) in PBS-T for 1 hr. Wells were then washed again with 3 x 300 µL of PBS-T and 250 µL of 3,3',5,5'-Tetramethylbenzidine (TMB) substrate added, the plate incubated for 15 minutes then the absorbance read at 450 nM. Preparation of the TMB substrate was as follows.

Acetate buffer pH 6 was made by combining 500 mL of 0.1 M sodium acetate and 23 mL of 0.1 M acetic acid. To make the TMB substrate 25 mL of acetate buffer pH 6 in a 50 mL polypropylene screw cap tube was warmed to 35 ° C and 250 µL of 0.1% TMB in dimethyl sulfoxide (DMSO) was added. The tube was wrapped in foil to exclude light and was incubated a further 15 minutes at this temperature to ensure thorough dissolution. The solution was cooled to 25° C and 10 µL of 30% H_2O_2 added immediately before use.

2.2.9 Protein assay

Protein concentration of cell lysates was determined using the bicinchoninic acid (BCA) assay (Pierce) in a multiwell format. A stock standard of 20 mg mL^{-1} bovine serum albumin in SDS PAGE lysis buffer (92.6 mM Tris-HCl pH 6.8, 3% SDS) was used to prepare standards in the range of 125 µg mL^{-1} to 2000 µg mL^{-1}. Duplicate 10 µL aliquots of each standard and sample were added to a 96 well polystyrene multiwell plate (Greiner Bio-One). BCA working reagent was prepared by

combining 50 parts of BCA reagent A (Pierce) and 1 part of 4% copper sulphate solution. 200 µL of working reagent was added to each sample or standard and the plate incubated for 30 minutes at 37 ° C. Absorbance was then read at 560 nM with a microplate reader (Biorad) connected to a PC and a standard curve and sample concentrations calculated using Microplate Manager® software (Biorad).

2.2.10 SDS PAGE

2.2.10.1 Gel casting

SDS PAGE was performed using Mini Protean 3® (Biorad) equipment and methods for gel casting were as outlined in the mini protean 3 instruction manual. Mini gels 80 x 60 x 0.75 mm were cast with a 15 % resolving gel and 4 % stacking gel using premixed 40% Acrylamide/Bis solution 37.5:1 (Biorad). Gels were allowed to polymerise for two hours before use.

2.2.10.2 Sample preparation

To monitor protein purification using SDS PAGE samples taken at various stages of the purification were mixed with at least 2 volumes of SDS sample buffer (62.5 mM Tris-HCl pH 6.8, 25% Glycerol, 2% SDS, 0.01% Bromophenol Blue, 75 mM DTT) , and heated to 95 ° C for 4 minutes and stored at room temperature until loading. Gels were run at a constant voltage of 200 V using standard Laemmli running buffer (25 mM Tris, 192 mM Glycine, 0.1% SDS) (Laemmli, 1970) until the dye front reached the bottom of the gel.

2.2.10.3 Gel staining

Gels were fixed for 1 hour with 50% (v/v) ethanol, 10% (v/v) acetic acid then left to soak overnight in a solution of 40% (v/v) methanol , 10% (v/v) acetic acid. Gels were stained for four hours with 0.1% (w/v) Coomassie blue R350, 20% (v/v) methanol, and 10% (v/v) acetic acid. De-staining was effected using several changes of a solution containing 50% (v/v) methanol and 10% (v/v) acetic acid.

2.2.11 Western blotting

Samples of the iron replete and iron limited cultures of *Cylindrotheca closterium* as well as purified ferredoxin and flavodoxin were run on gels and probed with antibodies in order to develop the immunoassays. Many trials of buffer composition, membrane type and assay conditions were conducted in order to optimise the assay. In particular the concentration of SDS in the gels and running buffer was found to significantly effect on the sensitivity and reproducibility of the ferredoxin immunoassay. Several immunoassays were conducted with varying amounts of SDS in the gels and SDS PAGE running buffer to optimise the concentration of this detergent. Optimal assay conditions found to provide the most intense banding for each protein with minimum background are described below.

2.2.11.1 Sample preparation

Preparation of proteins from cultured cell material for SDS PAGE used a slightly modified procedure to that described above for protein purification. These modifications were made so that the concentration of protein in the lysate could be quantified prior to loading on the gel. Firstly, total proteins from cell pellets were lysed by the addition of approximately 5 volumes of lysis buffer (92.6 mM Tris-HCl pH 6.8, 3% SDS, 0 .1 mM PMSF). Insoluble material was removed by centrifugation at 20000 x g for 10 minutes and duplicate 10 µL aliquots were taken for protein determination by the bicinchoninic acid method. After quantitation an aliquot of the lysate was diluted to an appropriate concentration and 0.325 volumes of a freshly prepared sample reducing buffer (300 mM DTT, 30% Glycerol, 0.04% bromophenol blue) was added and the solution heated at 95° C for 4 minutes. Samples were loaded at 25 µL per well. Samples of purified ferredoxin and flavodoxin for SDS PAGE were prepared by diluting stock solutions with whole SDS PAGE sample buffer (i.e. combined 1 volume of lysis buffer and 0.325 volumes of sample reducing buffer).

2.2.11.2 SDS PAGE

The SDS PAGE system used to separate proteins for western blotting was virtually the same as for monitoring protein purification but the amount of SDS in the gel and running buffer was reduced to 0.01%, which is on tenth of the original concentration. This was found to be necessary as excessive SDS was found to interfere with the detection of ferredoxin by western blotting.

2.2.11.3 Blotting procedure

Following electrophoresis gels were equilibrated 3 x 10 minutes with 50 mL per gel of transfer buffer (25 mM Tris, 192 mM Glycine, 20% Methanol) with agitation on a shaker table. This repeated washing was found to be necessary to remove SDS from the gel and thereby maximise binding of ferredoxin to the membrane. After equilibration of gels proteins were transferred onto 0.22 μm nitrocellulose membranes (Hybond ECL, Amersham) for 1 hr at 80 V using the Biorad Mini Trans-Blot® transfer cell. Gels were then air dried overnight at ambient temperature before immunodetection.

2.2.11.4 Immunodetection

The immunodetection procedure followed the method outlined in the ECL western blotting detection protocol supplied with reagents (Amersham Biosciences 2002). Membranes were blocked for 1 hr in 5% skim milk in PBS-T (10 mM phosphate pH 7.2, 0.1% Tween 20) then rinsed briefly with two changes of PBS-T (these and subsequent washes used 150 mL of buffer per membrane). Primary antibodies for both ferredoxin and flavodoxin were diluted 1/5000 (50 mL per membrane) and incubated for 1.5 hrs. Whilst optimising the immunodetection procedure membranes were incubated with only one primary antibody at a time however once optimum conditions were found membranes were incubated with both antibodies simultaneously. Membranes were then washed briefly (10 seconds) with two changes of PBS-T then for another 1 x 15 minutes followed by 3 x 5 minutes.

Membranes were then incubated with 1/25000 anti-rabbit HRP conjugate (Amersham) for 1 hr in 50 mL buffer per membrane. The above wash schedule used for the primary antibody was repeated, membranes were placed on a piece of cling wrap and 6 mL of ECL substrate was pipetted onto each membrane. After incubating for 1 minute membranes were wrapped in a fresh piece of cling wrap and the signal was captured on Hyperfilm X-ray film (Amersham) in an autoradiography cassette. Films were processed as per the instructions that accompanied the packet.

2.2.11.5 Densitometry

Gels were scanned with a Canon LiDE 50 scanner at 1200 dpi resolution and files saved in uncompressed TIFF format. Densitometry was performed using Image Quant V5.2® Software (Amersham). Bands were quantified by calculation of band volume using an object averaged background correction.

2.2.12 Determination of linear range

A solutions containing a mixture of pure ferredoxin and flavodoxin each at a concentration 8000 ng mL^{-1} was prepared in SDS PAGE loading buffer. This solution was used to prepare eight standard solutions in the range 224-8000 ng mL^{-1}. Triplicate SDS PAGE gels were loaded with 25 µL of each standard which resulted in wells being loaded with 5.6, 9.3, 15.6, 25.9, 43.2, 72, 120 and 200 ng of each protein. Gels were run, blotted, immunodetected and bands quantitated as described above. Autoradiography of blots was performed for 1 and 3 minutes. Plots of band volume versus protein were constructed to determine the linear range of the assay for each protein

2.3 Results

2.3.1 Growth of *Cylindrotheca closterium*

Growth characteristics of *Cylindrotheca closterium* in 15 L batch cultures were determined by extracted chlorophyll analysis. Figure 2.1 shows growth curves for cultures grown at three different concentrations of iron.

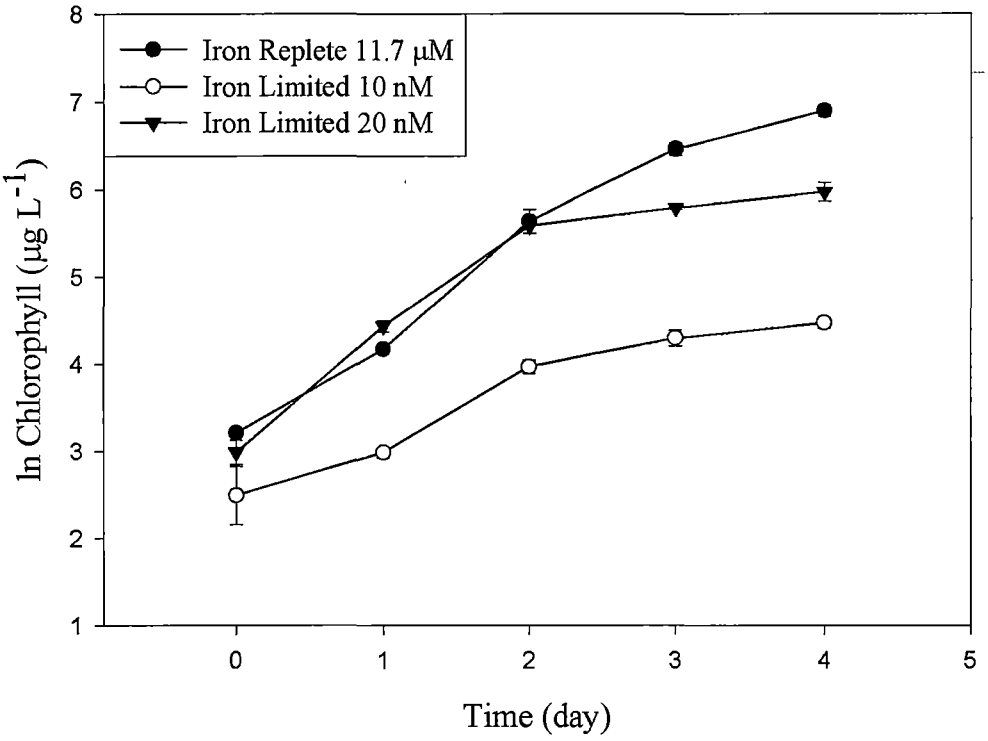

Figure 2.1 Daily change in ln chlorophyll (µg L^{-1}) of *Cylindrotheca closterium* grown in f/2 media with three concentrations of iron. Data points are means of duplicate cultures and error bars represent standard deviations.

Growth of all cultures was initially exponential. The mean growth rates during this exponential phase of cultures grown at three concentrations of iron are shown in Table 2.1. There was a significant effect of iron concentration on chlorophyll specific growth rates during the initial stage of growth (ANOVA $p<0.05$). Only the 10 nM iron cultures grew significantly slower than both the 20 nM culture and the

11 7 μM culture ($p<0.05$ Tukey's HSD). There was no significant difference between the chlorophyll specific growth rates of the 20 nM and the 11.7 μM grown cultures.

The latter stages of the growth curve shows that all cultures approached a stationary phase of growth however the maximum concentration of chlorophyll reached in the carboys was dependent on the amount of iron added (Table 2.1).

Table 2.1 Growth rate, final yield of chlorophyll and chlorophyll content of *Cylindrotheca closterium* cultures grown in f/2 media with three added levels of iron. Values are mean ± SD (n=2).

Added Iron	Growth (d^{-1})	Final Chlorophyll ($\mu g\ L^{-1}$)	Chlorophyll per cell (pg chl a $cell^{-1}$)
10 nM	0.74 ± 0.13	87.8 ± 5.4	0.179 ± 0.027
20 nM	1.30 ± 0.07	395 ± 41.7	0.444 ± 0.041
11.7 μM	1.22 ± 0.042	991 ± 67.2	1.96 ± 0.044

Cell counts proved to be problematic for *Cylindrotheca closterium* as cultures formed sticky aggregates, particularly as cell density increased. However, counts were carried out prior to harvesting, after separation of the aggregates by sonication at low power. These were used to calculate chlorophyll per cell (Table 2.1). Chlorophyll levels per cell at the time of harvest were highest for cultures grown with 11.7 μM iron and lowest for the culture with only 10 nM added iron. The cultures grown with 20 nM iron had chlorophyll per cell levels intermediate to the other two. The effect of iron on chlorophyll per cell levels were highly significant (ANOVA $p<0.001$) with both low iron cultures having significantly lower chlorophyll per cell than the high iron culture (Tukey's HSD, $p<0.001$), and the two low iron cultures being significantly different from each other (Tukey's HSD, $p<0.05$). There was an order of magnitude difference in cellular chlorophyll levels between the culture grown with 10 nM iron and 11.7 μM iron.

2.3.2 Ferredoxin purification

Ferredoxin was successfully purified from iron replete cultures of *Cylindrotheca closterium*. Figure 2.2 is an SDS PAGE gel showing separated proteins from various fractions obtained during the purification scheme. A band corresponding to ferredoxin could not be detected in any of the fractions prior to ion exchange chromatography including the fraction which was loaded on the DEAE column. The absorbance of fractions at 280 and 460 nM eluted from the DEAE column is shown in Figure 2.3. Fractions which eluted when the NaCl concentration was between 390 and 490 mM NaCl had an A_{460} greater than 0.05 and when run on an SDS PAGE gel and were found to be highly enriched with an 18 kDa protein which was later identified as ferredoxin from its characteristic absorbance spectrum (Figure 2.4). Although initial SDS PAGE gels found the presence of a single protein band for these fractions, latter gels run with increased protein load showed the presence still of a minor contaminant which, from its relative mobility, may have been flavodoxin (not shown). The removal of this contaminating protein was achieved using hydroxyapatite column chromatography. Ferredoxin was eluted from this column at a phosphate concentration of 50 mM whereas the contaminating protein remained on the column until the phosphate concentration was raised to 80 mM. After concentrating the ferredoxin containing fractions with a size exclusion spin column the resultant solution of pure ferredoxin had an A_{435}:A_{280} of 1.9. Protein concentration of this solution was 405 μg mL^{-1} determined by the bicinchoninic acid assay. The yield of ferredoxin from 19.8 g of cells (wet weight) was 420 μg. The absorbance spectrum of ferredoxin (Figure 2.4) showed absorbance maxima at 331, 403 and 435 nm.

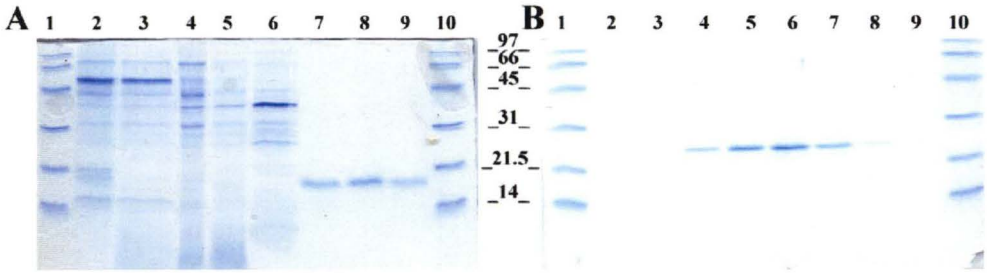

Figure 2.2 SDS PAGE gels of fractions obtained during protein purification. Numbers between the two gels show the molecular weight (kDa) of molecular weight markers which are loaded in lanes 1 and 10 on both gels.

A) Fractions obtained during ferredoxin purification; 2 soluble proteins, 3 soluble in 45% ammonium sulphate, 4 Soluble in 65% ammonium sulphate, 5 fraction loaded onto DEAE column, 6 Fraction eluted from DEAE column with 0.2M NaCl, 7-9 fractions eluted from DEAE column enriched in 18kDa protein (ferredoxin).

B) 2-9 Fractions eluted off DEAE column and enriched in 24 kDa protein (flavodoxin) during flavodoxin purification.

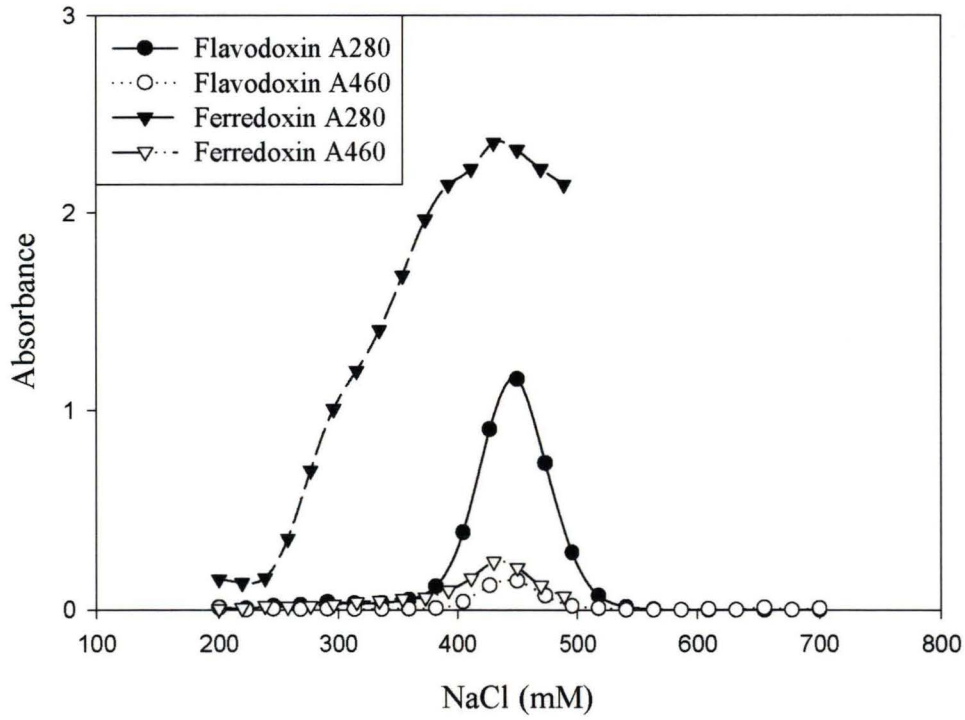

Figure 2.3 Absorbance at 280 nm and 460 nm of fractions that elute from DEAE column during purification of ferredoxin and flavodoxin.

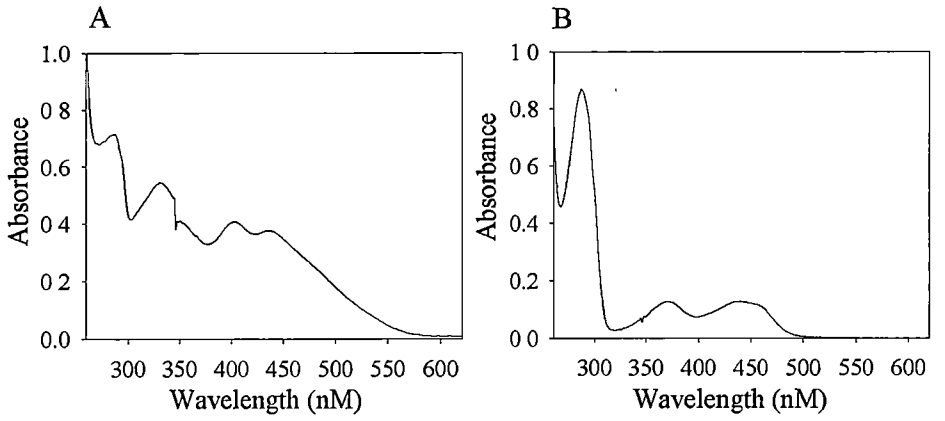

Figure 2.4 Absorbance spectra of A) Ferredoxin and B) Flavodoxin.

2.3.3 Flavodoxin purification

Both the 20 nM grown cultures and the 10 nM grown cultures were used to successfully purify flavodoxin. After precipitation of the 70-100% ammonium sulphate fraction the resultant pellet was redissolved, desalted and purified by DEAE chromatography. The elution profile of proteins monitored by absorbance at 280 nm and 460 nm is shown in Figure 2.4. A single peak of protein eluted between 400 and 500 mM NaCl. Fractions corresponding to this protein peak were found to contain a single protein by SDS PAGE (Figure 2.2) which had a molecular weight of 24000, and was identified as flavodoxin from its absorbance spectrum (Figure 2.4) which showed maxima at 280, 371 and 438 nm The yield was 2.4 mg from 9 g cells (wet weight) and the A_{438} : A_{280} of the combined fractions was 3.95.

2.3.4 Antibody production

High titre antisera were raised towards both ferredoxin and flavodoxin in New Zealand White rabbits. Serum titres for both rabbits were monitored by antibody capture ELISA and are presented in Figure 2.5. Pre immune sera from the two rabbits used in the study had low serum titres. Antibody titres between 1/2000-1/2500 were reached with only two immunisations for flavodoxin and three immunisations for ferredoxin. These continued to increase with further boosters

reaching a maximum of 1/17000 for flavodoxin after four immunisations and 1/22000 for ferredoxin after a total of five immunisations.

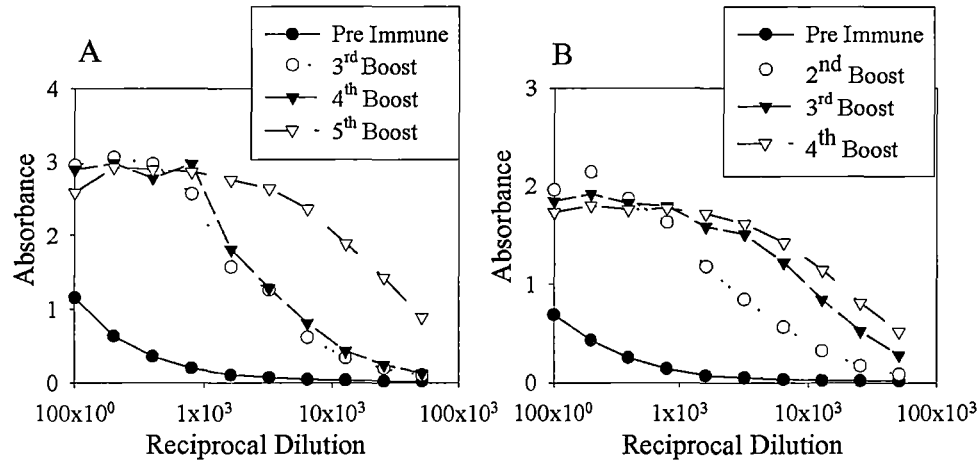

Figure 2.5 Serum titres of antibodies towards A) Ferredoxin and B) Flavodoxin measured by ELISA twelve days after each inoculation. Titres are taken as the inflection point of each curve

2.3.5 Establishment of western blotting protocol

As shown in Figure 2.6 A the flavodoxin antibodies immunodecorated a single band in lanes loaded with both purified flavodoxin or lysates prepared from *C. closterium* cells. There was a small amount of cross reactivity with high molecular weight proteins but no reactivity with other proteins in the vicinity of the target protein. The flavodoxin antibodies labelled a protein of the same molecular weight in lysates prepared from both iron replete and iron limited grown *C. closterium* cells.

Antibodies generated toward ferredoxin immunodecorated a single band in lanes loaded with purified ferredoxin and lanes loaded with lysates prepared from iron replete grown *C. closterium* cells (Figure 2.6 B). Again there was little non specific cross reactivity with other proteins in the whole cell lysates.

Flavodoxin antibodies did not cross react with ferredoxin as is evident from the lack of a band for ferredoxin in the lane loaded with proteins from the iron replete culture. Similarly ferredoxin antibodies did not immunodecorate pure flavodoxin (not shown).

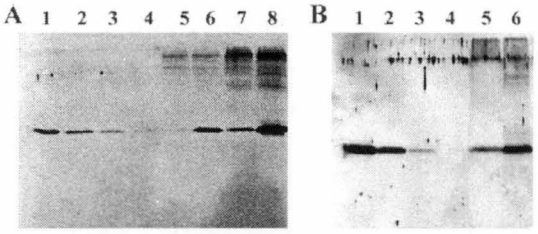

Figure 2.6 Western blots for ferredoxin and flavodoxin:

A) flavodoxin; lanes 1-4 purified flavodoxin 250 ng, 125 ng, 67.5 ng, 32.8 ng; lane 5-8 proteins from *C. closterium*, iron replete, iron limited, iron replete, iron limited (different loadings).

B) Ferredoxin; lanes 1-3 purified ferredoxin 250 ng, 50 ng, 10 ng; lane 4 empty, lanes 5 and 6 iron replete *C. closterium* (different loadings).

2.3.6 Ferredoxin and flavodoxin western blots: SDS concentration

Blots simultaneously immunodecorated for both ferredoxin and flavodoxin are shown in Figure 2.7. Blots taken from gels run with 0.01% SDS ($1/10^{th}$ normal concentration) are shown in Figure 2.7 A whilst Figure 2.7 B shows a similar blot taken from a gel from which SDS was omitted. Excluding SDS from the running buffer and gel resulted in good detection of ferredoxin but substantial band smearing for flavodoxin. In contrast when a standard concentration of SDS was used (0.1%) ferredoxin was not detected (not shown). The best compromise found to maximise ferredoxin staining without causing flavodoxin band smearing was found to be 0.01% SDS.

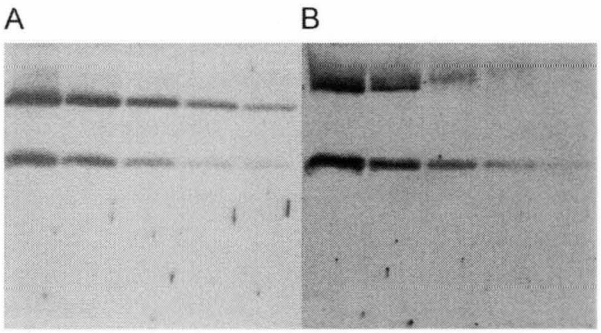

Figure 2.7 Two western blots for ferredoxin and flavodoxin taken of SDS PAGE gels run with different amounts of SDS. A=Five dilutions of flavodoxin (top bands) and ferredoxin (bottom bands) run on a gel with 0.01% SDS, B= Five dilutions of flavodoxin (top bands) and ferredoxin (bottom bands) run on a gel without SDS.

2.3.7 Linear range of western blots

An example of one of the blots performed on dilutions of ferredoxin and flavodoxin in the range of 5.6-200 ng of protein is shown in Figure 2.8. In these blots both ferredoxin and flavodoxin were detected simultaneously and autoradiographs were taken of the same gel for 1 and 3 minute. Plots of band intensity determined by densitometry, versus protein are shown for the 1 minute autoradiograph for both ferredoxin and flavodoxin (Figure 2.9). Both exposure times led to detection of both proteins over the entire range of the standards loaded. A linear response was observed for band intensity between 5.6 and 43.2 ng for flavodoxin and between 5.6 and 72 ng for ferredoxin with a Pearson's r^2 correlation coefficient above 0.99 within these ranges. Extending the linear regression outside this range resulted in significant declines in r^2 values. Similar linear responses were observed for both the longer and shorter exposure times with the latter exposure producing more visible signals for standards in the lower range.

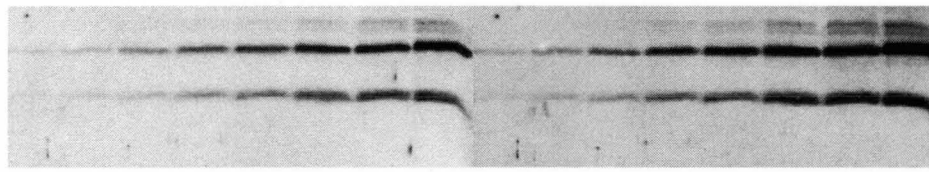

Figure 2.8 Westen blots run simultaneously for both flavodoxin (top bands) and ferredoxin (bottom bands). Autoradiographs taken for 1 minute (right) and 3 minutes (left). Standards are in the range from 5.6 ng to 200 ng for both proteins.

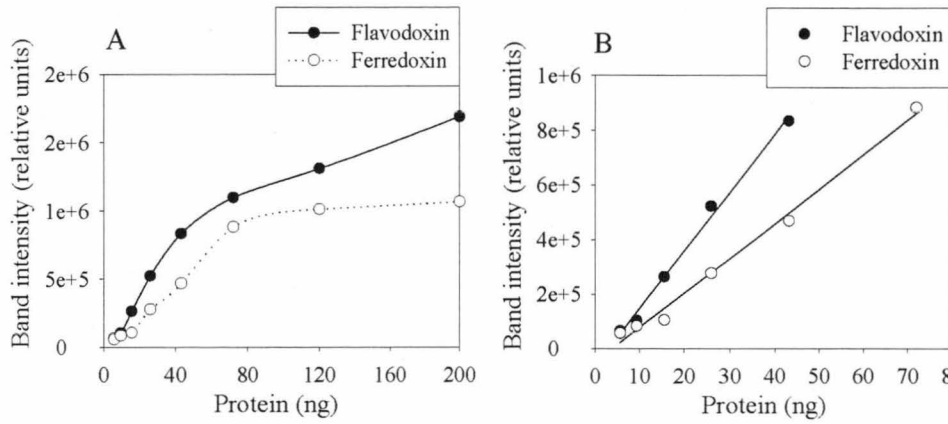

Figure 2.9 Results from densitometry conducted on gel from Figure 2.8 that was autoradiographed for one minute. A) Whole range for ferredoxin and flavodoxin; B) Linear range for flavodoxin and ferredoxin.

2.4 Discussion

Cylindrotheca closterium was grown into iron limitation in f/2 medium by reducing the added iron concentration to between 10-20 nM. The growth curves showed that the 20 nM grown culture grew at the same rate as the iron replete (11.7 μM Fe) culture suggesting that iron was not limiting growth at the start of the experiment but became limiting as it was taken up from the media by the diatom. The culture supplied with 10 nM iron grew at around 60% of the rate of the other two cultures suggesting that dissolved iron was sub optimal from the start of the experiment for cultures grown with this much iron. Chlorophyll per cell data showed that the culture grown at 10 nM iron were severely chlorotic with less than 1/10th of the chlorophyll per cell of the iron replete cultures. Similarly the 20 nM grown cultures had chlorophyll per cell levels of around 25% of the iron replete cultures. Chlorosis is a common response to iron limitation with declines in chlorophyll per cell of 50% being regularly observed for a range of diatoms grown under similar conditions (Davey & Geider, 2001; McKay *et al.*, 1997).

Low and high iron grown cultures of this organism were used as sources of the proteins flavodoxin and ferredoxin respectively. Purification schemes used for the two proteins were based on those reported previously (La Roche *et al.*, 1995; McKay *et al.*, 1999). However gradient elution was used in place of batch methods during ion exchange chromatography for both methods and the final step in the published ferredoxin purification scheme (native PAGE) was replaced by chromatography on hydroxyapatite. This latter step was necessary to remove small amounts of flavodoxin which co-purified with ferredoxin from the iron replete culture. Theses methods allowed ferredoxin and flavodoxin to be purified to homogeneity in high yields as evidenced by a single band on SDS PAGE and the characteristic absorption spectra obtained for both proteins. The ratio of absorbances of these proteins at 280 nm (peptide bond) and the visible maximum (438 nm for flavodoxin and 435nm for ferredoxin) have frequently been used as indicators of purity. The observed ratios for

flavodoxin (4.0) and ferredoxin (1.9) agree with published values of 5-6 for eukaryotic flavodoxins (Fitzgerald *et al.*, 1978; Peleato *et al.*, 1994) and (1.25-2) for eukaryotic ferredoxins (Bes *et al.*, 1999; Matsubara, 1968).

High affinity antibodies towards both flavodoxin and ferredoxin were produced in rabbits and these were used to develop western blots for both proteins. Flavodoxin was easily detected on SDS PAGE gels run with standard Laemmli buffer, however development of the ferredoxin western blot was problematic. Immunodecoration of ferredoxin was not observed during initial attempts to run the western blot with the standard protocol used successfully for flavodoxin. Therefore various trials were undertaken to determine why the assay was failing.

Poor transfer efficiency of proteins from the gel matrix to the membrane, and loss of antibody recognition upon denaturation of proteins prior to SDS PAGE are two common causes of failed western blots (Harlow & Lane, 1989). Therefore, western blots were run under a variety of conditions in order to determine the cause of the failed assay. A number of parameters were examined including running the assay under non-denaturing conditions and the use of alternate membranes to improve transfer efficiency (e.g. PVDF and 0.2 μm nitrocellulose, the former having a higher total protein binding capacity than nitrocellulose and the smaller pores in 0.2 μm compared to standard 0.45 μm nitrocellulose is reported to prevent "blow through" of low molecular weight proteins (Kurien & Scofield, 2003)) .

Ultimately, however, it was found that ferredoxin could be detected on nitrocellulose membranes if the concentration of SDS was decreased in both the gel and running buffer. The optimum SDS concentration was found to be 1/10th of the normal Laemmli buffer (Laemmli, 1970) concentration. This concentration resulted in sensitive detection of ferredoxin as well as tight banding for the flavodoxin protein. Along with reductions in SDS concentration stringent washing of the gels in transfer buffer containing 20% methanol was important for reproducible detection of

ferredoxin. The optimal wash protocol was found to be three washes of 10 minutes duration. Longer wash times resulted in substantial losses of ferredoxin from the gels, while fewer washes or shorter wash times did not effect removal of SDS, resulting in poor detection of ferredoxin. Inclusion of methanol in western blotting buffers is known to effect the removal of SDS with the result that proteins will bind more readily to the membrane (Biorad Mini Protein3 Instruction Manual). However, due to the low molecular weight of ferredoxin, extended washing of gels with buffer prior to transfer resulted in diffusion of the protein from the gel matrix. Hence sensitive reproducible detection of this protein could only be achieved by using short washes with several changes of wash buffer. This resulted in a favourable concentration gradient for SDS removal whilst minimising the time available for the protein to diffuse from the gel.

Western blots run on whole protein extracts from *Cylindrotheca closterium* detected both proteins with little cross reactivity towards other proteins in the homogenate. In low iron grown *C. closterium* flavodoxin was detected but not ferredoxin. However, western blotting performed on proteins from iron replete cells detected both ferredoxin and flavodoxin. No attempt was made at this stage to quantify the relative amounts of these proteins by densitometry, however comparison of flavodoxin band intensity of lanes loaded with the same total protein from iron replete and iron limited cells shows that flavodoxin is highly up-regulated in the latter. Moreover, the fact that flavodoxin, which co-eluted with ferredoxin off the DEAE column during ferredoxin purification, was a minor contaminant of ferredoxin (estimated a less than 10% from Coomassie stained band intensity) suggests that under iron replete conditions ferredoxin is the dominant protein expressed in *C. closterium*. La Roche *et al.* (1995) similarly observed constitutive expression of flavodoxin in this organism but noted that its expression was massively up-regulated under low iron conditions.

With an optimised blotting protocol and sufficient pure ferredoxin and flavodoxin to use as standards, the assay was trialled in a quantitative format. Similar lower limits of detection were achieved for both ferredoxin and flavodoxin. Furthermore, the linear ranges of both assays were similar. The two proteins could be successfully quantitated when applied to gels at between 5 to 50 ng in a volume of 25 µL (0.2 - 2 µg mL^{-1}). In comparison the HPLC technique established by Doucette *et al.* (1996) had a lower limit of detection of 1 µg mL^{-1} requiring 1 µg of sample to achieve this level of detection. The limit of detection of existing qualitative westen blot immunoassays for diatom ferredoxin (La Roche *et al.*, 1995) and flavodoxin (McKay *et al.*, 1999) have not been determined . However, a recently developed ELISA for ferredoxin and flavodoxin specific for the proteins from *Scenedesmus vacuolatus* achieves a linear range of 30-600 ng mL^{-1} (Inda & Peleato, 2003). Hence the western blot procedure described here is approximately an order of magnitude more sensitive than the HPLC technique but an order of magnitude less sensitive than the ELISA approach.

Chapter 3 : Ferredoxin and flavodoxin expression in iron replete polar diatoms

3.1 Introduction

In an attempt to provide a rapid and simple diagnostic test for iron limitation several research groups have investigated the possibility of using the proteins ferredoxin and flavodoxin as indicators of iron nutrition (Boyd *et al.*, 1999; Doucette *et al.*, 1996; Erdner *et al.*, 1999; La Roche *et al.*, 1996; La Roche *et al.*, 1995; McKay *et al.*, 1997; McKay *et al.*, 1999; McKay *et al.*, 2000).

Expression of flavodoxin in response to iron starvation has been observed in a number of marine algal taxa including diatoms (La Roche *et al.*, 1993; La Roche *et al.*, 1995) dinophytes and prymnesiophytes (Erdner *et al.*, 1999). Early attempts to use flavodoxin as a stand alone marker for iron limitation in natural samples showed great promise. Initial studies by La Roche *et al.* (1995) used a flavodoxin immunoassay to detect the protein in natural algal populations which had been driven into iron limitation by the addition of excess macronutrients. Flavodoxin abundance was also shown to vary inversely with dissolved iron concentration along a 900 km east-west transect from coastal waters to the open ocean in the north-eastern subarctic Pacific (La Roche *et al.*, 1996). This study also observed reductions in flavodoxin abundance when carboys containing phytoplankton from low iron waters were supplied with iron.

Other attempts to use flavodoxin or a combination of ferredoxin and flavodoxin to deduce iron nutritional status of phytoplankton communities have been inconclusive.

Using a HPLC method for ferredoxin and flavodoxin during IronExII, the second mesoscale iron enrichment experiment, Erdner & Anderson (1999) could not detect either of the two proteins before iron enrichment but detected flavodoxin but not ferredoxin after iron enrichment. Furthermore, pennate diatoms isolated from the bloom were found to completely suppress flavodoxin expression and induce ferredoxin in iron replete laboratory cultures

Similarly during SOIREE (Boyd *et al.*, 2000), the first mesoscale enrichment experiment conducted in the Southern Ocean, flavodoxin was detected both before and after iron enrichment despite other indicators of algal physiology suggesting that the community was no longer suffering from iron starvation. Ferredoxin was not probed for in this study. Timmermans *et al.* (1998) conducted iron enrichment bioassays in the Southern Ocean and observed increased levels of flavodoxin in enriched bottles as compared to control (iron limited) bottles. Only one study to date has observed complete suppression of flavodoxin expression upon iron enrichment with induction of ferredoxin expression (Boyd *et al.*, 1999).

Sustained flavodoxin expression in natural phytoplankton communities after addition of iron has generally been attributed to incomplete alleviation of iron stress. Indeed several studies on diatoms in laboratory culture suggest that flavodoxin expression is an early response to iron limitation. Diatoms experiencing falling iron availability replace ferredoxin by flavodoxin prior to decreases in growth rate or other changes in physiology (Davey & Geider, 2001; Erdner *et al.*, 1999; McKay *et al.*, 1997; McKay *et al.*, 1999).

However, a study conducted on *Rhizosolenia* mats in the central North Pacific gyre (McKay *et al.*, 2000) indicates that caution must be used in applying these markers. This study found that all mats sampled expressed flavodoxin but not ferredoxin. Furthermore, laboratory cultures of *R. formosa* expressed flavodoxin constitutively and ferredoxin expression was never observed. As immunoassays were used to

detect both proteins the lack of ferredoxin expression may have resulted from poor antibody recognition. This study does, however, demonstrate that flavodoxin cannot be used as a stand alone marker for iron limitation, particularly in communities in which the expression of this protein has not been thoroughly characterised. Constitutive expression of flavodoxin was also observed in cultures of *Cylindrotheca closterium* (La Roche *et al.*, 1995) and *Thalassiosira weissflogii* (Doucette *et al.*, 1996). In *T. weissflogii* flavodoxin expression was later found to be suppressed when the organism was grown in media containing very high levels of iron (Erdner *et al.*, 1999). However, Doucette *et al.* (1996) proposed that the ferredoxin index (flavodoxin abundance expressed as a fraction of the combined ferredoxin/ flavodoxin pool) could be used as a more reliable marker for iron stress in species which have a constitutive flavodoxin.

Hence to apply ferredoxin and flavodoxin as markers for iron nutritional status in Antarctic sea ice algae it is first necessary to determine the basal level of expression of these proteins in clones isolated from sea ice. There are relatively few algal species that thrive in Antarctic pack ice communities (Lizotte, 2001). Thorough characterisation of antibody cross reactivity and examination of key species from this environment for constitutive flavodoxin expression can therefore be achieved quite readily. One species that inhabits the pack ice, *Cylindrotheca closterium* has already been demonstrated to have constitutive expression of this protein.

The work outlined in the following chapter describes the isolation and growth of key Antarctic pack ice species as well as a few analogous species from the Arctic. Ferredoxin and flavodoxin expression are partly characterised in these species by looking at the extent to which constitutive flavodoxin expression occurs and by assessing the relative amounts of these two proteins in these organisms. As well as characterising expression of these proteins in polar diatoms the cross reactivity of the newly generated antibodies towards the species commonly found in sea ice will be established. Furthermore, measurements of ferredoxin and flavodoxin made on

these species will help to validate the quantitative immunoassay for use with these organisms.

3.2 Methods

3.2.1 Establishing clonal cultures of sea ice diatoms

Ice cores used to establish sea ice diatom cultures were collected from the Mertz Glacier region (66°S, 147°E) of the Southern Ocean during November 2001 during Voyage 1 of the RSV *Aurora Australis*. Soon after collection ice and associated biomass from the underside of several cores was scraped with scalpel into both filtered (GF/F) seawater and filtered seawater enriched with f/2 levels of nutrient (Guillard & Ryther, 1962) which had been pre-cooled to 2° C. Culture material was held on board the ship in 250 mL screw top polycarbonate jars at 2° C in a temperature controlled cabinet under 50 μmols m^{-2} sec^{-1} of light on a 20/4 light dark cycle.

Arctic cultures were isolated in a similar way from ice cores collected from the Barents Sea in April 2000.

Upon return to Australia individual diatom cells of various species were isolated from the mixed cultures by micro-pipette. All work was carried out in a cold-room at 4° C. Drops of the mixed culture were placed on a clean microscope slide on an inverted microscope. A cell of the desired species was drawn using mouth suction into a glass micro-pipette by way of fine bore silicon tubing. The cell was "washed" in a droplet of sterile f/2 media on another clean microscope slide, a process which was repeated three times. Between each wash the micropipette was sterilised by immersing in a beaker of boiling >18 MΩ Milli Q water Following washes each cell was transferred into a well of a sterile 24 well multi-well plate containing approximately 2 mL of sterile f/2 media and incubated in a temperature controlled cabinet at 2° C under 50 μmols m^{-2} sec^{-1} of light supplied by cool white fluorescent lights on a 20/4 light dark cycle.

Isolates were checked weekly for growth and purity. After 3-4 weeks wells that contained cells of only one species and which had grown to sufficient densities (i.e. those with observable pigmentation in the wells) were transferred into sterile 50 mL conical flasks containing 30 mL of sterile f/2 media and incubated under the conditions described above for initial isolation. The cultures were maintained by inoculating 1 mL of parent culture into 30 mL of fresh media every 3 weeks.

The identity of cultures were confirmed by Differential Interference Microscopy on both fresh cell material and frustules cleaned by oxidizing organic matter using a solution of hot 30% hydrogen peroxide (Sournia, 1978).

3.2.2 Species survey

A number of the isolated species were selected to test for cross reactivity of the ferredoxin and flavodoxin antibodies and to determine the basal level of expression of these proteins in cultures growing exponentially under nutrient replete conditions.

To initially assess the cross reactivity of antibodies single 50 mL cultures of each species were grown under conditions described above for culture maintenance. Antarctic species initially tested for cross-reactivity were *Entomoneis kjellmannii* (Cleve), *Navicula directa* (Wm. Smith), *Fragilariopsis curta* (Van Heurch), *Pseudonitzschia sp*, *Porosira glacialis* (Grunow), *Fragilariopsis cylindrus* (Grunow).

In the more detailed study growth rates of species were characterised and ferredoxin and flavodoxin levels were quantitated in cultures harvested in late exponential phase. Antarctic isolates used in the study were *F. cylindrus*, *F. curta*, *Fragilariopsis sublinearis* (Van Heurck), *Cylindrotheca closterium* (Ehrenberg), *E. kjellmanii*, *Nitzschia lecointei* (Van Heurck), *Polarella glacialis* (Montresor et al.). Two Arctic isolates were also examined *Nitzschia frigida* (Grunow) and *Fragilariopsis oceanica* (Cleve) Hasle.

Triplicate cultures of each species were grown in 250 mL fluorometer side arm flasks containing 125 mL of sterile f/2 media. Cultures were started by inoculating with 1 mL of parent culture and growth was measured by daily measurement of *in vivo* chlorophyll fluorescence. Cultures were harvested in mid exponential phase by concentrating the whole culture on a 2 μm (47 mm diameter) polycarbonate membrane (Osmonics) under less than 5 inHg vacuum then centrifuging the concentrate at 500 x g for 10 min at 2° C in an Eppendorf microcentrifuge. Cell pellets were then frozen at –80 ° C until further analysis.

3.2.3 Western blotting

Sample preparation and western blotting were performed as described in section 2.2.11. Protein content of lysates was determined by the bicinchoninic acid assay (Section 2.2.9). Blots for cross reactivity were loaded with 40 μg of protein whilst the protein load for quantitating proteins in the more detailed study was adjusted such that the intensity of the bands fell within the linear range of the standard curve. The loading was determined by running gels with several dilutions of protein lysate obtained from one of the replicate cultures for each species. Quantitation was performed by densitometry (Section 2.2.12) using Image Quant V5.2® Software (Amersham).

3.3 Results

A western blot run for both ferredoxin and flavodoxin on proteins from various Antarctic diatoms, as well as proteins from the temperate isolate of *Cylindrotheca closterium* from which antibodies were generated is shown in Figure 3.1. Significant heterogeneity of protein expression was observed despite all cultures being grown in iron replete f/2 medium. From the range of diatoms examined only one species, *Fragilariopsis cylindrus*, displayed the expected expression of ferredoxin only in iron replete media. Four of the isolates were observed to produce both ferredoxin and flavodoxin under iron replete condition. Ferredoxin was not detected in

Fragilariopsis curta and *Pseudonitzschia sp,* but distinct flavodoxin bands were observed in both of these organism. All species examined were observed to express either flavodoxin or ferredoxin or both of the proteins as determined by western immunoblotting.

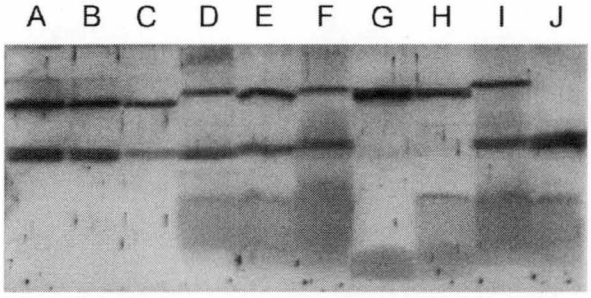

Figure 3.1 Western blot for ferredoxin and flavodoxin conducted on proteins extracted from various cultured diatoms. A-C=Dilutions of ferredoxin (bottom) and flavodoxin (top), D=*C. closterium*, E=*E. kjellmanii*, F=*N. directa*, G=*F. curta*, H=*Pseudonitzschia sp*, I=*Porosira glacialis*, J= *F.cylindrus*.

Cultures grown for the above blots were not monitored to ensure they were in exponential growth. A concern was that those species which were observed to express flavodoxin had reached a stationary, or nutrient limited stage of growth which induced flavodoxin expression.

Triplicate cultures of a range of species from Antarctic and Arctic origin were grown and their growth rates are shown in Table 3.1. All cultures were harvested in the mid exponential phase of growth.

Table 3.1. Growth rates (mean ± SD of three replicates) of Arctic and Antarctic microalgae used to study basal expression of ferredoxin and flavodoxin.

Species	Rate (d^{-1})
Fragilariopsis cylindrus	0.575±0 151
Fragilariopsis curta	0.398±0.019
Fragilariopsis sublinearis	0.176±0.006
Cylindrotheca closterium	0.353±0.376
Entomeneis kjellmannii	0.179±0.027
Nitzschia lecointei	0.320±0.040
Polarella glacialis	0.256±0.008
Fragilariopsis oceanica	0.283±0.030
Nitzschia frigida	0.381±0.016

For each culture ferredoxin and flavodoxin were quantified by western blot, with standards in the range of 5 to 50 ng. A representative set of blots obtained for these species is shown in Figure 3.2. Three of the four examined species from the genus *Fragilariopsis*, including two of Antarctic origin (*F. curta* and *F. sublinearis*) and one of Arctic origin (*F. oceanica*) produced flavodoxin only under iron replete exponential growth. The fourth species from this genus (*F. cylindrus)* produced only ferredoxin. *N. lecointei* and *N. frigida* were observed to express only ferredoxin, although the antibody reacted poorly with the protein from *N. frigida.* Both *E. kjellmannii* and *C. closterium* expressed both proteins under iron replete growth. No bands were immunodecorated in the lane loaded with proteins from the Antarctic flagellate *Polarella glacialis.*

Figure 3.2 Representative pair of gels used to quantify ferredoxin and flavodoxin in cultures of Antarctic and Arctic algae. A-E ferredoxin and flavodoxin standards, F *F. curta*, G *F. sublinearis*, H *N. lecointii*, I *Polarella glacialis*, J *F. oceanica*, K-O ferredoxin and flavodoxin standards, P *F. cylindrus*, Q *E. kjellmannii*, R *C. closterium*, S *N. frigida*.

Levels of ferredoxin and flavodoxin produced by each of these cultures are listed in Table 3.2. Results are expressed as nmoles of each protein per mg of algal protein and represent the means and standard deviations of triplicate cultures. The Antarctic strain of *C. closterium* was found to express the highest levels of flavodoxin as determined by western blotting with 60.5 nmoles per mg total soluble protein. This is over twice the amount of flavodoxin that any other species was observed to produce during this study. *N. frigida* produced the weakest signal for either of the proteins with only a very feint band detected for ferredoxin with 40 μg of soluble protein loaded on the gel. The intensity of this band was well below the lowest standard and therefore not quantifiable. For all other species 40 μg of protein was sufficient to produce a quantifiable band. There was a high degree of consistency in the amount of each protein expressed for all other species with a range of 25-34 nmole per mg protein for ferredoxin and 21 to 26 nmol per mg for flavodoxin. For the two species which expressed both flavodoxin and ferredoxin during iron replete exponential growth flavodoxin constituted 40% and 70 % of the combined ferredoxin + flavodoxin pool. Furthermore, ferredoxin was expressed at a similar concentration in these species as it was in the two species which expressed only ferredoxin.

Table 3.2 Ferredoxin and flavodoxin expression in Antarctic and Arctic diatoms grown under iron replete conditions and harvested during the exponential phase of growth. Protein levels are expressed as nmoles of ferredoxin and flavodoxin per mg of total soluble protein as measured in SDS extracts by the bicinochoninic acid method. Values are mean±SD (n=3). Flavodoxin index is the percentage of flavodoxin in the combined ferredoxin + flavodoxin pool. bq= below quantitation and nd=not detected

Species	Ferredoxin (nmoles mg^{-1})	Flavodoxin (nmoles mg^{-1})	Flavodoxin Index
Fragilariopsis cylindrus	34.0±6.5	nd	0
Nitzschia lecointei	33.8±1.5	nd	0
Nitzschia frigida	bq	nd	
Fragilariopsis oceanica	nd	26±.5	100
Fragilariopsis curta	nd	25.00±1	100
Fragilariopsis sublinearis	nd	24.5±4	100
Cylindrotheca closterium	25.00±7.0	60.5±7.8	70
Entomeneis kjellmannii	32.5±6.3	21.8±2.5	40
Polarella glacialis	nd	nd	

3.4 Discussion

Antibodies generated to ferredoxin and flavodoxin immunodecorated bands of appropriate molecular mass in all of the eleven polar diatom species examined. Of these only proteins from one species, *Nitzschia frigida* cross reacted poorly with the ferredoxin antibodies. Ferredoxin antibodies also failed to immunodecorate protein bands in the Antarctic flagellate *Polarella glacialis*. Flavodoxin expression was not observed in iron replete cultures of these two species. Bands detected for all proteins had similar relative mobility to the pure protein standards from *C. closterium*. Furthermore, ferredoxin stained as a single band in all species examined. This is in contrast to multiple ferredoxin bands observed when proteins from uni-algal cultures were blotted with antibodies generated towards ferredoxin from *T. weissflogii* (McKay *et al.*, 1999). The good cross reactivity observed for both proteins within the bacillariophyceace is similar to the reaction observed with antibodies for

Phaeodactylum tricornutum flavodoxin (La Roche *et al.*, 1995) and *Thalassiosira weissflogii* ferredoxin (McKay *et al.*, 1999) highlighting the conserved nature of these proteins at this taxonomic level.

Although induction of flavodoxin due to iron limited growth was not examined in this study, constitutive expression of this protein was observed in 7 of the 11 diatoms tested. Under iron replete growth four of these organisms produced flavodoxin exclusively (i.e. were not observed to produce ferredoxin)

These results differ from those previously observed , with constitutive flavodoxin appearing to be the norm rather than the exception. However, these differences can be largely explained if all organisms examined by all studies to date are classified as either neritic or oceanic. Prior to this study thirteen species of marine diatom had been examined for flavodoxin expression (Davey & Geider, 2001; Doucette *et al.*, 1996; Erdner & Anderson, 1999; Erdner *et al.*, 1999; La Roche *et al.*, 1995, McKay *et al.*, 2000). Eleven of these produced flavodoxin when grown under iron limited conditions and suppressed its expression completely when grown in an environment with sufficient iron. Of those organisms with an inducible flavodoxin, only one species was of oceanic origin (Erdner & Anderson, 1999). The remaining two of these thirteen species expressed flavodoxin constitutively, with the cosmopolitan species *Cylindrotheca closterium* producing both flavodoxin (La Roche *et al.*, 1995) and ferredoxin (McKay *et al.*, 1999) under iron replete growth (as was observed in this study) whilst the oceanic *Rhizosolenia sp* examined by McKay *et al.* (2000) was never observed to produce ferredoxin.

Contrary to the previous work conducted on diatom ferredoxin and flavodoxin the majority of the organisms used in this study inhabit a truly oceanic environment. They include species which are representative of Antarctic pack ice assemblages including *F. cylindrus* and *F. curta,* which often dominate in this environment (Lizotte, 2001), and an analogous species from the Arctic (*F. oceanica*). Of the

species examined in this study only three solely expressed ferredoxin under iron replete conditions. The combined data from this and other studies suggest that constitutive flavodoxin expression is a common adaptation of oceanic diatoms to life in a chronically low iron environment.

Iron concentrations in coastal waters are often several orders of magnitude higher than the extremely low levels found in oceanic regions distant from the influence of continents (Hutchins *et al.*, 1998; Wells *et al.*, 1995). The iron requirements for growth of marine algae of coastal and oceanic origin reflect these differences in iron availability (Brand, 1991; Brand *et al.*, 1983; Sunda *et al.*, 1991). The kinetics of iron uptake of coastal and oceanic species do not differ greatly (Sunda & Huntsman, 1995) as coastal species appear to take up iron at rates which approach the maximum predicted by diffusion and ligand exchange kinetics (Hudson & Morel, 1990). To survive in a low iron environment oceanic phytoplankton have either had to reduce their iron quota or become smaller (Sunda & Huntsman, 1997). Recently significant differences in photosynthetic architecture between a coastal and oceanic diatom have been identified (Strzepek & Harrison, 2004). Particularly evident was a reduction in the number of PS1 units and cytochrome b_6f complexes in oceanic species. Both of these components contain significant quantities of iron and a reduction in these components presumably results in a lower cellular iron quota (Strzepek & Harrison, 2004). Constitutive flavodoxin expression by oceanic diatoms can also be viewed as a mechanism to reduce the cellular iron quota. Among the various *Fragilariopsis* species examined, constitutive flavodoxin expression was seen in the three larger species, whilst the much smaller *F. cylindrus* expressed solely ferredoxin under iron replete conditions. Although based on only a limited number of species, the results suggest that *F.cylindrus* has reduced its iron quota by becoming smaller whilst the other species have reduced their cellular quota in part by permanently replacing an iron containing catalyst for a functionally equivalent protein which does not contain iron. Among these larger *Fragilariopsis* species expression of flavodoxin and the

absence of ferredoxin was observed in both Antarctic and Arctic species. Whether these "flavodoxin only" organisms are derived from a different lineage than *F. cylindrus* awaits confirmation by phylogenetic analysis.

Constitutive expression of flavodoxin in oceanic diatoms provides an alternative explanation for the observed increases in flavodoxin in iron enriched bottles during iron enrichment mesocosm experiments (Timmermans *et al.*, 1998) where large diatoms such as *Fragilariopsis kerguelensis* were observed to bloom in the iron enriched bottles. Similarly, during the IronExII (Erdner & Anderson, 1999) and the SOIREE (Boyd *et al.*, 2000) mesoscale fertilization experiments flavodoxin levels were observed to increase and in the former case increases tracked the increase in biomass. In both of these experiments the increases in flavodoxin levels occurred despite other indicators of iron stress (such as Fv/Fm) suggesting that the iron infusions had relieved the communities from iron stress.

Quantitation of protein bands for replicate cultures of each species against a standard curve generated with pure ferredoxin and flavodoxin proteins showed that the proteins could be measured by his method with a reasonable degree of precision. The amount (moles) of ferredoxin plus flavodoxin per unit weight of cellular protein was remarkably consistent for most species studied. However, the fact that highest flavodoxin levels were measured in the species to which antibodies were generated suggests that flavodoxin levels are somewhat underestimated in species other than this one. Polyclonal antibodies contain a range of antibody molecules that recognise different epitopes. It would be expected generally that proteins from the species to which the antibodies were produced would bind a greater number of epitopes and with higher affinity than similar proteins from other organisms, resulting in the strongest signal per unit protein for this species. Similarly, the faint banding observed for ferredoxin in total proteins from *N. frigida* is probably a reflection of poor cross reactivity rather than a low abundance of protein in this species. Despite the method having varying accuracy for different species the reasonable level of

precision achieved between gels means that quantitation against pure proteins standards will allow for comparison of many more samples of a single species than is currently possible with semi-quantitative western blots (La Roche *et al.*, 1995; McKay *et al.*, 1999).

The results suggest that the use of flavodoxin expression alone as an indicator of iron limitation in polar diatoms is questionable. Furthermore, indices such as the ferredoxin index (Erdner *et al.*, 1999) do not improve the reliability of using these proteins as iron stress indicators in these organisms. This index, which expresses flavodoxin abundance as a percentage of the total ferredoxin and flavodoxin pool was proposed as a means to correct for species which produce a small amount of constitutive flavodoxin, such as *T. weissflogii* (Doucette *et al.*, 1996). In this species the index is below 15% under iron replete condition rising to 100% under chronic low iron stress. Clearly with many polar species producing flavodoxin only (index of 100%), the index is as invalid as flavodoxin expression alone being used as an indicator of iron stress

Although uncertainty exists as to the exact levels of these proteins in the species measured, the fact that protein levels determined by this method generally varied by less than two fold in a range of species points to the calculated indices being close approximations to those measured by HPLC

The only other measurements of ferredoxin and flavodoxin in marine diatoms are those published for *T. weissflogii* (Doucette *et al.*, 1996). In this organism based on an HPLC method, flavodoxin was present at around 0.2 nmoles (mg soluble protein) $^{-1}$ in iron replete cells and 7 nmoles (mg soluble protein)$^{-1}$ in iron limited cells. Ferredoxin was measured at around 2.1 nmoles (mg soluble protein)$^{-1}$ in iron replete grown cells only. These values compare with those from this study where ferredoxin levels were between 25- 35 nmoles (mg soluble protein)$^{-1}$ for a range of species and flavodoxin levels were generally between 22-26 nmoles mg^{-1} soluble

protein, except for *C. closterium* where the levels were two fold higher for this protein. Some of the observed differences may be truly species differences. Use of standard proteins from *Chlorella* and Spinach for the HPLC method as well as incomplete extraction of the proteins by the HPLC method (Erdner *et al.*, 1999) and differences in the measurement and definition of "soluble protein" would have also contributed to the observed differences. Extraction of proteins in SDS buffer is commonly known to solubilise the majority of cellular proteins.

Use of protein standards from *C. closterium* would have led to accurate determination of ferredoxin and flavodoxin in this species. The fact that the measured values in other species are in agreement with the concentrations measured for *C. closterium* suggests that the determinations are reasonably accurate.

Chapter 4 : Iron responsive regulation of ferredoxin and flavodoxin in Antarctic sea ice diatoms

4.1 Introduction

The role of iron in regulating phytoplankton growth rates and influencing community composition in much of the Southern Ocean is well established (Boyd, 2002a). But despite the numerous studies directed towards elucidating the role of iron in the Southern Ocean there is very little information available on the response of individual Southern Ocean algal species to iron limitation Timmermans *et al.* (2001a; 2001b) studied the effects of iron on two Antarctic diatoms *Chaetoceros brevis* and *Chaetoceros dichaeta* grown in both natural seawater amended with iron (without excess chelator) as well as in EDTA buffered seawater. These investigators found clear differences in the iron requirements of these two species. The smaller species *C. brevis* was able to achieve rapid rates of growth at low iron concentrations and with low light. In contrast the results for *C. dichaeta* suggested that for this species to bloom it required relatively high iron concentrations, high light intensities and a long photoperiod. Timmermans *et al.* (2004) studied growth rates of large Southern Ocean diatoms to determine growth kinetics and macronutrient consumption of these organisms in relation to iron availability. Van Oijen *et al.* (2004a) also examined *C. brevis* under low iron conditions and high and low light. Among their findings were that iron limitation led to reduced pigment content, decreases in light absorption and a decrease in quantum yield. They also observed large decreases in storage carbohydrates and increased susceptibility to photoinhibition.

Similar studies on Antarctic sea ice diatoms are lacking. Although it is doubtful that any algal species can be designated exclusively a "sea ice species", *Fragilariopsis curta* (Grunow) , *Fragilariopsis cylindrus* (Van Heurck) and *Phaeocystis antarctica* (Karsten) have been identified as three organisms that dominate pack ice assemblages (Lizotte, 2001).

An estimated 80% of iron within the cells of eukaryotic marine algae is bound within prosthetic groups of chloroplast electron transport proteins (Raven, 1990). When the rate of iron uptake from the environment is insufficient to meet demand for cell division, phytoplankton cells reduce their cellular quota for iron in an attempt to maintain growth at maximum rates (Sunda & Huntsman, 1995; Sunda & Huntsman, 1997). Mechanisms thought to be responsible for the lowering of iron quotas under iron stress include a general decrease in the number of photosynthetic units (Sunda & Huntsman, 1997), decreased synthesis of specific iron containing proteins (Greene *et al.*, 1992) and substitution of iron containing proteins for functionally equivalent proteins without iron, such as the replacement of ferredoxin for flavodoxin (La Roche *et al.*, 1993; La Roche *et al.*, 1995).

Considerable differences in iron use efficiencies have been observed between different species. One of the most startling observations is the much lower (up to eight fold) iron requirements of oceanic species compared to coastal species (Brand, 1991; Sunda & Huntsman, 1995). Surface area normalised uptake rates of coastal and oceanic species are similar (Sunda & Huntsman, 1995) Iron transport rates in all marine algae is constrained by limits imposed by diffusion and ligand exchange kinetics and the number of transport molecules that can fit in a unit area of cell membrane (Morel *et al.*, 1991). Because oceanic species have not been able to develop more efficient uptake systems, evolutionary pressure has forced oceanic species to either become smaller or reduce their cellular requirements for iron (Sunda & Huntsman, 1995). The rearrangement of photosynthetic architecture through the reduction of the ratio of Photosystem 1 to Photosystem 2 has been identified as one

mechanism employed by oceanic species to reduce their demand for iron (Strzepek & Harrison, 2004). Other strategies utilised by oceanic microalgae to reduce their iron quota remain unknown but are to likely to involve the replacement of iron containing catalysts with functionally equivalent proteins that do not contain iron, and minimisation or avoidance of biochemical pathways that require iron (Sunda & Huntsman, 1995).

Because of their frequent occurrence in pack ice it can be assumed that species that thrive in this environment are well adapted to the conditions that exist in this habitat. The Antarctic pack ice pack is characterised by strong gradients of temperature, light, salinity, and nutrient supply (Arrigo, 2003; Brierley & Thomas, 2002; Thomas & Papadimitriou, 2003). These conditions may have placed significant evolutionary pressure on these organisms to develop efficient metabolism in regard to iron.

Here I describe experiments undertaken to examine the effects of iron limitation on *Fragilariopsis cylindrus* and *Fragilariopsis curta*, two diatoms that dominate Antarctic pack ice. Half saturation constants for growth in relation to iron availability are determined for these organisms. Physiological and biochemical responses to iron limitation are also examined. Particularly, relationships between ferredoxin and flavodoxin expression, iron availability and other biochemical/physiological responses to reduced iron supply are determined. This is done in order to assess the usefulness of ferredoxin and flavodoxin as markers for iron availability in these organisms.

4.2 Methods

Fragilariopsis cylindrus and *Fragilariopsis curta* and were grown in 250 mL (for acclimation) or 500 mL (final experiments) polycarbonate jars with polypropylene lids (Technoplas). Culture-ware and any material that came in contact with growth medium was soaked in 0.01% Triton X100 in >18.2 MΩ resistivity Milli Q water for 24 hours then rinsed with 5 rinses of Milli Q water It was then soaked overnight in

1 N HCl (Mallinkrodt AR select) followed by another 5 rinses with Milli Q water. All rinsing and subsequent handling of plastic ware was done in a trace metal clean laminar flow hood. For sterilisation, bottles or jars were filled with Milli Q water, lightly capped, placed in polyethylene zip lock bags and heated in a domestic 700 W microwave oven to boiling, then for a further ten minutes.

Media for culturing was prepared from natural seawater collected from the Mertz glacier region (66°S, 147°E) of the Southern Ocean in November 2001 during Voyage 1 of the RV *Aurora Australis*. Water was pumped from beneath an ice flow through a hole cut with a SIPRE ice corer. The pumping system consisted of polyethylene tubing connected to a peristaltic pump with a short length of silicone tubing. A 0.45 μm polycarbonate (Osmonics) membrane housed in a polypropylene inline filter housing was used to filter the water before being collected in a polycarbonate carboy. All components of the pumping system were cleaned as described for the culture-ware. Prior to collecting water the pumping system and carboys were flushed with 5 L of seawater. Seawater was stored in the dark at 4° C for approximately a year before being used in the experiment. Measurement of dissolved iron in the seawater by flow injection analysis showed that levels were sub nanomolar (A. Bowie personal communication) and therefore insignificant compared to the levels added when preparing the trace metal buffered media.

Seawater from the 20 L carboys was sterilised by passing through 0.2 μm acid cleaned capsule filter (Sartorius Sartobran 300) with the aid of a peristaltic pump. From the filter it was dispensed into trace metal clean and sterile 1 L polycarbonate bottles. Media composition was based on that of Aquil (Price *et al.*, 1989). To each bottle was added nitrate (300 μM) phosphate (10 μM) and silicate (100 μM) from stocks which had been passed through a Chelex column to remove contaminating trace metals (Morel *et al.*, 1979). A combined vitamin stock was then added. A trace metal mixture (without iron) was combined with EDTA (100 μM final concentration) before being added to the media. Final trace metal concentrations were Cu 19 6 nM,

Mn 121 nM, Zn 80 nM, Co nM, Mo 100 nM and Se 10 nM. For experiments with *Fragilariopsis curta* the final concentration of Zn was increased to 500 nM as initial experiments showed that this species had a high requirement for this element. The iron concentrations of each 1 L bottle of media was adjusted with an iron EDTA stock (1:1.1) which had been freshly prepared from 0.1 M $FeCl_3$ (in 0.01 M HCl) and 0.1 M EDTA stock. Total dissolved iron concentrations were 500 nM, 300 nM, 100 nM, 50 nM, 25 nM, 12.5 nM 6.25 nM. Metal speciation in the media at the start of the experiment was calculated by the method described in Appendix A, based on the method of (Gerringa *et al.*, 2000).

All cultures were grown at 1° C under 70 µmol photons m^{-2} sec^{-1} light supplied by cool white fluorescent lights (Philips). Prior to the start of the experiment each species was acclimated to each concentration of iron. This involved maintaining cultures in exponential growth at each level of iron for at least three transfers (4-9 weeks depending on iron concentration and species) at which point growth rates and Fv/Fm were stable.

The acclimated cultures were inoculated in triplicate into 500 mL jars containing 300 mL of media. The amount of inoculum used was that required to achieve a dark adapted fluorescence value (Fo) of 100 at PM gain setting 14 to 16 on a water PAM fluorometer (Walz, Effeltrich, Germany) zeroed with a filtered seawater blank. This level of fluorescence was determined to be the lowest that could be reliably measured by the instrument and corresponded to around 10000-20000 cells per ml for *F. cylindrus* and 4000 to 8000 cells per ml for *F. curta*. The twofold range in cell concentration for each species resulted from higher fluorescence per cell for the iron stressed treatments. Samples (3 mL) were withdrawn from each flask at regular intervals using trace metal clean and sterile techniques and Rapid Light Curves (RLC) were run under software control (WinControl, Walz, Effeltrich, Germany) after 10 seconds of quasi dark adaptation (Ralph & Gademann, 2004). These were used to calculate $rETR_{max}$ (maximum electron transfer rate), α (photosynthetic

efficiency) and E_k (light adaptation parameter). The same sample was then dark adapted for 30 minutes before assessing the quantum yield of fluorescence (Fv/Fm). Dark adapted Fo values were used to calculate growth rates of each treatment by linear regression of ln F vs time.

A weak measuring light (0 15 µmol photons m^{-2} s^{-1}) was used to measure the fluorescence yield, while a saturating pulse (> 3000 µmol photons m^{-2} s^{-1} for 0.8 s) was used to determine the maximum steady-state fluorescence. Chlorophyll fluorescence was detected at wavelengths above 710 nm. Blue light emitting diodes (LED) provided actinic light used in the rapid light curves at levels of 0, 37, 85, 125, 194, 289, 413, 577. Relative electron transport rate was derived according to the equation

rETR = Fv/Fm * PAR (Schreiber, 2004)

RLCs, are described using several characteristic parameters such as E_k, α and $rETR_{max}$ (McMinn et al., 2003). To determine these parameters, the RLC were fitted to an exponential curve following Platt *et al.* (1980). This process described the photosynthetic response as a single continuous function of light, covering both the initial linear response, as well as the photoinhibited region at elevated light. Data was exported from WinControl (Walz, Effeltrich, Germany) into SPSS (v12.0.1) Empirical data was mathematically fitted to a double exponential decay function (Platt *et al.*, 1980), using a Marquardt-Levenberg regression algorithm.

$$P = P_m(1-e^{-(\alpha E_d/P_s)})e^{-(\beta E_d/P_s)}$$

In the absence of photoinhibition (β=0), the function becomes a standard rectangular hyperbola, with an asymptotic maximum rETR value and can be simplified to:

$$P = P_m(1-e^{-(\alpha E_d/Ps)})$$

Where P_s is a scaling factor defined as the maximum potential rETR in the absence of photoinhibitory processes, P_m is the photosynthetic capacity at saturating light, α is the initial slope of the RLC before the onset of saturation, E_d is the downwelling irradiance (400-700 nm), and α characterizes the slope of the RLC beyond the onset of photoinhibition (Heneley, 1993). E_k is the photoadaptive index or minimum saturating irradiance and is calculated as;

$$E_k = rETR_{max}/\alpha$$

The proportions of energy dissipated as heat (non photochemical quenching) was calculated according to the following equation (Schreiber, 2004).

Non photochemical quenching (NPQ) = (Fm – Fm') / Fm'

Where Fm is the maximum fluorescence in the dark, Fm' is the maximum fluorescence in the light, F_0 is the minimum fluorescence in the dark.

When cultures had grown to a fluorescence value between 3000 to 4000 relative units with the instrument set on the PM gain chosen at the beginning of the experiment, aliquots were taken for cell counts, and duplicate chlorophyll determination. The remainder of the culture was concentrated on a 2 µm (*F. cylindrus*) or 5 µm (*F. curta*) polycarbonate membrane (Osmonics) under vacuum less than 5 inHg then washed from the membrane into a micro-centrifuge tube. Cell material was pelleted by centrifugation at 1000 x g and the pellets frozen at –80° C until analysis of the proteins by western blotting (Chapter 3).

4.3 Results

4.3.1 Growth

There was a clear effect of iron on growth rate for both *F. cylindrus* and *F. curta* (Figure 4.1). The growth rate data was fitted to a Monod growth function where:

$$\mu = \frac{\mu \max \times [Fe']}{Km + [Fe']}$$

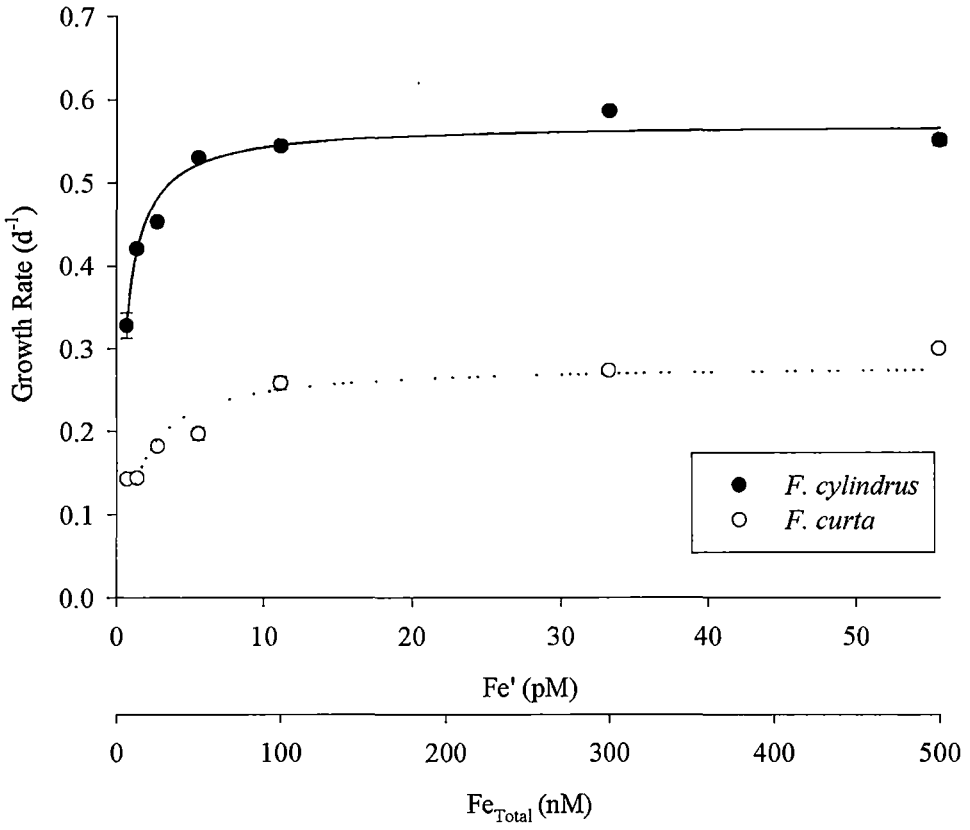

Figure 4.1 Growth rates of *F. cylindrus* and *F. curta* in relation to inorganic (Fe') and total (Fe_{total}) iron concentrations. Error bars indicate SE (n=3) and when not observed are smaller than symbols. Solid lines represent modelled Monod growth curve.

Maximum growth rates (μ_{max}) were 0.57 d^{-1} for *F. cylindrus* and 0.28 d^{-1} for *F. curta* whilst K_m for growth was 0.51 x 10^{-12} M and 1.3 x 10^{-12} M for *F. cylindrus* and *F. curta* respectively where the concentrations represent the sum of all inorganic iron

species ([Fe']= $[Fe^{+3}]$ + $[Fe(OH)^{+2}]$ + $[Fe(OH)_2^{+}]$). At its lowest growth rate of 0.34 d^{-1} in media containing 0.69 pM Fe' (6.25 nM Fe_{total}), *F. cylindrus* was growing at 60% of its calculated μ_{max}. Under similar conditions *F. curta* grew at a rate of 0.14 d^{-1} which was 50% of its maximum rate.

For *F. cylindrus* mean growth rates at the four highest concentrations of iron ranged from 0.530 to 0.586 d^{-1} and therefore represent growth at close to maximum rates. For this species the level of iron required to achieve a decrease in growth of 10% (a reduction seen as biologically significant and representative of the onset of iron limited growth) was 2.78 pM Fe' (25 nM Fe_{total}).

For *F. curta* cultures grown with 55.5pM, 33.3pM and 11.1 pM Fe' (500, 300 and 100 nM Fe_{total}) grew at rates which were within 10% μ_{max}. For this species, growth rate decreased below 90% μ_{max} when supplied with 5.55 pM Fe' (50 nM Fe_{total}) or less.

4.3.2 PAM fluorometry

For both *F. cylindrus* and *F. curta* Fv/Fm was highest for the cultures grown with the highest concentration of iron and lowest for the cultures grown with the least iron. The relationship between Fv/Fm and iron was similar to that observed for growth rate (Figure 4.2) For both species cultures grown with the three highest concentrations of iron had Fv/Fm values close to maximum. More distinct reductions in Fv/Fm occurred for organisms growing at Fe' concentrations below 5.55 pM (50 nM Fe_{total}).

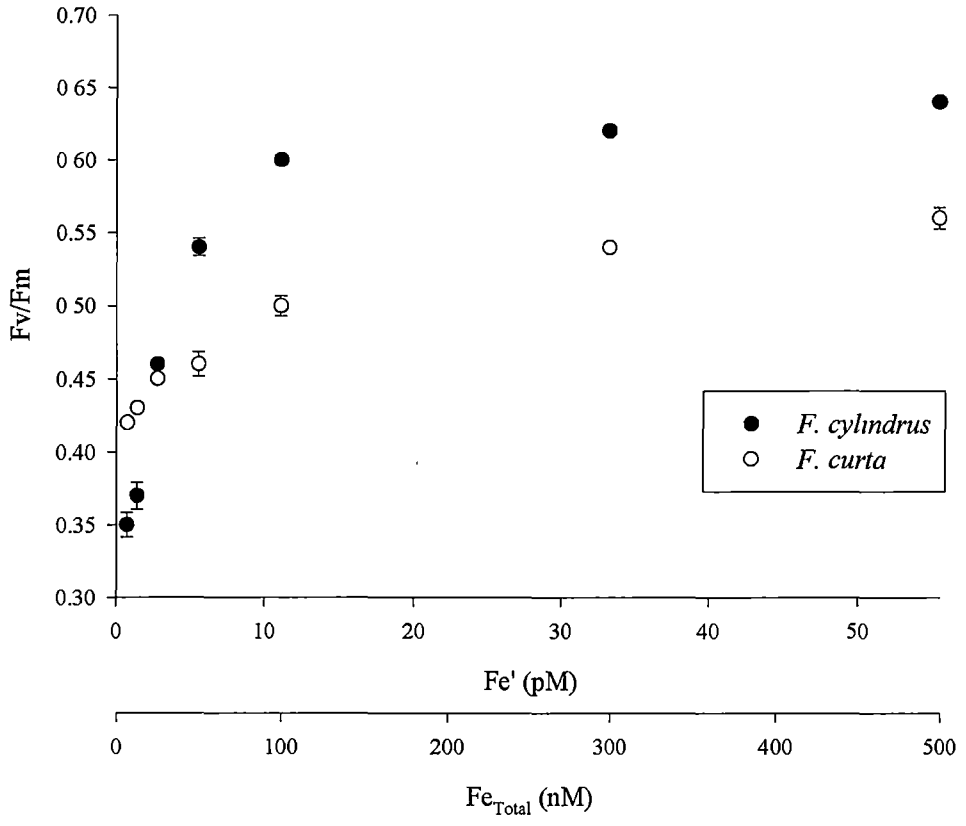

Figure 4.2 Fv/Fm as a function of inorganic iron (Fe') and total iron (Fe_{total}) for *F. cylindrus* and *F. curta*. Error bars indicate SE (n=3) and when not observed are smaller than symbols.

For *F. cylindrus* the maximum observed Fv/Fm was 0.64 and the most iron limited cultures of this species had an Fv/Fm of 0.34. This level of reduction is indicative of moderate to severe nutrient stress.

Maximum observed Fv/Fm for *F. curta* was somewhat lower (0.56), but still within the range expected for nutrient sufficient phytoplankton. In this species Fv/Fm was less responsive to iron stress than growth rate. For cultures grown at the lowest concentration of iron 0.69 pM Fe' (6.25 nM Fe_{total}) Fv/Fm was reduced by 25% of that observed for the 500 nM grown culture whilst growth rate was suppressed by 50%.

Representative rapid light curves (RLC) for *F cylindrus* and *F. curta* grown at each concentration of iron are shown in Figure 4.3 and Figure 4.4. The corresponding cardinal points, $rETR_{max}$, α and E_k derived from curves taken of triplicate cultures of each species at each treatment level are presented in Table 4.1.

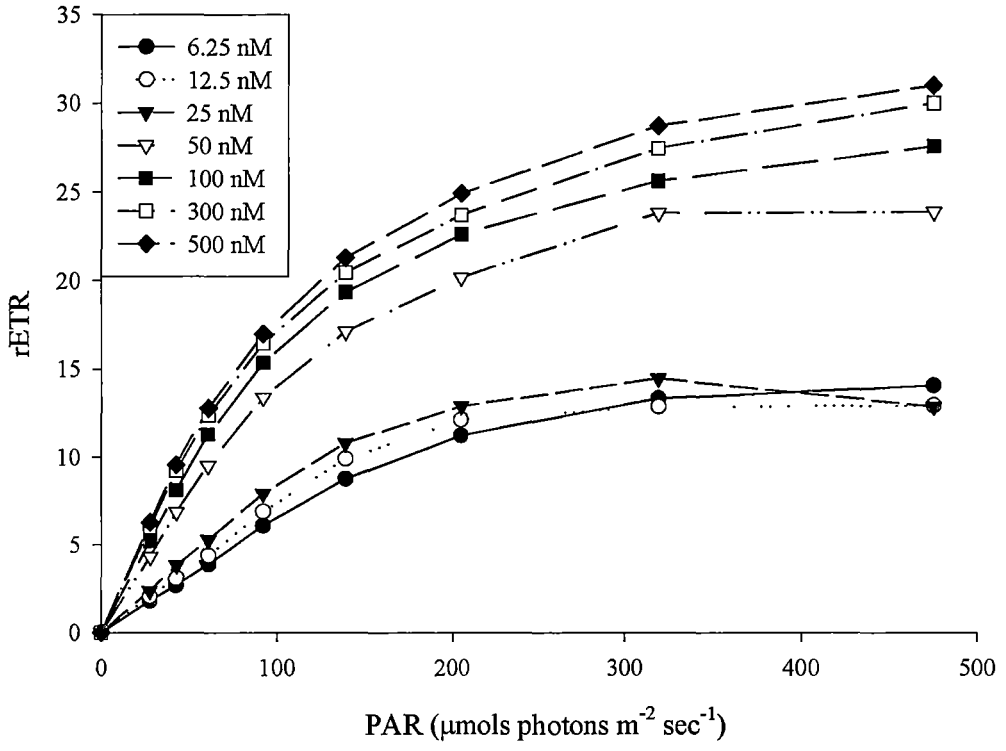

Figure 4.3 Representative Rapid Light Curves for *F. cylindrus* grown at seven concentrations of iron.

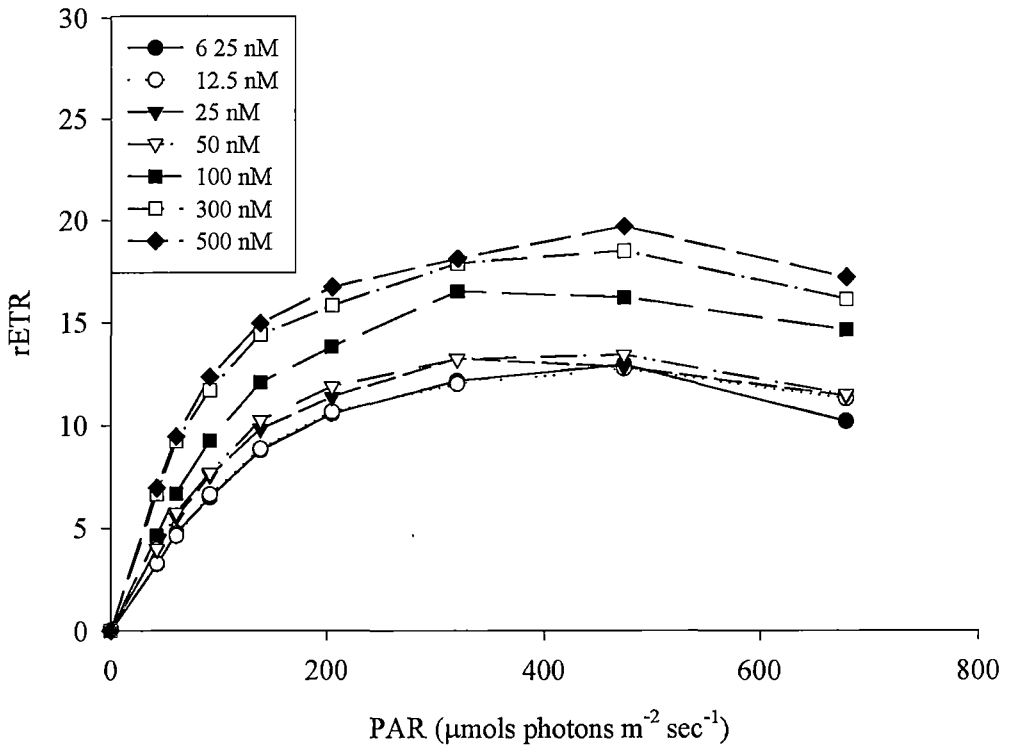

Figure 4.4 Representative Rapid Light Curves for *F. curta* grown at seven concentrations of iron.

Table 4.1 Rapid light curve parameters for *F. cylindrus* and *F. curta* grown at seven concentrations of iron. Values represent mean ±SE (n=3).

Iron (nM)	$rETR_{max}$		α		E_k	
	F. cylindrus	*F. curta*	*F. cylindrus*	*F. curta*	*F. cylindrus*	*F .curta*
6.25	37.6±2.1	32 1±1 0	0 212±0 017	0.236±0 014	181±22	139±12
12.5	33.3±1.9	31.7±0.2	0.252±0.010	0.240±0.010	133±2	133±6
25	39 5±6.4	32 4±0 0	0.283±0 021	0.288±0.014	145±35	112±6
50	60 0±3 1	33.3±1.7	0.479±0 021	0.298±0 010	126±12	112±9
100	66 4±1 9	40 7±1.2	0.552±0 005	0 343±0.014	120±4	119±5
300	71.2±1.4	44 0±2 1	0 590±0.010	0 481±0.029	120±1	93±10
500	74.0±3 1	45 7±0 0	0.619±0 005	0.495±0.017	120±6	93±3

For both species there was a clear reduction in both $rETR_{max}$ and α with decreasing iron availability. For *F. cylindrus* grown with the lowest concentration of iron $rETR_{max}$ was half of the iron replete value while α was reduced by 65%. For *F. curta* the reductions in these parameters were slightly lower (30% for $rETR_{max}$ and 50% for α). Changes in E_k were not as well defined as the other two parameters but did show the general trend of higher values at the lowest iron concentrations. This trend is more evident from plots of relative $rETR_{max}$ vs relative α for each species (Figure 4.5). For both species the linear trend had a slope greater than unity. This demonstrates that for both species declines in α were greater than reductions in $rETR_{max}$ resulting in E_k shifting to higher values for the low iron cultures. This effect was more pronounced for *F. curta* (slope 1.28) than *F. cylindrus* (slope 1.13).

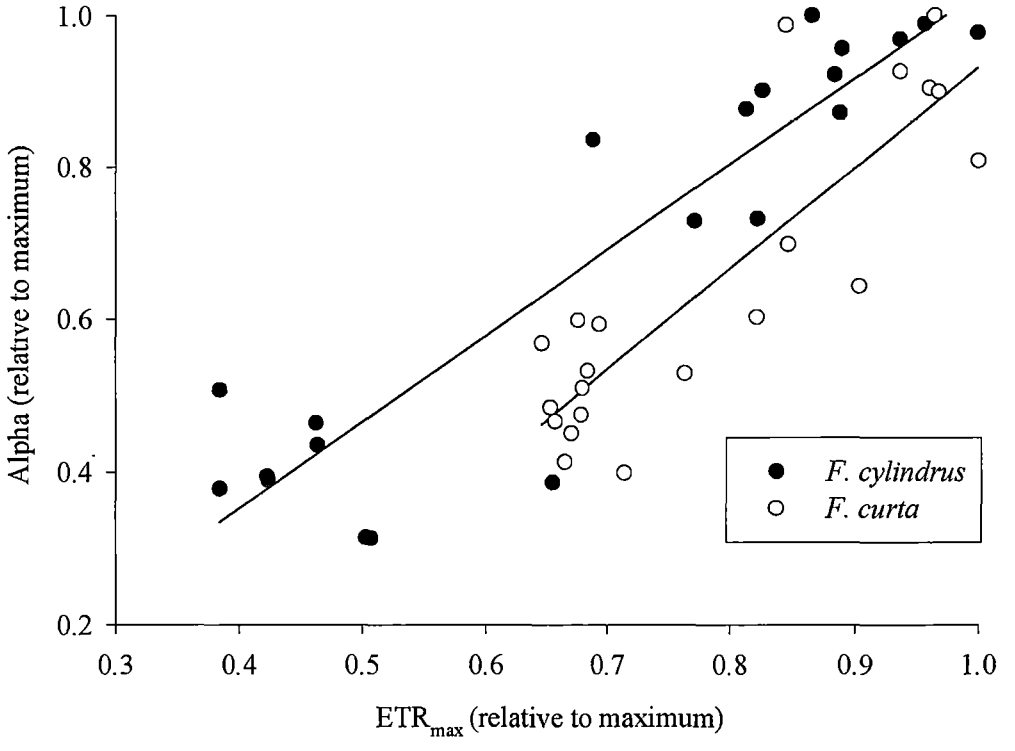

Figure 4.5 Plot of relative ETRmax versus relative α for cultures of *F. cylindrus* and *F .curta* grown at seven concentrations of iron.

The ability of cultures to develop non photochemical quenching (NPQ) as light levels increased during rapid light curves are shown in Figure 4.6 for *F. cylindrus* and Figure 4.7 for *F. curta*. Iron replete *F. cylindrus* showed the ability to develop a moderate level of NPQ. For these cultures the NPQ coefficient approached 0.4 for the highest light level experienced during the rapid light curves. There was a clear effect of iron on the ability to develop NPQ by this organism. Iron stress led to a decreased ability to dissipate excess light energy by nonphotochemical mechanisms. *Fragilariopsis cylindrus* grown with the lowest concentration of iron developed approximately 35% of the NPQ of iron sufficient cells at the highest light level. *Fragilariopsis curta* developed less NPQ than *F. cylindrus* despite higher light levels (final irradiance of light curve was 678 for *F. curta* compared to 475 for *F. cylindrus*) and the ability to develop NPQ did not vary with the level of iron.

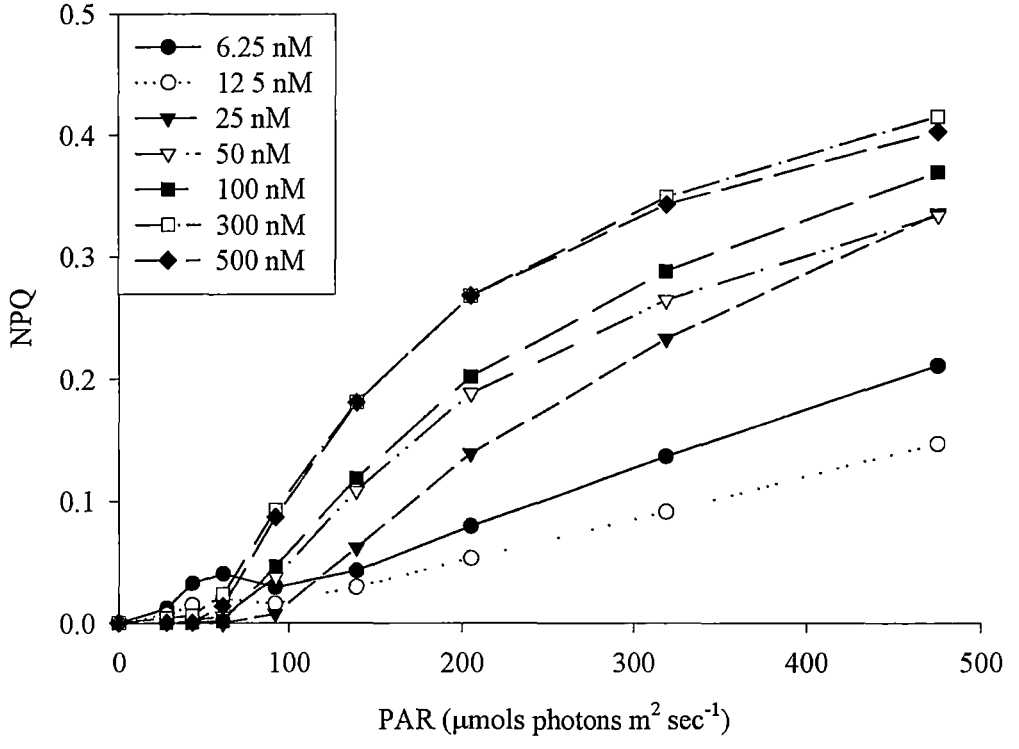

Figure 4.6 Non Photochemical Quenching (NPQ) developed during rapid light curves by *F. cylindrus* cultures grown at seven concentrations of iron

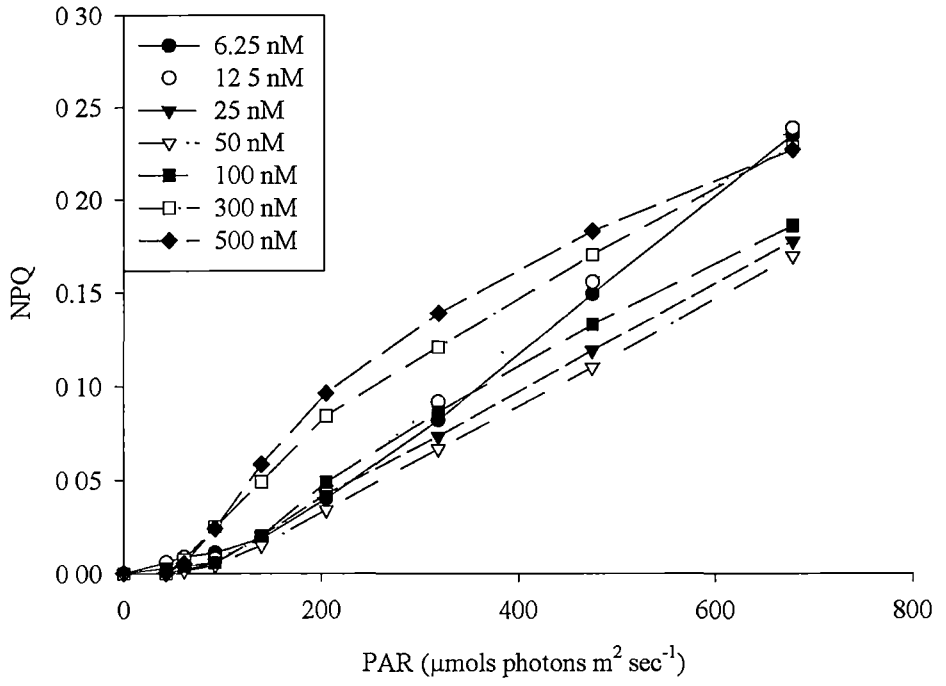

Figure 4.7 Non Photochemical Quenching (NPQ) developed during rapid light curves by *F. curta* cultures grown at seven concentrations of iron.

4.3.3 Chlorophyll and protein

Results for chlorophyll and total protein are expressed on a per cell basis in Table 4.2. Chlorophyll content of cells was highest for organisms grown at the highest iron concentrations for both species. For both species decreasing iron in the media led to progressively lower cellular chlorophyll concentrations. The relative stepwise decrease in chlorophyll content at each concentration of iron was similar for the two species. The lowest per cell concentrations were observed in the cultures grown with the least iron and were 55-60% of maximum values for both species. For both species cellular protein content did not show any consistent response to iron availability.

Table 4.2 Chlorophyll and protein content of *F. cylindrus* and *F. curta* grown at seven concentrations of iron.

Iron (nM)	Chlorophyll (fg cell^{-1})		Protein (fg cell^{-1})	
	F. cylindrus	*F. curta*	*F. cylindrus*	*F. curta*
6.25	9 5±1.1	1.06± 06	0 85±0 04	54.1±4 2
12.5	9 6±0.6	1 01±0 06	0 86±0 05	49 2±8.5
25	11.6±2 8	1 15±0.01	0.64±0 03	55.1±4.6
50	13 7±0 9	1.09±0.09	0.82±0.07	53 5±5 0
100	16 1±1 0	1 54±0.06	0.73±0.08	67.5±7 8
300	18 6±1 2	1.33±0 09	1.00±0.10	56.5±7 1
500	17 5±0.9	1 76±0 06	0 93±0 11	73 0±4.4

4.3.4 Ferredoxin and flavodoxin

An example of a western immunoblot for ferredoxin and flavodoxin conducted on total proteins extracted from *F. cylindrus* is shown in Figure 4.8. Iron had a clear effect on the expression of these proteins in this organism. Cultures grown with 55.5 pM Fe′ (500 nM Fe_{total}) produced predominantly ferredoxin, with a small amount of flavodoxin staining detectable but well below the lowest standard loaded on the gel and therefore not quantifiable. Ferredoxin was replaced by flavodoxin for cultures grown with less iron but the response was not a simple switch from one protein to another. Cultures grown with both 33.3 pM Fe′ (300 nM Fe_{total}) and 11.1 pM Fe′ (100 nM Fe_{total}) expressed both proteins with a greater amount of ferredoxin compared to flavodoxin produced by the organism at the higher iron concentration. For cultures supplied with 5.55 pM Fe′ (50 nM Fe_{total}) or less only flavodoxin was expressed. The amounts of each protein produced under each treatment level were quantified against a standard curve of known amounts of the pure proteins from *C. closterium* (Figure 4.9). When both proteins are expressed as moles of catalyst, flavodoxin appeared to replace some but not all of the ferredoxin expression leading

to a decline in the total concentration of catalyst with increasing iron stress. When ferredoxin expression was completely suppressed (50 nM Fe_{total}) flavodoxin levels were maximal and did not increase for cultures that were suffering from a greater level of iron stress.

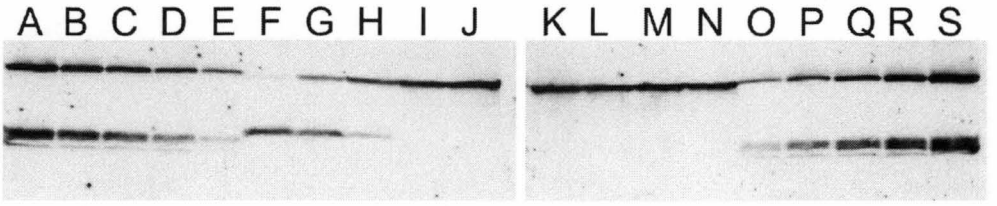

Figure 4.8 Western Immunoblots characterising expression of ferredoxin and flavodoxin in cultures of *F. cylindrus*. Lanes A-E and O-S are purified standards of flavodoxin (top) and ferredoxin (bottom) in the range of 5-50 ng. Lanes F-N are proteins from *F. cylindrus* cultures grown with the following amounts of iron; F 500 nM, G 300 nM, H 100 nM, I 50 nM, J 25 nM, K 6.25 nM, L 12.5 nM, M, 25 nM, N 50 nM.

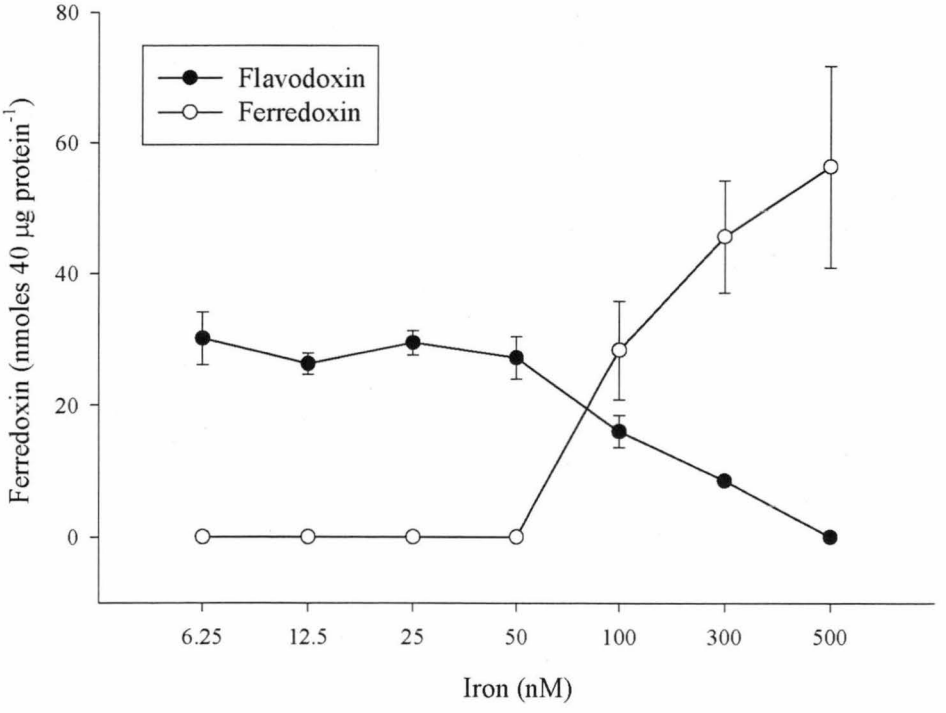

Figure 4.9 Flavodoxin and ferredoxin expression in cultures of *F. cylindrus* grown in media with different iron concentrations.

The equivalent blots and graph for *F. curta* (Figure 4.10 and Figure 4.11) suggest that the ability to produce ferredoxin is absent in this organism. The data presented for replicate cultures at each treatment level (Figure 4.11) shows relatively constant levels of flavodoxin across all treatments.

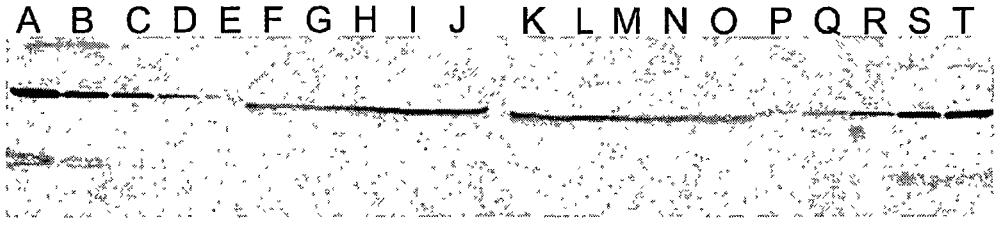

Figure 4.10 Western Immunoblots characterising expression of ferredoxin and flavodoxin in cultures of *Fragilariopsis curta*. Lanes A-E and P-T are purified standards of flavodoxin (top) and ferredoxin (bottom) in the range of 5-50 ng. Lanes F-N are proteins from *F. curta* cultures grown with the following amounts of iron; F 500 nM, G 300 nM, H 100 nM, I 50 nM, J 25 nM, K 6.25 nM, L 12.5 nM, M, 25 nM, N 50 nM O 100 nM.

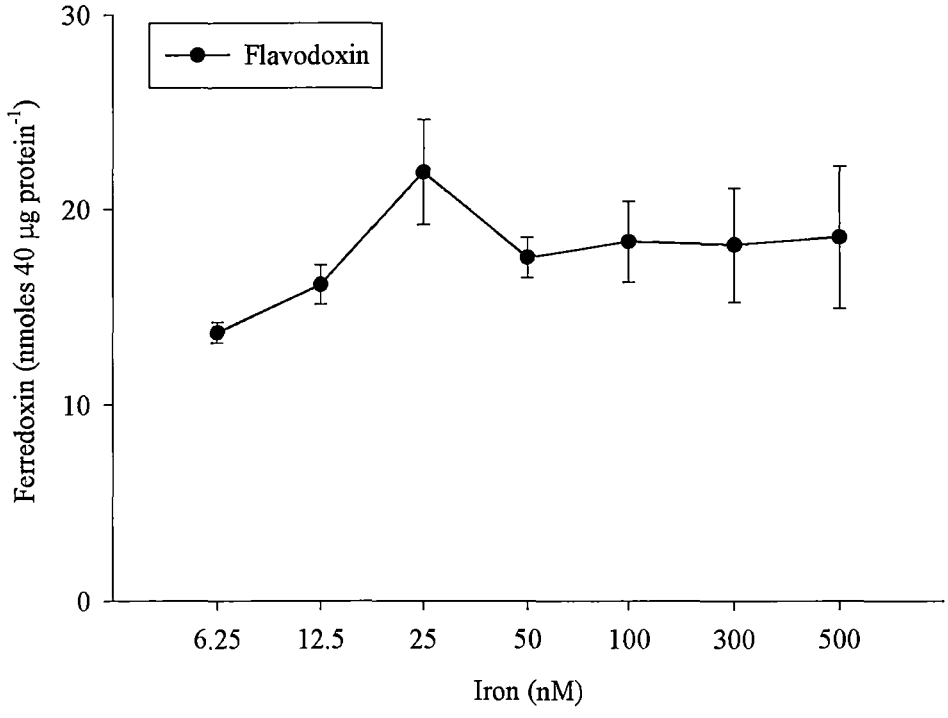

Figure 4.11 Flavodoxin expression in cultures of *Fragilariopsis curta* grown in media with different iron concentrations.

4.3.5 Temporal changes upon recovery of *F. cylindrus* from iron limitation

PAM fluorometry, extracted chlorophyll analysis and western blotting were used to monitor the recovery of *F. cylindrus* cultures from iron stress. There were considerable differences in the rates of change of the various measured parameters. Changes in the photosynthetic parameters Fv/Fm, α and $rETR_{max}$ are shown in Figure 4.12, Figure 4.13 and Figure 4.14 respectively.

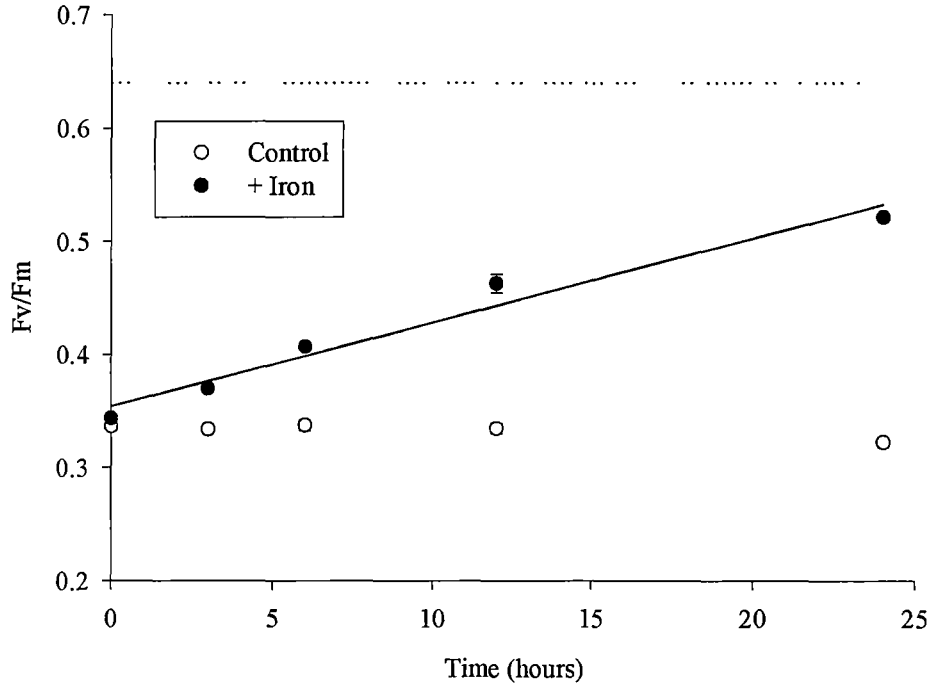

Figure 4.12 Recovery of *F. cylindrus* from iron stress. Changes in Fv/Fm. Broken line represents Fv/Fm of 500 nM grown culture.

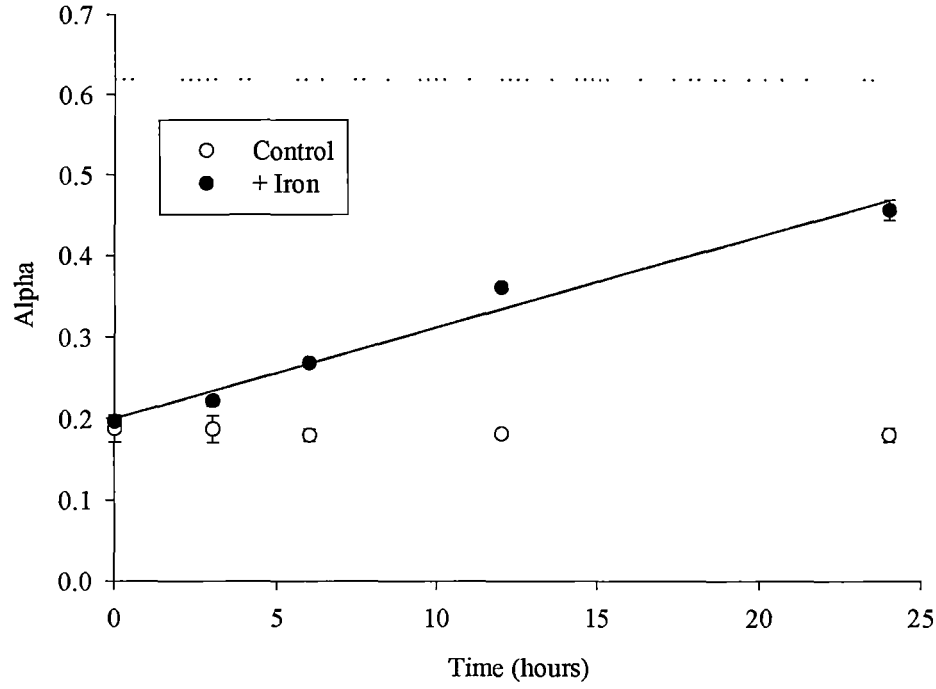

Figure 4.13 Recovery of *F. cylindrus* from iron stress. Change in α. Broken line represents α of 500 nM grown cultures.

Small changes in Fv/Fm and α were evident within 3 hrs of adding iron to iron stressed cultures The increase in these two parameters was linear over the 24 hour period. Twenty four hours after addition of iron Fv/Fm had recovered to approximately 80% of iron replete levels and α to within 70%. If recovery of these two parameters were to continue at the observed rates α and Fv/Fm would have reached iron replete values after approximately 40 hours.

Recovery of $rETR_{max}$ occurred with different kinetics. Recovery of this parameter in the first 6 hours occurred at a similar rate to increases in Fv/Fm. During the second six hour period the recovery rate of this parameter accelerated and reached iron replete levels within 12 hours of iron addition and remained at this level for the final sampling time point.

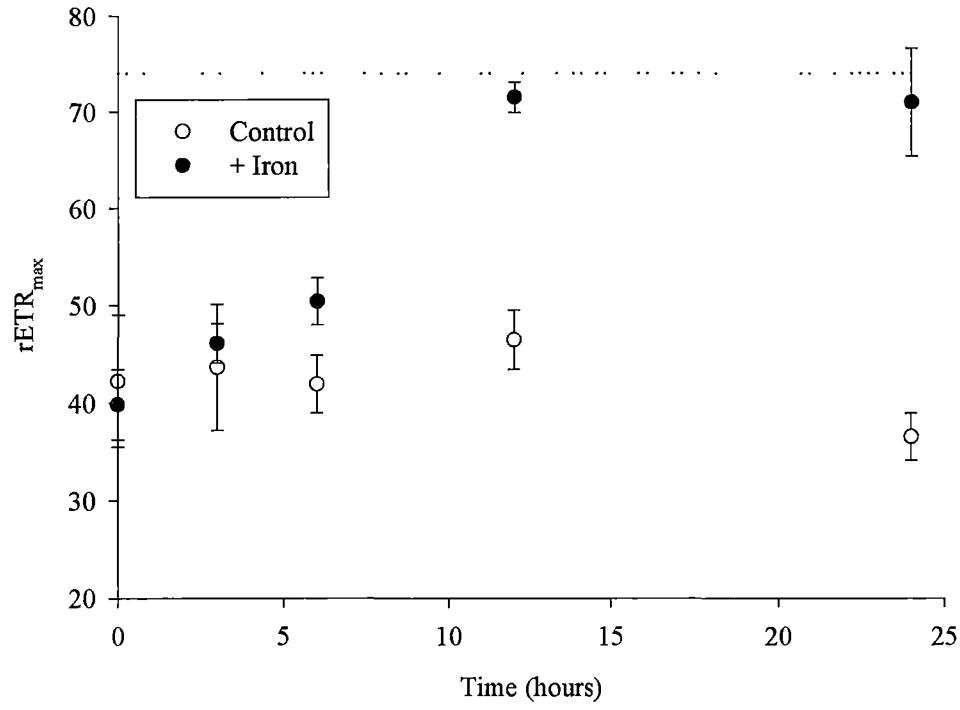

Figure 4.14 Recovery of *F. cylindrus* from iron stress. Changes in rETRmax. Broken line indicates rETRmax of 500 nM grown cultures.

Chlorophyll per cell (Figure 4.15) and ferredoxin expression (Figure 4.16) were much slower to show signs of change. There was no change evident in cellular chlorophyll levels until the 24 hour time point where chlorophyll levels had increased by 20% compared to control levels. Recovery to iron replete levels would involve a doubling of pre recovery chlorophyll per cell levels.

After 12 hours a faint band for ferredoxin was observed but was well below the lowest standard loaded on the gel and therefore below quantitation (Figure 4.15). After 24 hours, expression of ferredoxin was more sustained and had increased to a similar level (in terms of moles catalyst) as flavodoxin. At the same time there was no significant decline in flavodoxin expression Ferredoxin and flavodoxin levels at this time point were similar to the 100 nM grown cultures although by comparison Fv/Fm and α was close to that of the 50 nM culture, chlorophyll per cell was at levels comparable to the 25 nM culture whilst $rETR_{max}$ was equivalent to that of the 500

nM culture. Hence although synthesis of ferredoxin began slowly it recovered more fully than Fv/Fm α or cellular chlorophyll concentrations but not as rapidly as $rETR_{max}$.

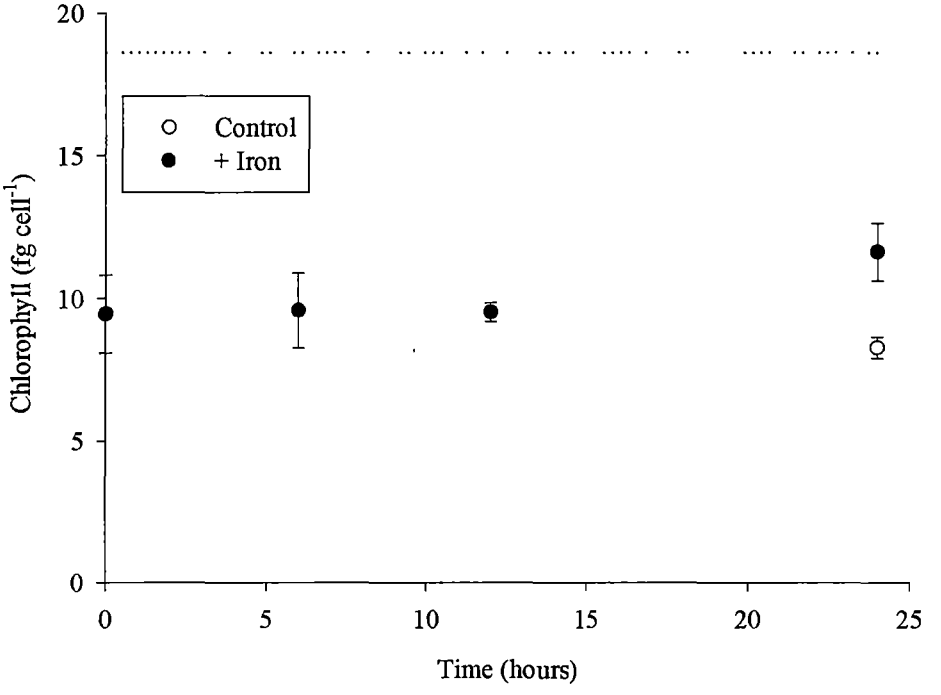

Figure 4.15 Recover of *F. cylindrus* from iron stress. Changes in chlorophyll per cell. Dashed line represents chlorophyll per cell level of 500 nM grown culture.

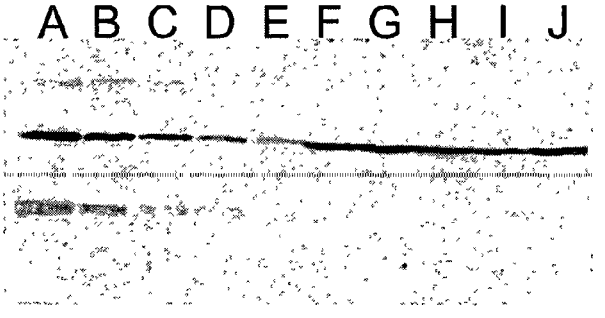

Figure 4.16 Expression of ferredoxin and flavodoxin in *F. cylindrus* during recovery from iron stress. Lanes A-E Proteins standards in range or 50 to 5 ng (flavodoxin top, ferredoxin bottom) F T=0, G +Fe 6hrs, H +Fe 12hrs, I +Fe 24hrs, J control 24hrs.

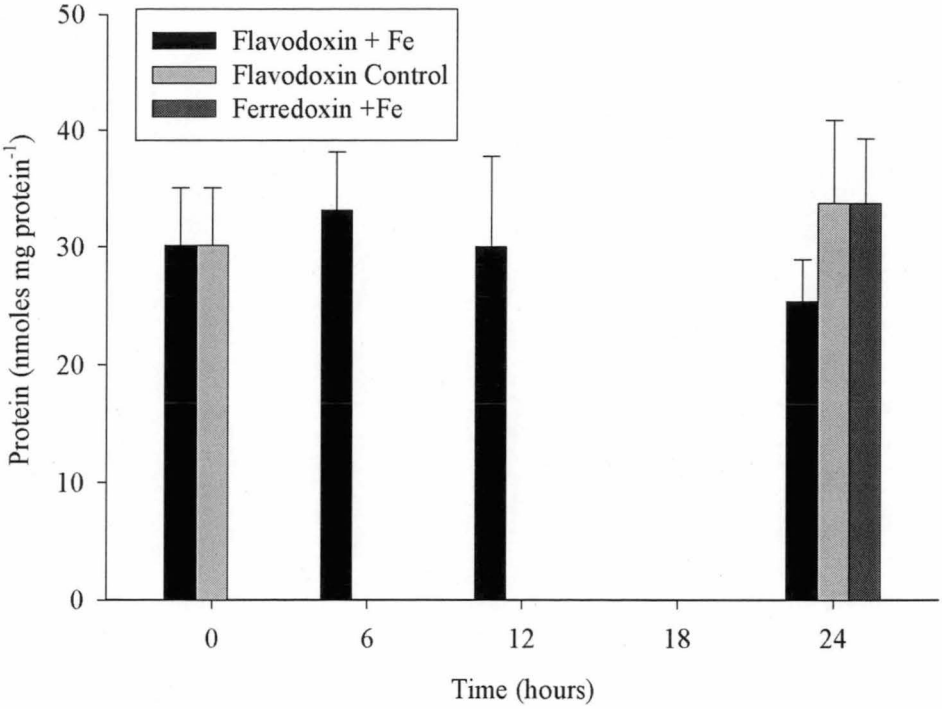

Figure 4.17 Ferredoxin and flavodoxin during recovery of *F. cylindrus* from iron limitiation. Values are expressed as moles of protein per 40 µg of cellular protein (standard amount loaded per gel). Error bars representr SE (n=3).

4.4 Discussion

4.4.1 Growth

The maximum growth rate of *F. cylindrus* (0.57 d^{-1}) in trace metal buffered media was similar to that observed by Fiala & Oriol (1990) under equivalent light and temperature conditions in *f* medium, and identical to the rate observed in f/2 medium for this strain (Chapter 3). Growth of *F. curta* in this medium was 75% of what we observed for this strain in f/2 medium under similar light intensity (Chapter 3).

The growth rate data fitted to a Monod function yielded similar K_m values for both species. In respect to total inorganic iron [Fe'] these were 0.51 x 10^{-12} for *F. cylindrus* and 1.3 x 10^{-12} for *F. curta*. For both species reductions in growth rate to below 90% of maximum occurred around 2.8 to 5.6 pM Fe' (25-50 nM Fe_{total}) and

at the lowest concentration of iron in the experiment both species grew at around half their maximum rates.

Comparison of these K_m values to those reported in the literature for other phytoplankton is complicated by differences in methods used to estimate inorganic iron and uncertainties in which chemical species of iron are available for uptake by phytoplankton in various media. For example, K_m for Fe′ of the Antarctic diatom *Chaetocerous brevis* grown in media buffered with EDTA was 2×10^{-12} M (Timmermans *et al.*, 2001a). The same species and strain grown in low iron seawater with added desferrioxamine had a K_m for [Fe′] two orders of magnitude lower but a K_m for dissolved iron (the sum of Fe′ and the concentration of iron bound to the natural organic ligands in seawater) of 0.59×10^{-12} M (Timmermans *et al.*, 2001b). Shaked *et al.* (2005) recently presented evidence for an iron uptake model for diatoms where both inorganic iron and organically bound iron are available for uptake but all species must undergo reduction to +2 oxidation state at the cell surface prior to uptake. In this model uptake in EDTA buffered media largely occurs through reduction of inorganic iron species at the cell surface.

Growth rate data for other diatoms grown in EDTA buffered media was used to calculate K_m values based on [Fe′] calculated using metal speciation calculations used in this study and that by Timmermans *et al.* (2001a). The values fall within a range of approximately one order of magnitude (Table 4.3). Those reported here for *F. cylindrus* and *F. curta* are in the middle of the range of presented values. The calculations used ignore the photo-dissociation of iron EDTA complexes that increase steady state inorganic iron concentrations (Gerringa *et al.*, 2000). Hence, actual K_m [Fe′] are likely to be higher than the values reported here. However values reported for *C brevis* are directly comparable to those of *F. cylindrus* and *F. curta* because the same light and temperature conditions were used in both experiments. Although light intensity and temperature were higher during the experiments conducted on the temperate species (500 μ mol photons m^{-2} sec^{-1}, 20° C) compared to

during the experiments on polar organisms the increase in steady state [Fe′] (and hence K_m [Fe′]) due to iron EDTA photodissociation are likely to be of similar magnitude.

At low temperatures rates of thermal dissociation and association of iron EDTA complexes are lower but photodissociation rates remain largely unchanged (Sunda & Huntsman, 2003). Based on the observed changes in rates of thermal reactions compared to photolysis at 10° C compared to 20° C (Sunda & Huntsman, 2003), the increase in [Fe′] caused by 70 μmol photons m^{-2} sec^{-1} light at 1° C would be similar to the increase due to 500 μmol photons m^{-2} sec^{-1} light at 20 ° C, approximately a factor of 3.5. Hence, the values are comparable and suggest that within the narrow size range of these organisms there is no clear effect of size or habitat (neritic/oceanic or polar/temperate) on an organisms K_m [Fe′] for growth

Table 4.3 K_m [Fe′] and cell volume for temperate and polar phytoplankton of both neritic and oceanic habitat.

Species	K_m [Fe′]	Cell Volume (μm^3)
T. oceanica‡	0.18×10^{-12}	90
T. pseudonana‡	3.6×10^{-12}	30
T. weissflogii‡	3.0×10^{-12}	840
C. brevis #	2.0×10^{-12}	50
F. curta§	1.3×10^{-12}	750
F. cylindrus§	0.51×10^{-12}	90

‡ Results from study of Sunda and Huntsman (1995) with Fe′ recalculated
# From Timmermans et al. (2001a)
§ This study

K_m [Fe′] growth represents the concentration of iron required to achieve a growth rate half of maximal and therefore provides an indication of an organisms overall ability to maintain growth under low iron conditions. With falling iron concentrations an organism with a high K_m [Fe′] will experience physiological

impairment sooner than an organism with a low K_m [Fe'] growth. The values do not represent the quota or iron use efficiency of the organism, which is a measure of the amount of iron an organism requires to generate a unit amount of biomass.

Sunda & Huntsman (1997) suggest that the options available to oceanic species to grow under low iron conditions are to become smaller, which increases the SA:volume ratio, reduce intracellular iron quotas or to grow more slowly. The reduced maximum growth rate of the larger species, *F. curta,* clearly contributes to its ability to maintain growth at similar iron concentrations to its smaller competitor *F. cylindrus.*

4.4.2 Effects of iron on photosynthesis and pigments

As well as the observed halving of growth rate there were significant changes to photosynthetic parameters and cellular chlorophyll levels. The magnitudes of these changes were similar for both organisms. One of the most consistent and obvious effects of iron limitation was a reduction in α values.

Decreases in α have also been observed in iron limited cultures of *Chaetoceros muelleri* (Davey & Geider, 2001) and the Antarctic flagellate *Pyramimonas sp.* (van Leeuwe & De Baar, 2000). In other studies α values were not affected by iron limitation in cultures of the Antarctic diatom *Chaetoceros brevis* (van Oijen *et al.*, 2004a) or the neritic diatom *Phaeodactylum tricornutum* (Greene *et al.*, 1991). In all but one of the above mentioned studies α values were calculated from ^{14}C uptake and normalised to a per chlorophyll basis. Alpha values obtained by PAM rapid light curves reflect the probability of light energy captured by an antenna unit being used for PSII photochemistry (quantum yield for PSII charge separation) under weak actinic illumination Hence α reflects the effective quantum yield of PSII under low light conditions. Chlorophyll specific α values from traditional photosynthesis vs irradiance curves are irradiance specific rates of photosynthetic oxygen evolution or carbon assimilation and are equivalent to the product of the

quantum yield of photosynthesis (Φ which is proportional the quantum yield for PSII charge separation) and the chlorophyll specific light absorption coefficient (a*). In the study on *P. tricornutum* iron limitation led to a decrease Φ but an increase in a* (due to reductions in pigment content and a decreased in the package effect) with the net result that α remained unchanged (Greene *et al.*, 1991). The clear decreases in α observed in iron limited *Pyramimonas sp* and *C. mueller*ı suggests that in these studies decreases Φ were much greater than increases in a*. These results as well as those observed here for *F. cylindrus* and *F. curta,* suggest that a consistent effect of iron limitation is to decrease quantum yield of photosynthesis, most likely due to changes that occur to PSII to reduce the efficiency of charge separation. In the marine algae *Dunaliella tertiolecta* alterations to PSII resulting from iron limitation included an uncoupling of pigment antenna units from PSII reaction centres which coincided with lower expression of a number of PSII associated proteins (Vassiliev *et al.*, 1995).

Rapid light curve α values and Fv/Fm measure the quantum yield of PSII under light limited photosynthesis and dark adapted states respectively. A comparison of the two can provide information about the functioning of the photosynthetic apparatus at sub-saturating irradiances. Alpha values were consistently lower than Fv/Fm for all cultures but the difference between α and Fv/Fm was not the same for iron limited and iron replete cultures. For the most iron limited treatments for both organisms α was 60% of Fv/Fm whilst for cultures grown with the highest concentration of iron α was > 90% Fv/Fm. This suggests that for the most iron limited cultures weak illumination caused a relatively large percentage of reaction centres to close. Conversely, the majority of reactions centres remained open for the iron replete cultures under the weak illumination experienced during the early steps of the RLC.

Plots of F and Fm' against irradiance for iron replete and iron limited grown *F. cylindrus* and *F. curta* showed similar features. These plots for *F. cylindrus* only are shown in Figure 4.18.

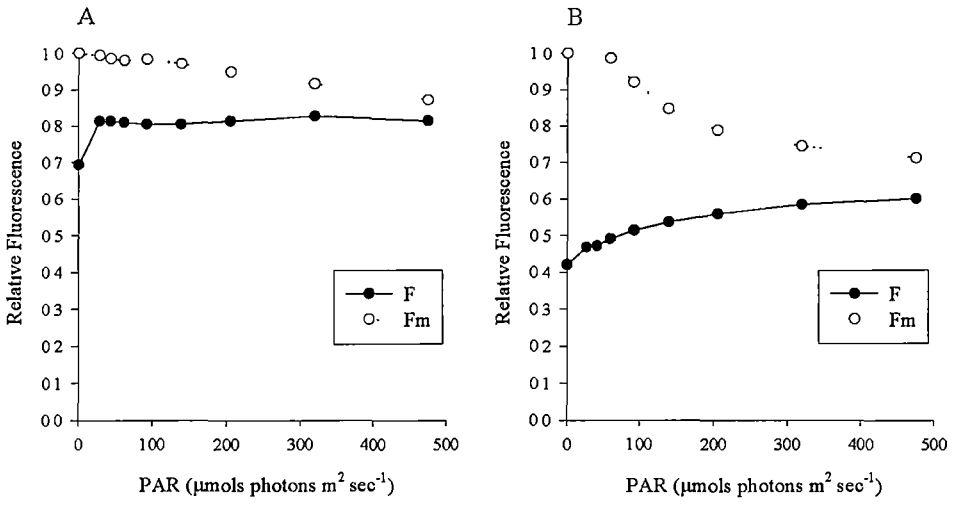

Figure 4.18 Changes in steady state (F) and maximum (Fm) fluorescence during rapid light curves for iron limited (A) and iron replete cultures of *F. cylindrus*.

For iron replete cultures (Figure 4.18B) increasing light intensity during the RLC caused a gradual increase in the minimal steady state fluorescence value F to approximately 150% of the quasi dark adapted value. Furthermore, when irradiance exceeded environmental levels maximum fluorescence Fm' declined in a sigmoidal fashion. The Fm' of iron limited cultures (Figure 4.18A) also declined with rising light levels however the overall decrease in Fm' was less and began at higher irradiance. Steady state fluorescence F of iron limited cells showed a very different response to iron replete cells, increasing only at the first level of actinic light and then remaining constant for all subsequent light levels.

Declines in Fm' are characteristic of the induction of non-photochemical quenching mechanisms which are usually associated with the build up of a proton gradient across the thylakoid membrane (energy dependent quenching qE) (Buchel & Wilhelm, 1993). The relaxation kinetics observed for this quenching i.e. complete relaxation within 30 minutes of dark adaptation, is also consistent with the quenching being of the qE variety (Krause & Weis, 1991). Smaller declines in Fm' of iron limited cells indicates less development of non-photochemical quenching, which is consistent for the observed lower NPQ coefficient for iron limited *F. cylindrus* cultures compared to cultures of this organism grown under iron replete conditions.

That non-photochemical quenching began to develop at higher irradiance in iron limited cells suggests that higher photon fluxes were required to build the trans thylakoid proton gradient (ΔpH) in iron limited cells.

Increases in steady state fluorescence F upon illumination are thought to reflect the oxidation state of the plastaquinone pool (PQ) and as a consequence the proportion of reduced primary accepter Q_A (Kolber & Falkowski, 1993). As more of the plastaquinone pool becomes reduced less is available to reoxidize Q_A resulting in more reaction centres being closed to the transfer of absorbed photon energy. Gademann & Ralph (2004) suggest that an increase in F during a RLC reflects insufficient "sink" capacity to remove the electrons generated at the PSII reaction centres. This is particularly evident in low light adapted organisms which maximize light capture at low irradiance but have limited ability to process high electron fluxes (Ralph & Gademann, 2004). Hence iron replete *F. cylindrus* and *F. curta* showed characteristics of adaptation to moderate light levels. F increased steadily with increasing irradiance suggestive of an imbalance between electron generation by PSII and usage of these reducing equivalents through carbon fixation.

In iron limited cells the increase in F at quite low irradiance and only at the onset of actinic illumination could similarly be due to an increase in the extent of reduction of the plastaquinone pool. However, as it occurred under very low light levels with the effective quantum yield (and F) remaining relatively constant for the following five steps of the light curve, it more likely indicates a closure of a subset of the reaction centres under low light. Such closures could occur if a subset of reaction centres were of the Q_A non-reducing type (Krause & Weis, 1991) That F remained constant with further increases in irradiance suggests that capacity to utilise electrons was greater than ability to generate them. This is consistent with the observation that iron limited cells began to develop nonphotochemical quenching at higher irradiance. Only when photon flux densities are relatively high can iron limited cells generate enough ΔpH to induce the build up of nonphotochemical quenching.

Iron limited growth also resulted in suppression of the maximum relative electron transport rates ($rETR_{max}$). Furthermore, declines in $rETR_{max}$ were not as great as the observed decreases in α causing E_k to shift to higher irradiance. This further demonstrates that iron limitation caused larger reductions to light capture and primary charge separation relative to electron processing capacity downstream from PSII. In iron replete cultures E_k was close to environmental light levels indicating that the organisms were growing at close to light saturation with limited ability to photochemically utilise the increased photon fluxes when light levels exceed environmental levels. Iron limited cultures however were growing at sub-saturating irradiance where the capacity to process energy downstream of PSII is greater than the capacity to carry out light capture and primary charge separation.

The results presented here are consistent with iron induced changes in photosynthesis being mainly due to effects on PSII. Various alterations to the photosynthetic electron transport chain have been postulated to cause a reduction in maximal quantum yield for PSII due to iron limitation. Vassiliev *et al.* (1995) reported that iron limitation causes a significant reduction in the abundance of LHCII proteins which coincided with PSII reaction centres becoming energetically isolated. Reduced transfer of excitation energy from closed PSII reaction centres to open centre was also observed, along with changes in the rate of electron transport through the photosynthetic electron transport chain. These latter changes were thought to be the result of decreased abundance of certain functional proteins on the acceptor side of PSII (eg cytb559) which resulted in less efficient reduction of the primary acceptor Q_A. Evidence for alterations to the rate of electron transfer through PSI has also been observed (Greene *et al.*, 1992) as a result of a reduction in certain iron containing proteins in this photosystem. Although alterations to PSI may have occurred in *F. cylindrus* and *F. curta,* they were masked by more substantial relative changes to PSII.

4.4.3 Ferredoxin and flavodoxin expression in relation to iron supply, growth and physiology

Phytoplankton faced with falling concentrations of an essential nutrient respond to the stress by initiating changes to cellular biochemistry which attempt to mitigate the effects of falling nutrient availability. These changes may include the induction of acquisition systems, for example, the up-regulation of membrane bound metal transport ligands, replacement of one catalyst for another, as occurs with the replacement of ferredoxin and flavodoxin, and the progressive down regulation of metabolic processes (La Roche *et al.*, 1999).

Alterations to cellular composition and biochemical processes in response to decreased nutrient availability can precede reductions in growth rate. For example, Morel *et al.* (1991) suggest that microalgae growing with replete amounts of a given trace metal express sub-maximal densities of membrane bound transporters for that metal. When the availability of a trace metal falls to a critical level, where the organisms full quota cannot be met, the number of transport ligands increases. This allows the organism to maintain growth at near maximum rates. This physiological state, where growth rate is near maximum but compensatory mechanisms have been induced is called metal stress (Morel *et al.*, 1991) When ligand transport density reaches a maximum level, and other mechanisms cannot compensate for the decreased metal availability, growth rates fall and the organism enters metal limitation. A useful definition of the onset of metal limitation is a growth rate 90% of maximum (Morel *et al.*, 1991). Hence, changes in cellular biochemistry or physiology that result from reduced trace metal availability but that are not accompanied by a reduction in growth rate are evidence of metal stress.

Based on the above definitions for metal stress and metal limitation the substitution of ferredoxin for flavodoxin in *F. cylindrus* begins as an early response to iron stress. For this organism the cultures grown with 300 nM and 100 nM iron contained both ferredoxin and flavodoxin and showed photosynthetic parameters and cellular

chlorophyll concentrations that were around 90% of the values observed for the 500 nM (iron replete) cultures. Full replacement of ferredoxin for flavodoxin was observed in the 50 nM cultures which grew at rates which were still above 90% μ_{max}, i.e. the organisms were not growing under iron limitation. These cultures grown with 50 nM of iron showed only minor symptoms of iron stress with photosynthetic parameters and per cell chlorophyll concentrations suppressed by around 20% compared to maximum.

Davey & Geider (2001) observed that substantial increases in flavodoxin expression caused by iron stress had little effect on growth rates, light saturated photosynthesis rates, variable fluorescence or intersystem electron transport in cultures of the diatom *Chaetocerous muelleri*. These authors also observed that under the highest levels of iron stress small increases in flavodoxin were accompanied by large changes in photosynthetic parameters. *F. cylindrus* grown at a pFe' of 2.8 (25 nM Fe_{total}) or less grew at rates which were substantially limited by iron availability. For these treatment each incremental reduction in iron caused a drop in growth rate and further reductions α, rETRmax, Fv/Fm, however flavodoxin concentrations expressed as per protein or per cell remained constant for these cultures. The differences observed in these two species may reflect that *F. cylindrus* was growing acclimated to the iron concentration whereas *C. muelleri* was experiencing falling iron levels. Under such circumstances rates of change to photosynthetic parameter through processes such as damage and degradation to photosynthetic units may be more rapid than protein synthesis rates. Hence, an acclimated state where flavodoxin expression is truly related to iron supply may not have been reached. Erdner *et al.* (1999) similarly observed that flavodoxin was expressed in *Thalassiosira weissflogii* at growth rates of 80-90% maximum These authors also examined ferredoxin expression in this organism and suggested that when growth rates were limited by iron the relative abundance of ferredoxin and flavodoxin (the ferredoxin index) had the potential to indicate the severity of iron stress. McKay *et al.* (1999) observed that accumulation

of flavodoxin coincided with impairment of photochemistry in *Phaeodactylum tricornutum,* however, the level of impairment observed was minor, corresponding to the small decrease observed for *F. cylindrus* grown at 100 nM Fe_{total} compared to 500 nM.

Fragilariopsis curta showed similar trends to *F. cylindrus* in terms of growth rate, α, $rETR_{max}$ and Fv/Fm. For this organism, significant limitation of growth by iron occurred in the four treatments supplied with less than 5.6 pM [Fe'] (50 nM Fe_{total}) Apart from a 30% decrease in α for the 100 nM grown culture the cultures supplied with the three highest concentration of iron showed little other evidence of physiological impairment. Furthermore, ferredoxin was never detected in this species and flavodoxin levels were constant across all treatments.

Constitutive expression of flavodoxin has previously been observed in *Rhizosolenia sp.* but the expression of ferredoxin was not examined in this organism (McKay *et al.*, 2000). In *T. weissflogii* a constitutive flavodoxin was also reported but was a minor fraction of the combined ferredoxin + flavodoxin pool (Doucette *et al.*, 1996), and was later found to be turned off by very high iron concentrations (Erdner *et al.*, 1999). The lack of detection of ferredoxin in *F. curta* could have conceivably resulted from a lack of antibody cross reactivity towards the protein from this organism. If ferredoxin was the dominant catalyst in *F. curta* but was simply not detected in iron replete cultures, an up-regulation of flavodoxin would be expected under iron stress. The observed constant concentration of this catalyst in *F. curta* suggests that ferredoxin is either a minor component or completely absent from this organism.

4.4.4 Recovery of *F. cylindrus* from iron limitation

To conduct analyses for ferredoxin and flavodoxin on algae extracted from sea ice the organisms must be extracted from the ice matrix by melting. The melting process can be completed within approximately 12 hours. A key concern was that during this

time unavoidable contamination of samples with iron may result in changes to *in situ* ferredoxin and flavodoxin expression. Therefore experiments were conducted to observe the temporal changes in recovery from iron limitation in *F. cylindrus*.

Changes in Fv/Fm, α, $rETR_{max}$, chlorophyll and ferredoxin/flavodoxin occurred with different kinetics following the addition of iron to iron limited cultures. The parameter that recovered first was $rETR_{max}$, which attained iron replete levels within 12 hours of iron addition. Both Fv/Fm and α increased with similar linear kinetics, and recovered to 80% and 70% of iron replete values over the course of the 24 hour experiment. Changes in α were therefore primarily due to increases in primary charge separation and are most likely due to an increase in functional PSII centres as has been observed previously (Vassiliev *et al.*, 1995). Although both α and $rETR_{max}$ increased substantially during 24 hours of recovery, E_k remained at higher than iron replete levels. Hence despite a recovery in the maximum relative electron transport rate, higher photon flux densities were required to achieve this rate.

Despite significant relaxation of constraints on photochemistry in the 24 hour period, changes to protein expression and cellular chlorophyll concentrations occurred more slowly. Cellular chlorophyll concentrations increased only marginally in the 24 hour period and only at the final time point. There was evidence of ferredoxin induction after 12 hours with a faint band discernable on western blots. Significant expression of this protein was not observed until the 24 hour time point. During this time flavodoxin levels did not change significantly.

In cultures of the temperate diatom *P tricornutum* complete replacement of flavodoxin with ferredoxin occurred within eight hours of iron resupply and major reductions in flavodoxin were observed prior to the detection of significant amounts of ferredoxin suggesting active degradation of this protein (McKay *et al.*, 1999). In this organism complete replacement of flavodoxin for ferredoxin was accompanied by an approximate doubling of Fv/Fm (from 0.25 to 0.45)

The relative rates of recovery of Fv/Fm and protein expression are similar in both species but the slower absolute rates of *F. cylindrus* compared to *P. tricornutum* are consistent with the temperature dependence of biochemical processes.

Recovery of Fv/Fm in both of these culture experiments are rapid compared to rates observed during open ocean iron enrichment in the Southern Ocean (Boyd *et al.*, 2000) and Equatorial Pacific (Coale *et al.*, 1996). During the experiment in the polar ocean a doubling of Fv/Fm occurred in four days while a similar degree of recovery was observed in 24 hours during the temperate ocean experiment. Slower recovery rates during field conditions compared to laboratory trials suggest that the more ideal light and iron regimes of laboratory studies accelerate the recovery process. During extraction of algae from ice cores conditions for recovery are far from ideal. Contamination by iron is likely to only marginally increase iron supply. Furthermore, light can be excluded from the samples and changes in salinity that occur during melting are known to physiologically stress these organisms (Ryan *et al.*, 2004) which would likely further impair the process. Hence, changes in ferredoxin and flavodoxin levels during melting are unlikely.

4.4.5 Ferredoxin and flavodoxin as markers for iron nutritional status in Antarctic sea ice algae

In *F. curta* flavodoxin expression was found to be constitutive. The constant level of expression of this protein in this organism under conditions ranging from iron replete growth to severe iron limitation clearly precludes the use of this protein as a marker for iron nutritional status in this species. Widespread constitutive expression of flavodoxin by other sea ice associated diatoms from both the Arctic and Antarctic (Chapter 3) would be expected to be under similar regulatory control to that of *F. curta*. Hence neither flavodoxin abundance nor flavodoxin presence can be used to signify iron nutritional status in sea ice communities In light of these results it is interesting to reassess the observed persistence of flavodoxin expression during the first Southern Ocean iron enrichment experiment (SOIREE) (Boyd *et al.*, 2000). In

this experiment Fv/Fm attained values close to 0.5 but flavodoxin expression persisted. This was thought to be due to incomplete alleviation of iron stress. The bloom that formed was dominated by *Fragilariopsis kerguelensis*. Based on the observed constitutive expression of flavodoxin in other closely related large oceanic *Fragilariopsis* species from both the Arctic and Antarctic (Chapter 3) it is likely that the observed persistence of flavodoxin was due to constitutive expression of flavodoxin in *F. kerguelensis* and other diatoms that bloomed in response to iron enrichment.

That flavodoxin is expressed as an early response to iron limitation in *F. cylindrus*, and that its expression is maximal under conditions where neither growth was reduced nor photosynthesis significantly impaired means that neither the presence of this protein nor the ferredoxin index can be used to signify a level of stress which would have significant environmental consequences.

Although not all polar diatoms are capable of expressing ferredoxin the ability to express this protein is retained in many Antarctic diatoms (Chapter 3) *Fragilariopsis cylindrus* which retains this ability has an almost ubiquitous distribution in this environment (Lizotte, 2001). Some species capable of expressing ferredoxin would be present in most sea ice communities. The likely presence of ferredoxin producing microalgae in most sea ice communities, coupled with the fact that this protein is present in *F. cylindrus* only when growth rates are maximal suggests that the presence of this protein is likely to serve as an indicator of iron sufficiency in Antarctic sea ice. Finally, that the induction of ferredoxin in iron limited *F. cylindrus* is slower than the time taken to process sea ice samples indicates that analyses conducted for these proteins will accurately reflect protein expression *in situ*.

Chapter 5 : Profiles of ferredoxin and flavodoxin in pack ice cores from Eastern Antarctica

5.1 Introduction

Over the past two decades a significant research effort has sought to determine the role of iron in the Southern Ocean (Boyd, 2002a). This has taken the form of precise iron measurements (e.g. de Baar *et al.*, 1999; Fitzwater *et al.*, 2000; Loscher *et al.*, 1997), iron enrichment bottle incubation experiments (e.g. Sedwick *et al.*, 2000; Timmermans *et al.*, 1998) and studies that have correlated oceanic iron concentrations and algal biomass (de Baar *et al* , 1995). Additionally, several mesoscale *in situ* iron enrichment experiments have been conducted in the vicinity of the Polar Front (Boyd, 2002b; Boyd *et al.*, 2000; Coale *et al.*, 2004; Gervais *et al.*, 2002). The emerging view is that in the low iron waters of the Southern Ocean picoplankton and nanoplankton dominate with their growth and abundance controlled by grazers and light (Gervais *et al.*, 2002; Veldhuis & de Baar, 2005). Increased iron supply to these waters results in a floristic shift to larger, faster growing algal species, notably diatoms, which are able to escape grazing pressure and reach high cell densities (Boyd *et al.*, 2000; DeBaar & Boyd, 2000; Gervais *et al.*, 2002). The dominance of small algal species in low iron waters appears to result from their high surface area to volume ratios which provide favourable conditions for iron uptake (Sunda & Huntsman, 1997)

In contrast to the large effort undertaken to elucidate the role of iron in the Southern Ocean pelagic ecosystem little research has been conducted on the role of iron in the Antarctic sea ice microalgal community. Sea ice is a dominant feature of the

Southern Ocean growing to cover 19 million square kilometres each year (Comiso, 2003).

As surface waters of the remote Southern Ocean contain low concentrations of iron (Coale *et al*, 2005; Croot *et al.*, 2004; de Baar *et al.*, 1999; Loscher *et al.*, 1997; Martin *et al.*, 1990b, Measures & Vink, 2001; Sohrin *et al.*, 2000). It has thus been suggested that sea ice forming from such low iron waters is also likely to contain low concentrations of this micronutrient, resulting in growth limitation of resident sea ice microalgae (Thomas, 2003).

However, contrasting evidence from analysis of iron in sea ice indicates that sea ice may contain significant amounts of iron, possibly as entrained sediments or within the accumulated snow on the surface of floes (Fitzwater *et al.*, 2000; Loscher *et al.*, 1997, Sedwick & DiTullio, 1997; Sedwick *et al*, 2000). Furthermore, indirect evidence for high concentrations of iron in sea ice has been gained from studies that have observed high iron levels and phytoplankton blooms in the presence of melting sea ice (Croot *et al*, 2004; Sedwick & DiTullio, 1997). Much of this research has been conducted on pack ice in waters associated with the continental margin where iron concentrations are significantly higher than in remote oceanic waters (Coale *et al.*, 2005; de Baar *et al.*, 1999; Fitzwater *et al.*, 2000; Measures & Vink, 2001; Sedwick & DiTullio, 1997; Sedwick *et al.*, 2000; Sohrin *et al.*, 2000) and so the applicability of these observations to ice forming in remote Southern Ocean waters remains largely unknown.

There has currently been no wide scale study on the distribution of iron in Antarctic sea ice Furthermore, there is currently no information on the availability of iron to Antarctic sea ice microalgae. These organisms inhabit distinct micro-habitats within the ice, such as bottom communities that live on the under surface of ice floes, interior communities within the network of brine channels and surface communities existing in the layer between the ice surface and overlying snow (Eicken, 1992).

The light, salinity, temperature and nutrient supply regimes experienced by these communities vary substantially (Arrigo, 2003; Eicken, 1992; Thomas & Papadimitriou, 2003). Strong gradients of physical and chemical conditions within the ice may also influence the iron requirements of the organisms inhabiting it. For example, evidence from culture studies on temperate phytoplankton suggests that phytoplankton grown on nitrate have higher iron requirements than those grown with ammonia as a source of nitrogen (Maldonado & Price, 1996). High ammonia concentrations have sometimes been detected in sea ice (Arrigo *et al.*, 2003a). Another factor that is likely to influence iron quotas of sea ice algae is the light environment which varies substantially through the vertical profile of a floe. Low light levels have also been shown to increase the iron quota of phytoplankton (Strzepek & Price, 2000; Sunda & Huntsman, 1997).

Lack of research into the availability of iron to Antarctic sea ice microalgae reflects both logistical difficulties in studying sea ice and technical problems associated with adapting methodologies used to study iron-phytoplankton interactions, such as bottle enrichment experiments (e.g. Martin & Fitzwater, 1988; Sedwick *et al.*, 2000; Timmermans *et al.*, 1998) to sea ice. One potential avenue available to investigate the bioavailability of iron in this environment is to examine the expression of iron regulated proteins in sea ice algal communities. Ferredoxin and flavodoxin are two such proteins known to be regulated by iron availability in marine microalgae (La Roche *et al.*, 1995; McKay *et al.*, 1997; McKay *et al.*, 1999). Flavodoxin expression in natural phytoplankton communities has been suggested be an indicator of low iron availability (La Roche *et al.*, 1996). Conversely detection of ferredoxin *in situ* is thought to signify iron replete conditions (Boyd *et al.*, 1999)

The following study investigates the distribution and abundance of ferredoxin and flavodoxin in pack ice cores from Eastern Antarctica. The results provide some of the first insights into the bioavailability of iron in Antarctic sea ice.

5.2 Methods

5.2.1 Sampling

Ice cores were collected from level first year pack ice at five stations in the Mertz Glacier region (63-66°S, 143-148°E) of the Southern Ocean during Voyage 1 of the RS *Aurora Australis* in October-November 2002 (Table 5.1;Figure 5.1). Snow was cleared from the surface with an aluminium snow shovel and cores were obtained with a 14 cm diameter ice corer. Triplicate cores were taken from each flow within a 2 m radius. Cores were wrapped in black plastic and transported back to the ship where they were processed immediately. Each core was cut into 10 cm sections which were thawed into 1.5 L of 0.2 μm filtered (Sartobran 300 capsule filter, Sartorius) seawater in the dark

Upon melting, the total volume was measured in order to calculate the dilution factor and a sub sample of 20-100 ml was filtered through a 47 mm diameter GF/F filter (Whatmann) and analysed for chlorophyll as described below. Sub samples for species identification (10 mL) were taken from all sections derived from one of the triplicate cores at both stations 1 and 3. These were preserved with Lugol's iodine and stored at 4° C. The dominant species in these samples were identified in wet mounts using differential interference microscopy. Approximately 200 cells were identified in each of these samples The remainder of the thawed core sections (or as much as could be filtered through a single membrane) was filtered through a 3 μm pore size 47 mm diameter polycarbonate membrane (Osmonics). The membrane was folded with forceps, placed in a 2 mL screw cap microcentrifuge tube and frozen at -80° C These samples were later analysed for ferredoxin and flavodoxin by western immunoblotting as described below.

5.2.2 Chlorophyll analysis

Pigments were extracted from filters into 10 mL of methanol for 24 hours at -20° C. The fluorescence of the extract was measured with Turner Designs model 10AU field fluorometer both before and after acidification with HCl. Chlorophyll *a* (chl *a*) concentrations were calculated as described by Arar (1997). The fluorometer was calibrated with a solution of pure chl *a* in methanol. The concentration of the primary standard was determined from its absorbance 665 nm and calculated using an extinction coefficient of 79.95 $g^{-1}cm^{-1}$ (Porra *et al.*, 1989).

5.2.3 Ferredoxin and flavodoxin analysis

Tubes containing membranes were removed from the freezer and kept on ice while 1 mL of lysis buffer (3% SDS, 100 mM Tris pH 6.8, 1 mM DTT, 1 mM PMSF) was added. Tubes were placed in a sonicator bath for 10 min on high power. After removing the membrane the extract was centrifuged at 20000 × g for 10 min in a microcentrifuge.

A fixed volume of the supernatant (900 µL) was transferred to a 15 mL polypropylene screw cap centrifuge tube (Greiner) and proteins were precipitated with 9 mL acetone at -20° C overnight. After centrifugation for 10 min at 4000 x g and -10° C the supernatant was removed and residual solvent was evaporated under reduced pressure (-30 inHg) in a desiccator for 1 h. The pellet was dissolved in 60 µL of fresh lysis buffer (without DTT or PMSF) and after transfer to a new microcentrifuge tube, insoluble material was removed by centrifugation at 20000 × g. Duplicate 5 µl aliquots were taken for protein determination by the Bicinchoninic acid method (Chapter 3). The final extracts were used to prepare samples for SDS PAGE and subsequent western blotting by adding 0 325 volumes of a solution containing a mixture of DTT, glycerol and bromophenol blue (Chapter 2). Standards in the range of 5-50 ng of pure ferredoxin and flavodoxin from *Cylindrotheca closterium* (Chapter 2) were loaded in the first five lanes of each gel and quantitation

was performed against these standards by densitometry as outlined previously (Chapter 3). Where possible protein extracts were diluted prior to the addition of 0.325 volumes of the DTT/glycerol/bromophenyl blue mixture such that 40 μg of protein could be loaded for each sample in a volume of 25 μL (the capacity of the lane). However, extracts resulting from some core sections contained insufficient protein to enable this amount to be loaded. For these samples 0.325 volumes of the DTT/glycerol/bromophenyl blue mixture was added to the undiluted extract and lanes were loaded with 25 μL of the resultant solution.

5.3 Results

5.3.1 Sea ice

Sampling locations, replicate core numbers, core lengths and snow depth are shown in Table 5.1. Location of ice stations in relation to ocean bathymetry are outlined in Figure 5.1. All cores were taken from level first year ice and ranged in length from 0.40 m to 0.80 m. The three most southern sites occurred in waters immediately to the north of the continental shelf, while stations 1 and 5 were in remote oceanic waters greater than 3500 m deep. Fifteen ice cores obtained from the five stations were sectioned into 0.1 m intervals from the bottom up. The bottom 0.1 m of cores obtained from stations 3 and 4 were sectioned further into the bottom most 2 cm (which contained the majority of the visible biomass) and an 8 cm interval. This resulted in a total of 102 samples which were processed for ferredoxin, flavodoxin, total protein and chl *a*.

Table 5.1 Location, core length and snow cover of sea ice sampling stations.

Station	Location	Core	Length (m)	Snow (m)
1	63.89°S	1A	0.43	0.1
	143.76°E	1B	0.49	
		1C	0.40	
2	65.72°S	2A	0.54	0.1- 0.15
	147.55°E	2B	0.55	
		2C	0.54	
3	65.72°S	3A	0.74	0.2
	146.55°E	3B	0.73	
		3C	0.75	
4	65.55°S	4A	0 55	0.15
	146.53°E	4B	0.50	
		4C	0.56	
5	64.42°S	5A	0.75	0.15
	145.66°E	5B	0.75	
		5C	0 80	

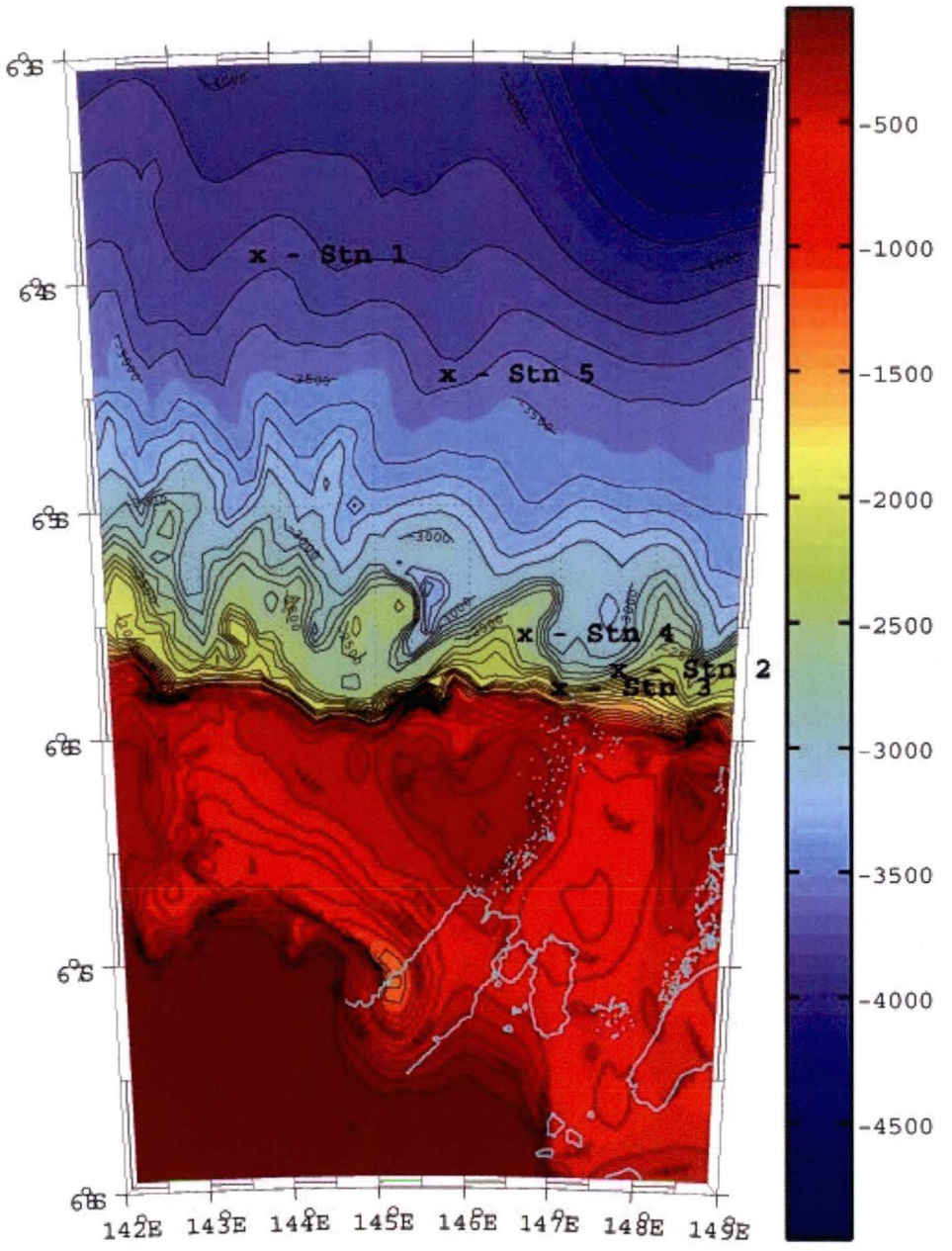

Figure 5.1 Sea ice sampling stations off the Adelie Land coast in relation to ocean bathymetry.

5.3.2 Chlorophyll *a* and total protein

Chlorophyll *a* content and distribution in sea ice from the five stations samples are shown in Table 5.2. Mean integrated areal chlorophyll standing stocks were 4.99 ± 2.39 mg m^2 and mean volumetric chlorophyll concentrations were 8.02 ± 4.51 mg m^3. Integrated standing stocks of individual cores ranged from 0.75 mg m^2 in the thinnest ice (0.4 m) at the most northern site to 9.33 mg m^2 at site 4 in ice which was approximately 0.55 m thick. Highest chlorophyll standing stocks were observed in floes at the three southern most stations (2, 3 and 4) which all had distinct bottom communities. For these floes >70% of the chl *a* occurred in the bottom 10 cm of the ice. The concentration of chl *a* in this bottom section was an order of magnitude greater than the concentration in all sections higher in the core. For the other two floes chl *a* was more evenly distributed within the profile of the cores, the relatively high percentage of chl *a* in the bottom section of cores from site 1 due to the ice being substantially thinner at this location.

Table 5.2 Total chlorophyll *a* content (areal and volumetric) of ice cores taken from five stations off the Adelie Land coast and the percentage of chlorophyll *a* in the bottom 10 cm of each floe. Values are mean ± SD of three replicate cores.

Station	Areal chl a (mg m2)	Volumetric chl a (mg m3)	chl a in bottom 10 cm (%)
1	1.30 ± 0.58	1.74 ± 0.86	41.7 ± 3.4
2	6.27 ± 0.31	11 54 ± 0.49	72.3 ± 7.1
3	6.65 ± 0.34	8.98 ± 0.36	73.7 ± 1.9
4	6.97 ± 2.05	12.93 ± 3.33	85.4 ± 6.2
5	3.75 ± 0.16	4.90 ± 0.35	15.0 ± 1.7
Mean	4.99 ± 2.39	8.02 ± 4.51	57.6 ± 27 0

Protein content of the cores was significantly correlated with chlorophyll content (Pearsons r=0.927; n=102; p<0.001) suggesting that the majority of protein extracted from samples was of autotrophic origin. The mean (± SD) ratio of chl *a*:protein was 33.0 μg (± 68.0) protein (μg chl *a*)$^{-1}$.

5.3.3 Profiles of flavodoxin and ferredoxin

SDS PAGE gels used for ferredoxin and flavodoxin analyses were each loaded with 5 unknown samples and five standards for each protein. The bottom ferredoxin and flavodoxin standards were loaded at 5 ng, a concentration found to afford reliable detection (Chapter 2). However, the method was capable of detecting both proteins at concentrations lower than these bottom standards. Hence quantitation of ferredoxin and/or flavodoxin was undertaken only when band intensity was above the bottom standard. When the band intensity was below that of the bottom standard only the presence of the protein was recorded.

Bands corresponding to ferredoxin and/or flavodoxin were observed in all but eight of the one hundred and two core sections analysed for these proteins. Samples in which ferredoxin and/or flavodoxin were not detected were almost exclusively derived from the uppermost section of cores. During sample preparation it was noticed that samples generated from the tops of cores often formed copious amounts of an unknown precipitate during the acetone concentration step. The nature of this material was not investigated but it is possible that these precipitates interfered with the assay.

In the remaining ninety four samples flavodoxin was detected in all but three samples. In addition a band corresponding to ferredoxin was observed in almost half of these samples. In those samples in which a flavodoxin band was observed the band intensity fell within the range of the standard curve in >90% of these samples, allowing the concentration to be determined. Ferredoxin immumo-staining was

sufficiently intense to quantify the amount of protein in approximately one third of samples in which the protein was detected.

The data was used to construct profiles of flavodoxin, ferredoxin and chlorophyll for the fifteen cores (Figure 5.2-Figure 5.6). Profiles are constructed to emphasise the concentration of ferredoxin and flavodoxin in the majority of core sections. As such the high concentration of chl *a* and flavodoxin within the bottoms of many of the cores are off scale and represented with numerical values. When ferredoxin and flavodoxin were present in concentration high enough to allow quantitation the concentration of the protein within the core section is shown. In instances when proteins were detected in small amounts, the presence only is indicated by a coloured symbol.

For samples processed from the bottom 0.1 m section of cores from sites 3 and 4 the concentrations shown for flavodoxin, ferredoxin and chl *a* were calculated from combining the data from analyses conducted on the bottom most 2 cm and uppermost 8 cm of these sections. It should be noted that ferredoxin was present only in the upper 8 cm fraction of these bottom sections, i.e. this protein was never detected in the lower most 2 cm of these cores.

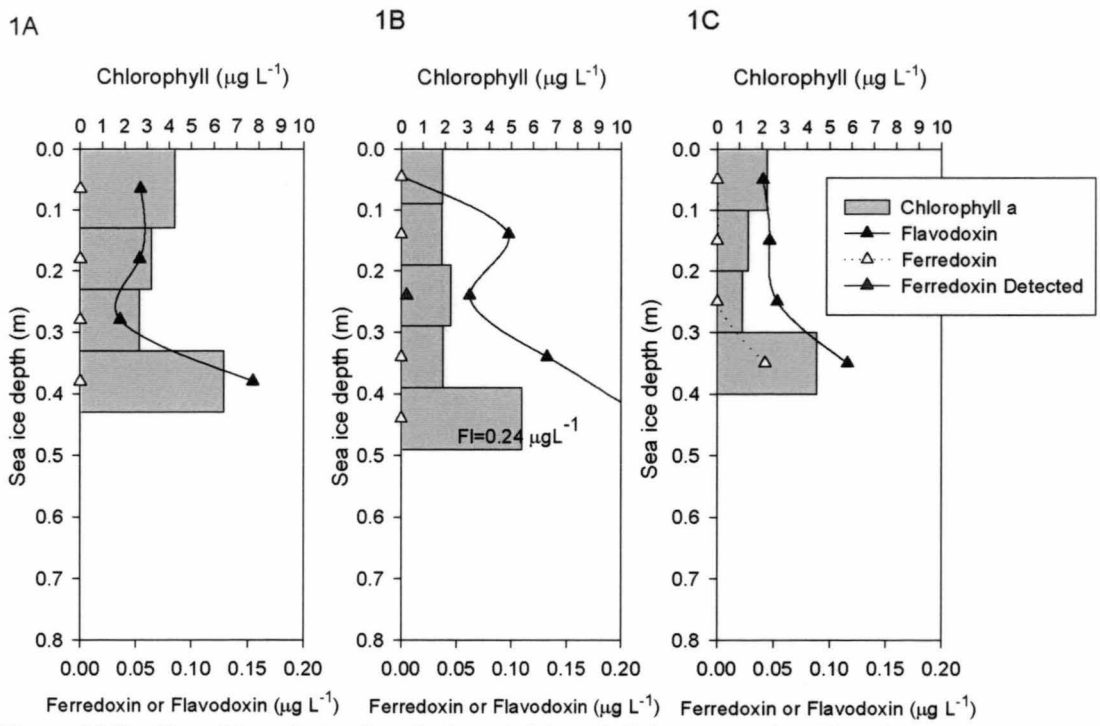

Figure 5.2 Profiles of ferredoxin, flavodoxin and chlorophyll from cores 1A, 1B and 1C.

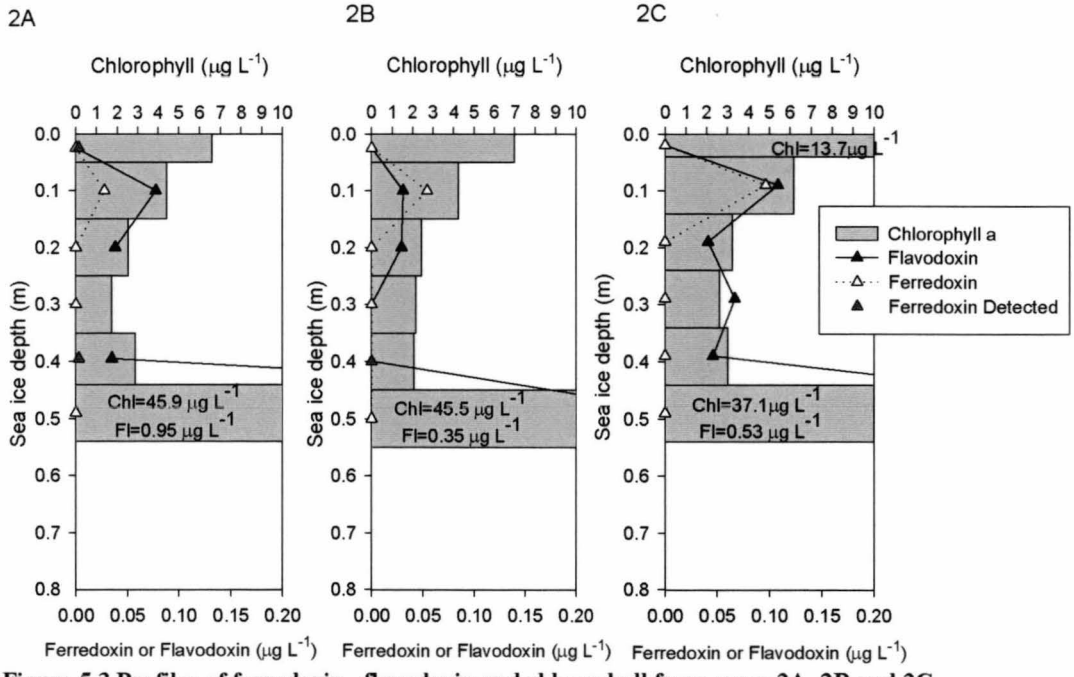

Figure 5.3 Profiles of ferredoxin, flavodoxin and chlorophyll from cores 2A, 2B and 2C.

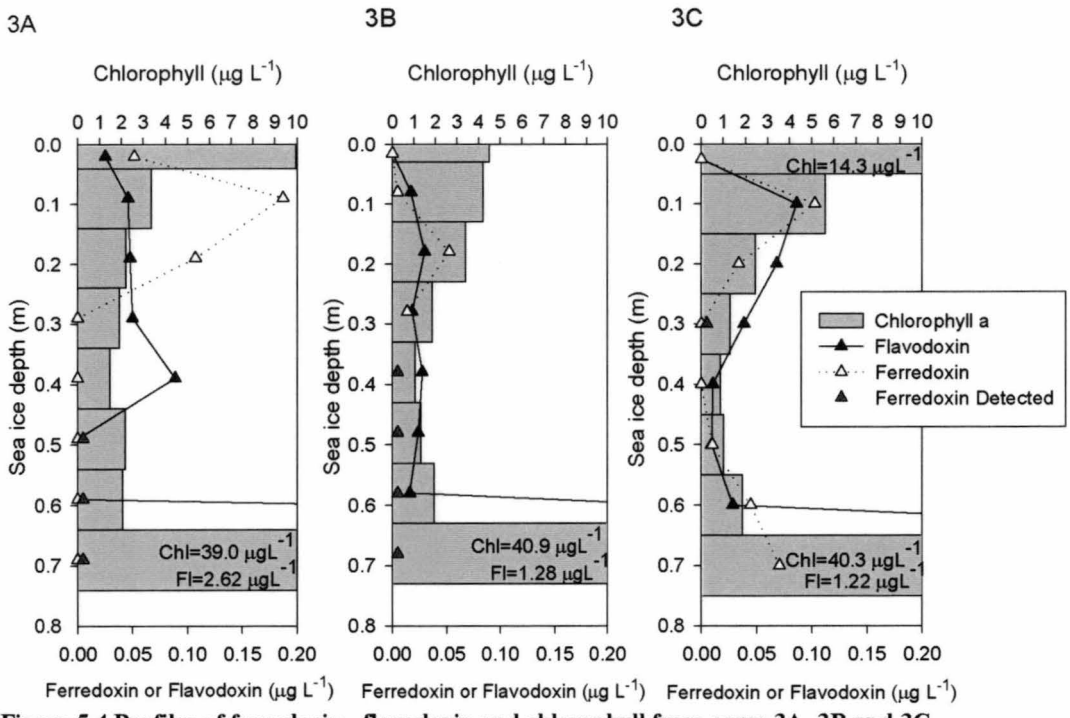

Figure 5.4 Profiles of ferredoxin, flavodoxin and chlorophyll from cores 3A, 3B and 3C.

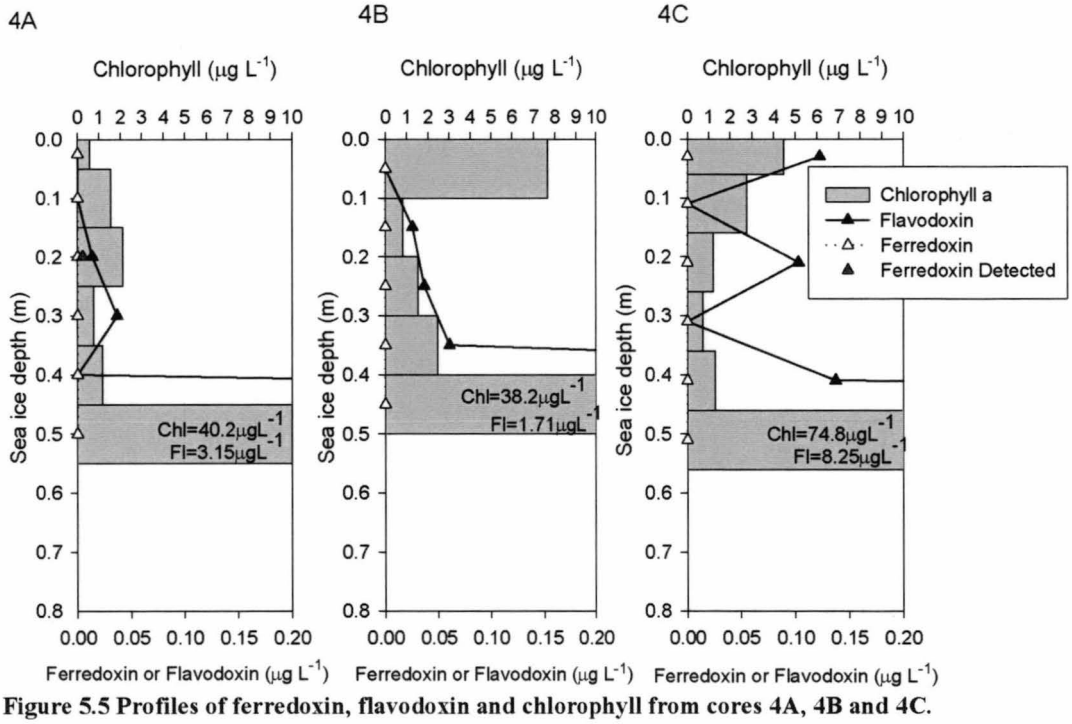

Figure 5.5 Profiles of ferredoxin, flavodoxin and chlorophyll from cores 4A, 4B and 4C.

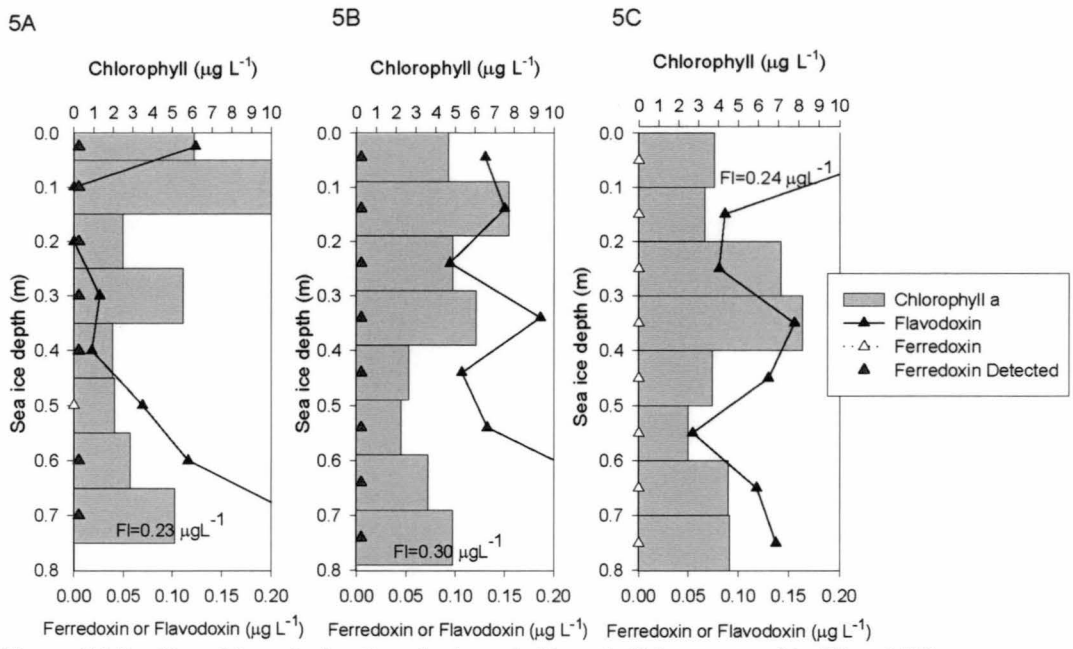

Figure 5.6 Profiles of ferredoxin, flavodoxin and chlorophyll from cores 5A, 5B and 5C.

Replicate cores from each floe generally showed similar distributions and concentrations of ferredoxin and flavodoxin. The range of flavodoxin concentrations observed in all samples in which flavodoxin was quantified was 9 to 8247 ng L^{-1}. This range of values is similar to the highly variable distribution of chl *a* within these core sections (0.75- 75 µg L^{-1}). For these samples, flavodoxin concentrations correlated significantly with both chl *a* and total protein (Pearson r= 0.806; n=76; p<0.001);(Pearson r= 0.851; n=76; p<0.001). The mean ratio of chl *a* to flavodoxin was 59 µg chl *a* (µg flavodoxin)$^{-1}$ (SD=58) and flavodoxin on average constituted 0.064 % (SD=0.050) of total protein.

In samples that contained quantifiable ferredoxin (n=13) the range of concentrations observed was smaller than that of flavodoxin (13.6 ng L^{-1} to 187 ng L^{-1}, mean 68 ng L^{-1} (SD=46)). However, the larger range and higher maximum protein concentrations observed for flavodoxin was due to the occurrence this protein in the dense bottom communities. These communities were not observed to contain significant ferredoxin. Removal of these high biomass bottom sections from the flavodoxin results, brings the flavodoxin concentrations down to similar levels

observed for ferredoxin (range 9-245 ng L^{-1}, mean 72 ng L^{-1}, (SD=53)). Chlorophyll and ferredoxin or protein and ferredoxin were not significantly correlated (Pearsons r=0.030; n=13; p=0.922), (Pearsons r=0.066; n=13; p=0.83). The mean ratio of chlorophyll to ferredoxin was 121 ug chl *a* (μg ferredoxin)$^{-1}$ (SD=144) and this protein represented 0.04% of total protein (SD=0.028). Samples that contained quantifiable amounts of ferredoxin also contained significant amounts of flavodoxin, however there was no correlation between the concentration of these two proteins (Pearsons r=0.03;n=13; p=0.923).

5.3.4 Significance of differences in patterns of ferredoxin and flavodoxin expression

The majority of core sections processed fell into one of the following three categories.

Those that contained quantifiable amounts of both ferredoxin and flavodoxin (n=13).

Those that contained quantifiable amounts or flavodoxin with detectable amounts of ferredoxin (n=23).

Those that contained quantifiable amounts of flavodoxin only (n=46).

Comparisons were made between these three categories to determine the significance of these patterns of expression.

5.3.4.1 Protein load

The lower limit of detection of the immunoassay is ultimately determined by the amount of biomass that can be concentrated on a membrane, which dictates how much protein is available to load onto gels Processing of cores did not always result in sufficient protein to enable gels to be loaded with maximum amounts of protein

(40 µg). Protein load was compared for categories 1, 2 and 3 in order to determine if variable protein load contributed to the observed patterns of expression.

The amount of protein loaded onto gels for each sample category are represented with box and whisker plots in Figure 5.7. Plots for the three categories show that the amount of protein loaded for samples in each category had similar distributions. Furthermore, there was no significant difference in the mean amount of protein loaded for each category (One way ANOVA, n=82, p=0.906).

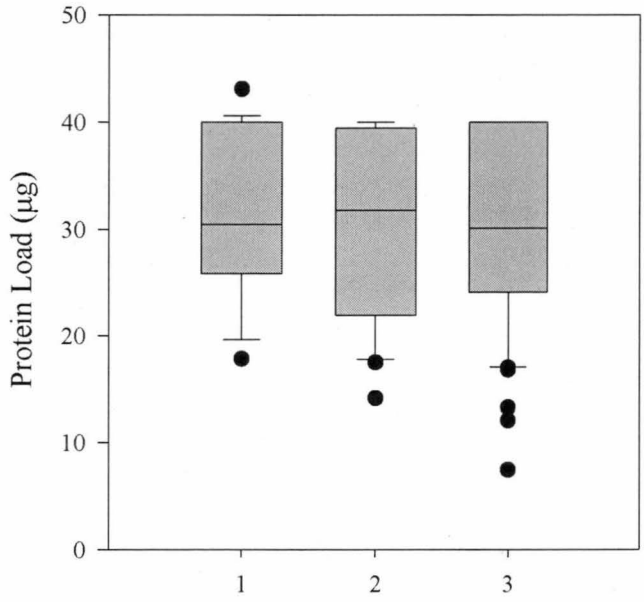

1= quantifiable ferredoxin and flavodoxin
2= quantifiable flavodoxin and detectable ferredoxin
3= quantifiable flavodoxin only

Figure 5.7 Box and whisker plots showing amount of protein loaded onto gels for samples that fell into the three dominant categories of protein expression. The centre line of the boxes indicate the median protein load for each category. Top and bottom box edges represent the 25th and 75th percentile values and the ends of the whiskers show the protein loads of the 10th and 90th percentile values. Dots represent outlier values.

5.3.4.2 Chlorophyll:Flavodoxin and Protein:Flavodoxin

The chlorophyll:flavodoxin ratio for samples in each category are represented with box and whisker plots in Figure 5.8. This ratio was highest for samples that contained quantifiable amounts of ferredoxin. The ratio for category 1 (quantifiable

ferredoxin and flavodoxin) was significantly different from that of category 3 (quantifiable flavodoxin only) (ANOVA, planned comparison, df=12.8, $p<0.1$, unequal variances assumed). Other pairs of categories were not significantly different from one another. This shows that when ferredoxin was present in significant amounts there is a clear replacement of flavodoxin. Analogous results were observed for the protein:flavodoxin ratio (not shown).

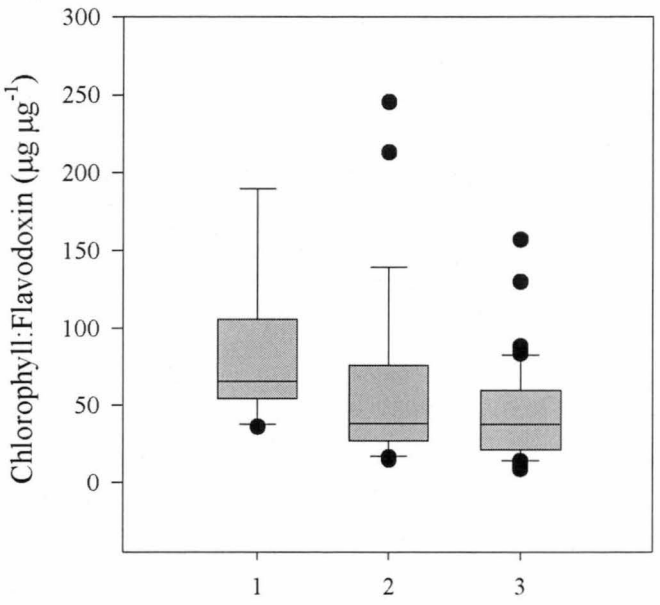

1= quantifiable ferredoxin and flavodoxin
2= quantifiable flavodoxin and detectable ferredoxin
3= quantifiable flavodoxin only

Figure 5.8 Box and whisker plots showing chlorophyll:flavodoxin ratios for samples that fell into the three dominant categories of protein expression. The centre line of the boxes indicate the median protein load for each category. Top and bottom box edges represent the 25th and 75th percentile values and the ends of the whiskers show the protein loads of the 10th and 90th percentile values. Dots represent outlier values.

5.3.4.3 Flavodoxin:Ferredoxin

Box and whisker plots of the flavodoxin:ferredoxin ratio are shown for the two categories that contained this protein (Figure 5.9). For samples that contained quantifiable amounts of ferredoxin the ratio was calculated from actual ferredoxin and flavodoxin concentrations determined by densitometry. Although an exact value cannot be placed on the amount of ferredoxin in samples with only detectable

quantities of this protein, the lowest ferredoxin standard loaded on gels was 5 ng. This amount was that found to be reliably detected in western blots. If it is assumed that detectable amounts of ferredoxin were below 4 ng, flavodoxin:ferredoxin ratios can be calculated for these samples based on actual flavodoxin staining intensity and an assumed maximum ferredoxin band intensity of 4 ng. The ratio calculated for samples in this category therefore represent the lowest probable ratio, in reality values for some samples would likely be higher.

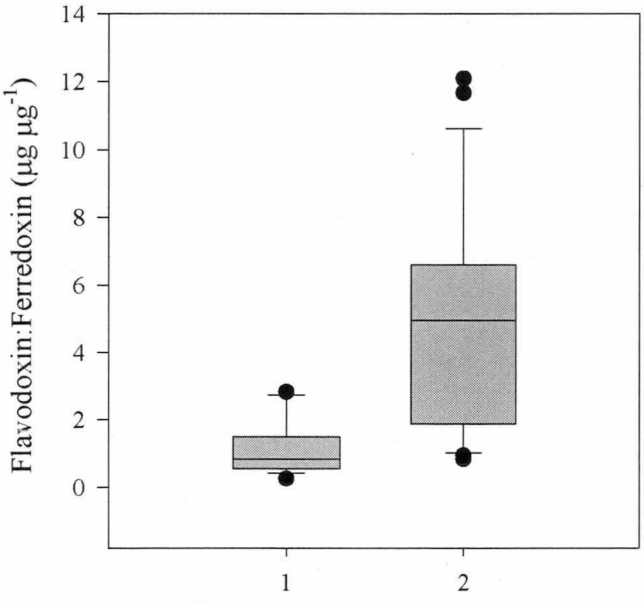

1= quantifiable ferredoxin and flavodoxin
2= quantifiable flavodoxin and detectable ferredoxin

Figure 5.9 Flavodoxin ferredoxin ratios for samples that contained quantifiable ferredoxin (actual ratio) and samples that contained detectable ferredoxin (estimated ratio). The centre line of the boxes indicate the median protein load for each category. Top and bottom box edges represent the 25th and 75th percentile values and the ends of the whiskers show the protein loads of the 10th and 90th percentile values. Dots represent outlier values.

Mean flavodoxin:ferredoxin value of samples containing only detectable amounts of ferredoxin was 5 (SD=3.4) with a range from 0.83 to 12.1. In samples that contained quantifiable ferredoxin, apart from one sample from the bottom of core 3C which had a very high flavodoxin:ferredoxin ratio of 18, the remaining samples with quantifiable ferredoxin and flavodoxin had ratios in the range of 0.25 to 2.8 with a mean ratio of 1.13 (SD=0.85). The differences observed for the two categories were

highly significant (ANOVA, df=35, $p<0.001$) and demonstrate that when the protein was detected in amounts less than the lowest standard it was present as a significantly smaller percentage of the combined flavodoxin + ferredoxin pool than when it was detected in quantifiable amounts.

5.3.5 Distribution of ferredoxin and flavodoxin

A summary of the distribution of samples containing quantifiable flavodoxin only, quantifiable flavodoxin with detectable ferredoxin and quantifiable ferredoxin and flavodoxin is presented in Table 5.3. High concentrations of ferredoxin were predominantly derived from core sections from station 3. Profiles of these cores (Figure 5.4) show that these high concentrations were located in the upper portion of this floe. This floe also produced a considerable number of samples that contained detectable amounts of ferredoxin. Core sections from the upper ice at station 2 were also observed to contain high concentrations of ferredoxin. Significant quantities of this protein were not associated with any of the other floes, however small amounts were detected in a significant number of core sections throughout the profile of floes from station 5.

Table 5.3 Summary of ferredoxin distribution in core sections derived from derived from five ice floes.

Floe	Ferredoxin quantified	Ferredoxin detected but not quantifiable	Ferredoxin not detected	Total
1	1	1	10	12
2	3	1	8	12
3	9	8	3	22
4	0	0	11	11
5	0	13	9	22
Total	13	23	41	77

One notable observation is the lack of significant ferredoxin expression in the high biomass bottom communities that were evident at sites 2, 3 and 4. The profiles presented for station 3 (Figure 5.4) suggest that all bottom sections from this site contained ferredoxin. However these detections did not occur in the bottom 2 cm of these cores but were observed in the 8 cm interval higher in the core. For these cores this bottom 2 cm contained 86% (SD= 2.8) of the chl *a* in the bottom 10 cm of the core.

5.3.6 Species composition

Species composition was determined for samples taken from cores at stations one and three only. The community inhabiting the relatively thin ice at station one (Table 5.4) was numerically dominated by *Fragilariopsis cylindrus* which generally comprised greater than 50% of the species count throughout the floe. Towards the bottom half of this floe *Cylindrotheca closterium* made a significant contribution to the biomass whereas in the top half of the floe other *Fragilariopsis* species including *F. curta* and *F. sublineuris* comprised the bulk of the balance of the species count

Table 5.4 Species composition of core taken at station 1.

Interval (cm from surface)	**30-40**	**20-30**	**10-20**	**0-10**
Fragilariopsis cylindrus (%)	57	67	23	50
Cylindrotheca closterium (%)	24	18	38	2
Other *Fragilariopsis sp* (%)	10	5	32	45
Other Species (%)	9	10	7	3

Table 5.5 Species composition of core taken at station 3.

Interval (cm from surface)	78-80	70-78	60-70	50-60	40-50	30-40	20-30	10-20	0-10
Entomeneis kjellmanii (%)	5	4	0	0	2	1	0	0	0
Fragilariopsis curta (%)	18	15	10	3	7	4	0	0	1
Fragilariopsis cylindrus (%)	37	26	21	42	37	27	54	75	96
Other *Fragilariopsis* (%)	4	4	2	5	4	9	11	16	1
Cylindrotheca closterium (%)	10	1	3	6	25	35	23	4	0
Pseudonitzschia sp (%)	8	26	38	17	1	2	0	0	1
Nitzschia lecointei (%)	8	19	23	22	15	8	3	1	0
Other (%)	8	5	4	4	9	14	8	5	1

The species composition at station three was more diverse than at station 1, particularly towards the ice water interface. Again *Fragilariopsis cylindrus* was a dominant organism at this location. Of particular note, this species increased in relative abundance towards the surface of the floe where the community was almost mono-specific for this species.

5.4 Discussion

5.4.1 Flavodoxin expression

The expression of flavodoxin is a common response to low iron availability in a number of marine microalgal taxa but has predominantly been studied in marine diatoms (Doucette *et al.*, 1996; Erdner *et al.*, 1999; La Roche *et al.*, 1995, McKay *et al.*, 1997; McKay *et al.*, 1999). This protein has been detected in natural phytoplankton communities, for example, in the northeast Pacific ocean where the abundance of flavodoxin was shown to vary inversely with the concentration of dissolved iron (La Roche *et al.*, 1996). During the study by La Roche *et al.* (1996) flavodoxin levels were observed to decrease when water samples containing iron

stressed phytoplankton were enriched with iron (La Roche *et al.*, 1996). These observations led the authors to suggest that flavodoxin could be used as an *in situ* marker for iron stress.

In the present study flavodoxin was detected in the majority of samples throughout the profile of ice cores from Eastern Antarctica. The widespread distribution of flavodoxin would at first appear to suggest that microalgae in sea ice commonly suffer from iron stress. However many of the diatoms identified (e.g. *Fragilariopsis curta*, *Cylindrotheca closterium* and *Nitzschia lecointei*) express flavodoxin under iron replete conditions in laboratory cultures (Chapter 3). Furthermore, the majority of samples that contained ferredoxin also contained significant amounts of flavodoxin. Hence, the significant correlation between flavodoxin and measures of biomass (chlorophyll and protein) is more likely to be the result of widespread constitutive flavodoxin expression amongst diatoms that commonly inhabit sea ice.

Similar constitutive flavodoxin expression has been observed in at least two temperate diatom species (La Roche *et al.*, 1995; McKay *et al.*, 2000). Sustained or even increased flavodoxin levels have been observed after iron enrichment during several iron enrichment bioassay experiments (Boyd *et al.*, 2000; Erdner & Anderson, 1999; Timmermans *et al.*, 1998). Such results have usually been attributed to incomplete alleviation of iron stress. For example, during the first mesoscale iron enrichment experiment in the Southern Ocean (SOIREE) (Boyd *et al.*, 2000) flavodoxin expression persisted following iron enrichment despite other parameters suggesting that the community had been released from iron limitation. However, sustained flavodoxin expression could equally have resulted from the presence of diatoms that express this protein constitutively. In contrast, complete suppression of flavodoxin expression and the induction of ferredoxin was observed in an iron enriched mesocosm experiment conducted in Subantarctic waters (Boyd *et al.*, 1999). These contrasting results suggest that the species composition is likely to play a major role in the observed patterns of ferredoxin and flavodoxin expression.

As such, experiments conducted on natural samples of microalgae must be interpreted with caution.

5.4.2 Ferredoxin expression

The distribution of ferredoxin in pack ice cores was more heterogeneous than flavodoxin. The majority of samples fell into one of three categories. In all three categories there was significant flavodoxin expression but some samples contained quantifiable amounts of ferredoxin, in others ferredoxin was detected but the concentration was below the limit of quantitation, and in other samples ferredoxin was absent.

The concentration of total protein in the final extract was often too low to allow gels to be loaded with the maximum amount of protein. This occurred as a result of both low levels of biomass within core sections and because membranes became clogged during the filtration process, resulting in less then ideal amounts of biomass on some membranes. Because of the sub optimal amount of protein loaded for some samples there was some concern that the observed heterogeneity of ferredoxin expression may have resulted from unequal sample loading.

Comparison of the amount of protein loaded for samples that contained only detectable amounts of ferredoxin with samples that contained significant (quantifiable) amounts of ferredoxin showed that there was no significant difference in protein load for these categories. Hence the observed patterns of expression were not an artefact of sample loading.

Substitution of ferredoxin for flavodoxin is a more likely explanation for the differences. Evidence for this substitution can be seen in sea ice core sections that contained quantifiable amounts of ferredoxin where this protein constituted a larger fraction of the combined ferredoxin + flavodoxin pool than samples in which ferredoxin was detected in low amounts. Further to this, highest ferredoxin

concentrations also coincided with reduced biomass specific levels of flavodoxin compared to samples with flavodoxin only.

It has generally been shown that ferredoxin is replaced by flavodoxin under iron stress in marine phytoplankton (Erdner & Anderson, 1999; Erdner *et al.*, 1999; McKay *et al.*, 1999). Furthermore, a number of species which produce ferredoxin under iron replete conditions and flavodoxin under iron stress express both proteins under moderate iron stress (Doucette *et al.*, 1996; Erdner *et al.*, 1999; McKay *et al.*, 1999)(Chapter 3). In such species the relative abundance of these two proteins has been suggested to be a better indicator of the degree of iron stress than flavodoxin alone (Doucette *et al.*, 1996). However, in the present study the observed variability in the flavodoxin·ferredoxin ratio may not simply reflect the iron nutritional status of the community, but could in part result from changes in the abundance of species capable of expressing ferredoxin. There is some evidence of a species effect in cores from station 3 with the greatest abundance of *Fragilariopsis cylindrus* coinciding with high ferredoxin levels in the upper ice at this floe. In laboratory culture this species expresses only ferredoxin under iron replete conditions, gradually replacing this protein with flavodoxin as iron availability decreases (Chapter 4). Despite the fact that the concentration of this protein could be influenced by species composition, the high abundance of this protein in the upper ice at this site, in conjunction with a relatively simple species composition is a clear indication that a significant proportion of the organisms inhabiting this community had access to an ample supply of iron.

In contrast, the community inhabiting the extreme bottom of this floe showed a distinct absence of ferredoxin. All samples generated from this bottom section of each ice core contained sufficient biomass to enable gels to be loaded with maximum amounts of protein, and a distinct flavodoxin band was evident in western blots from these samples Species capable of producing ferredoxin, including *Fragilariopsis cylindrus*, *Cylindrotheca closterium* and *Nitzschia lecointei* constituted greater than

50% of the species count in this community. The lack of ferredoxin expression in the bottom community at this site suggests that the availability of iron is suboptimal.

Similarly samples derived from station 1 were all numerically dominated by *F. cylindrus* and *C. closterium* which together comprised greater than 50% of the population. However, the absence of ferredoxin in the majority of samples derived from this floe suggests that the community was experiencing some degree of iron stress.

For samples that contained low amounts of ferredoxin (i.e. detectable but below quantitation) the flavodoxin:ferredoxin ratio was substantially higher than samples containing quantifiable amounts ferredoxin. The significance of these low ferredoxin samples is unclear. Low concentrations of this protein could conceivably result from an iron limited community which contains a relatively low abundance of species that are incapable of replacing ferredoxin with flavodoxin, i.e. organisms that continue to express this protein when suffering from iron stress. Some temperate phytoplankton sustain expression of this protein when suffering the effects of low iron availability (Erdner *et al.*, 1999).

Samples from station three, that contained small amounts of ferredoxin, had a species composition similar to core sections above and below these samples which expressed flavodoxin only. In these core sections, derived from the lower half of the floe at station 3, organisms capable of expressing ferredoxin (*Fragilariopsis cylindrus, Cylindrotheca closterium* and *Nitzschia lecointei*) generally constituted around 50% of the total species count, similar to what was observed for bottom community at this site. It appears that organisms inhabiting this region of the floe, where small amounts of ferredoxin were detected, may have experienced reduced iron supply similar to bottom communities at this site. However, if the observed low levels of ferredoxin expression are a true indicator physiological state the degree or iron stress would be low and unlikely to limit growth (Chapter 4).

5.4.3 Iron availability in bottom communities compared to surface communities

The highest concentration of biomass was found within bottom communities at the three southern most sites (stations 2, 3 and 4). Such bottom communities are dominant in Eastern Antarctica where it is estimated that they contribute around 76% of total primary production (Grose & McMinn, 2003). The algal standing stocks observed at the southern sites during this study are typical for sea ice in Eastern Antarctica (Grose & McMinn, 2003) and about twice the level observed for bottom communities in the Ross Sea at a similar time of year, where bottom communities were also dominant (Arrigo *et al.*, 2003a).

Despite greater than 75% of the chlorophyll specific biomass occurring in these bottom communities ferredoxin expression was not observed suggesting that iron was not available in replete amounts. Samples derived from these high biomass bottom communities provided sufficient biomass to enable gels to be loaded with the maximum amount of protein (40 μg). Hence the lack of ferredoxin detection was not caused by inadequate amounts of sample and is more likely to reflect a lack of expression of this protein by the community. Within the community from station 3 species that are known to express ferredoxin such as *Cylindrotheca closterium*, *Entomeneis kjellmanii*, *Fragilariopsis cylindrus* and *Nitzschia lecointei* constituted approximately 60% of the population. Based on the flavodoxin band intensity from these samples and a lower limit of detection of 2.5 ng for ferredoxin it can calculated that if ferredoxin was present the abundance of this protein was less than $1/10^{th}$ that of flavodoxin. A flavodoxin:ferredoxin ratio of 10 is well above the mean ratio and range for all samples in which ferredoxin was quantified (mean 1.14 range 0.25-2.8) and above the estimated mean ratio for samples that contained detectable ferredoxin (mean 5) and close to the 90^{th} percentile value for this category (10.3).

A lack of ferredoxin expression in these communities and the presence of distinct amounts of this protein higher in the floe suggests differences in iron supply to these

communities. Interior communities near the floe surface have available replete amounts of iron whereas bottom communities from the same location have a sub optimal supply of this trace nutrient. However, despite the higher availability of iron in the upper ice the accumulation of biomass within this portion of the floe was limited compared to bottom communities. This is despite the fact that communities within the upper portions of ice 0.5-0.7 m may have had substantially longer to develop than bottom communities.

These observations suggest that factors other than iron are limiting the growth of organisms within the upper ice at this location. Several studies which measured macronutrients in brine samples from Antarctic pack ice noted that macronutrients were not depleted to the point of limiting growth (Arrigo *et al.*, 2003a; Trevena *et al.*, 2000). However in pack ice surface communities both nitrate and phosphate depletion has been observed (Kristiansen *et al.*, 1998; Syvertsen & Kristiansen, 1993). The studies that observed macronutrient depletion in surface communities also observed decreases in nutrient concentrations at distance from the floe edge (Kristiansen *et al.*, 1998; Syvertsen & Kristiansen, 1993). The latter author suggested that typical pre spring nitrate concentrations of 30-35 μmol L^{-1} can produce algal biomass of 50 μg L^{-1} (Syvertsen & Kristiansen, 1993). In all core sections other than those with bottom communities chlorophyll concentrations were generally well below 10 μg L^{-1}.

Temperature is the other dominant factor that may limit biomass in these surface communities, which inhabit the coldest regions of the ice where temperatures can fall to below -20° C. Results obtained by Mock, (2002) while conducting *in situ* primary production measurements during autumn in the Weddell Sea suggest that upper ice communities were limited by high brine salinities and low temperature. Similar limitation by low temperatures and high salinity may have contributed to the low biomass in iron replete communities observed in the upper ice during the present study.

Although indicating that iron is in reduced supply, the lack of ferredoxin expression in bottom communities does not necessarily imply that growth rates are limited by this micronutrient. In these communities macronutrients definitely do not limit growth as they remain high in the water column year round (Trull *et al.*, 2001). In cultures of *Fragilariopsis cylindrus* complete replacement of ferredoxin expression by flavodoxin occurred before any reductions in growth rate were observed (Chapter 4). Hence ferredoxin can be completely replaced by flavodoxin but growth can continue at maximum rates.

The location of the floe sampled to the extreme north coincides with the Southern Boundary of the Antarctic Circumpolar Current (Bindoff *et al.*, 2000) and the southern most sites were in waters immediately north of the continental shelf. Measurements of surface water dissolved iron concentrations in this same region during December found that concentrations were generally below 0.2 nM (Sambrotto *et al.*, 2003). However some waters with higher iron concentrations (0.5 nM) were identified to the east of the Mertz glacier tongue and the authors suggested that these higher levels may be typical throughout the region earlier in the season prior to the onset of phytoplankton blooms which utilise this iron In this region nutrient rich upper circumpolar deep water intrudes onto the shelf during winter where it remains identifiable as highly modified upper circumpolar deep water (Bindoff *et al.*, 2001). Sambrotto *et al.* (2003) suggest that surface waters in this region may be replenished with iron through entrainment of deep water through mixing, resulting from the influence of strong katabatic winds. However, despite this likely supply of iron into surface waters, algae inhabiting bottom communities in this region appear to have access to suboptimal amounts of iron.

Increased iron availability in interior communities in the upper ice at this location suggests that either the upper ice was formed in waters which contain significantly greater concentrations of iron or that during sea ice formation iron becomes more biologically available in ice. Higher iron concentrations in surface ice due to

formation of the ice in other locations cannot be ruled out. Floes sampled at the southern locations were likely to have originated further in the east. Sambrotto *et al.* (2003) noted that ice was advected into this same region from the north east. However, other processes occurring during ice formation and modification are more likely sources of iron.

During ice formation seawater salts and nutrients are concentrated in brines leading to nutrient concentrations that are elevated relative to those in the seawater from which the ice forms (Eicken, 2003). For the majority of ions the degree of concentration is proportional to the increase in salinity (Eicken, 2003). In the coldest parts of floes near the surface salinities above 100 ‰ are common (Gleitz *et al.*, 1995). Iron is predominantly bound to strong organic ligands in seawater (Ussher *et al.*, 2004). Although little is known about how iron speciation is affected by increases in salinity such a threefold concentration effect could potentially elevate iron concentrations in sea ice brines to levels above those required to limit growth rates. Lytle *et al.* (2001) also identified that snow was commonly incorporation into sea ice forming in the Mertz glacier region with 16 out of 22 ice cores having snow incorporated into the top few centimetres Edwards & Sedwick (2001) identified significant concentrations of iron in snow from Eastern Antarctica with concentrations as high as 53 nM reported for some samples. Although low dissolved iron concentrations (0.36 nM) were detected in snow from the region around 140°E the authors suggested that these low concentrations resulted from inter annual variation rather than regional variation (Edwards & Sedwick, 2001). High concentrations of this micronutrient have also been measured in snow on sea ice in other regions of the Southern Ocean (Loscher *et al.*, 1997; Sedwick *et al.*, 2000). The final factor that may contribute significant iron into sea ice may be the incorporation of sediments and other particulate material. Several authors have provided indirect evidence that sea ice may contain significant quantities of sediment derived iron (Sedwick & DiTullio, 1997). Additionally, during sea ice formation it is

known that algal cells can become enriched in sea ice as they adhere to frazil ice crystals which form in the upper water column (Garrison *et al.*, 1983). The incorporation of such material into sea ice and subsequent regeneration of this cellular material would serve to further elevate iron concentrations in sea ice brines. The observation that not all communities inhabiting the upper sea ice produced significant amounts of ferredoxin suggests that either elevated iron concentrations are not universal in the upper sea ice or that there is substantial heterogeneity in the availability of this iron.

Both ferredoxin and flavodoxin have been detected in sea ice cores from Eastern Antarctica. Although it appears that the presence of flavodoxin does not indicate iron stress in these communities the detection of this protein in combination with ferredoxin provides some information about the iron nutritional status of the community. The absence of ferredoxin is likely to indicate a reduced supply of iron. However the significance of this reduced iron supply cannot be inferred on the basis of protein expression alone To determine the significance of the lower availability of iron in these communities other methods will need to be employed. The use of alternate protein or RNA markers for iron limitation is one possible avenue for further study. However to provide more useful information on the degree of iron stress in these communities, markers must be carefully validated in laboratory cultures of key sea ice species such as *Fragilariopsis cylindrus*. Because of its almost ubiquitous distribution in Antarctic sea ice, RNA probes targeted at iron regulated genes from this species may provide a way to investigate the availability of iron in sea ice. Designing RNA probes that target genes from a single species such as *F. cylindrus* would overcome the confounding effects of differential regulation of certain genes in different algal species

Chapter 6 : Conclusions and future research

A sensitive western blot immunoassay for ferredoxin and flavodoxin was developed using antibodies generated towards the proteins from *Cylindrotheca closterium.* These immunoassays were used to characterise the expression of these proteins in Antarctic sea ice diatoms both *in vitro* and *in situ.*

Good antibody cross reactivity was observed with a range of Antarctic sea ice diatoms as well as several sea ice diatoms of Arctic origin. This demonstrates that the amino acid sequences for these proteins are highly conserved. However, the expression of ferredoxin and flavodoxin shows substantial heterogeneity in these organisms. Some species grown under iron replete conditions express ferredoxin without flavodoxin, the situation expected from previously conducted work on temperate diatoms. However, equally common in organisms from this habitat are both the expression of flavodoxin only, and the expression of both ferredoxin and flavodoxin under iron replete growth. This permanent, full or part substitution of ferredoxin for flavodoxin would reduce the organisms demand for iron and suggests that there has been significant evolutionary pressure on these organisms to reduce their iron quotas.

Two closely related diatoms that dominate Antarctic pack ice, *Fragilariopsis cylindrus* and *Fragilariopsis curta,* show vastly different expression of these proteins. Under iron replete growth *F. cylindrus* expresses only ferredoxin, which is incrementally replaced by flavodoxin under condition where iron availability is reduced. The level of iron stress required to cause full substitution of ferredoxin for flavodoxin does not significantly impair growth or photosynthesis in this organism.

As such flavodoxin expression indicates iron stress rather than iron limited growth in this species, whereas the presence of ferredoxin indicates that the growth of this organism is not limited by iron availability In contrast, *F curta* has lost the ability to express ferredoxin and the level of flavodoxin expression in this organism is not influenced by iron availability.

Despite differences in ferredoxin and flavodoxin expression other effects of reduced iron supply on these two species are remarkably similar. Both organisms have similar K_m for growth in relation to total inorganic iron concentration (K_m [Fe']). The slower maximum specific growth rate of *F. curta* enables this larger organism to achieve a similar K_m to that of the smaller *F. cylindrus*. Both organisms growing near their K_m [Fe'] under iron limitation showed reductions of around 50% in the photosynthetic parameters Fv/Fm, alpha, and $rETR_{max}$ compared to iron replete cultures. Furthermore, at this degree of iron limitation *F. cylindrus* and *F. curta* cells had half the chlorophyll content of iron replete cells and a reduced capacity to develop non-photochemical quenching.

Iron limited *F. cylindrus* and *F. curta* have a greater capacity for electrons transport downstream of photosystem two (PS II) than photon capture at PS II. In combination with the observed decreases in Fv/Fm and alpha this suggest that reduced iron availability predominantly causes alterations to PS II which results in an impaired ability to capture light

During recovery of *F. cylindrus* from iron limitation Fv/Fm, alpha and $rETR_{max}$ recover with faster kinetics than replacement of flavodoxin for ferredoxin or chlorophyll synthesis. This suggests that restoration of the ability to undergo primary charge separation at PSII is the main priority in recovering from iron stress. Furthermore, little alteration to ferredoxin levels occurred within twelve hours of iron resupply. Hence, when analysing ferredoxin and flavodoxin in natural sea ice

samples the process of melting ice cores to extract algal cells is not likely to change the *in situ* levels of expression of these proteins.

Analysis of ferredoxin and flavodoxin in sea ice cores has provided confirmation of widespread constitutive flavodoxin expression in Antarctic sea ice diatoms *in situ*. Both proteins were observed in these communities with flavodoxin being detected in the majority of ice core sections analysed, including those sections of cores in which substantial amounts of ferredoxin were observed. Furthermore, flavodoxin concentrations correlated significantly with measures of biomass.

Compared to flavodoxin the distribution of ferredoxin is more heterogeneous in Antarctic sea ice microalgal communities. It was found to be absent from some core sections, present as a significant proportion of the combined ferredoxin + flavodoxin pool in others and detected as a small component of the combined ferredoxin + flavodoxin pool in a third fraction of the ice core sections analysed. Inferring iron nutritional status of the sea ice algal community from the ferredoxin abundance data is complicated by the variable species composition of sea ice which may cause the relative flavodoxin:ferredoxin ratio to change in the absence of any significant iron stress.

The significance of samples which contain ferredoxin as a minor component of the ferredoxin + flavodoxin pool is uncertain. In these samples low but detectable ferredoxin levels could arise from the presence of organisms that maintain ferredoxin expression under iron stress (i.e. organisms with a non repressible ferredoxin), or alternately these low levels may result from the community suffering from moderate levels of iron stress which cause the partial substitution of ferredoxin for flavodoxin.

In sea ice cores substantial ferredoxin expression most probably signifies a community with access to an ample supply of iron. Conversely, the expression of flavodoxin only is likely to arise from reduced iron availability. However, because complete substitution of ferredoxin for flavodoxin occurs with very mild levels of

iron stress the environmental significance of this reduced iron supply remains to be elucidated.

Communities which expressed high levels of ferredoxin and that were likely to have access to replete amounts of iron were associated with the upper ice at floes sampled close to the Antarctic continental shelf. Likely sources of iron for these communities include the overlying snow cover which may have also been incorporated into the upper ice as snow-ice. In the upper sea ice elevated concentrations of iron may also result through brine concentration. Particulate material derived from sediments or the biota may also contribute to the pool of biologically available iron after being solubilised by biological and physico-chemical processes. However, the upper sea ice is not iron replete throughout this region with other floes showing the absence of significant quantities of ferredoxin in samples derived from the upper ice. This shows that ability of organisms to access iron in the upper ice is likely to be highly variable.

The absence of ferredoxin in the high biomass bottom communities of the same floes, which had replete amounts of iron in the upper sea ice, further suggests that there is substantial spatial heterogeneity in the availability of iron in sea ice, even at scales of meters to centimetres. Being located near the edge of the continental shelf these waters are likely to experience iron concentrations which are towards the upper end of the range of concentrations in Antarctic waters. Despite the relatively high iron concentrations experienced by these bottom communities, and favourable conditions for the exchange of nutrients with the water column, iron supply was still sub optimal. These results suggest that diatoms growing on the underside of sea ice are likely to experience some degree of iron stress throughout much of the Southern Ocean. However, the degree of iron stress experience by the communities examined near the continental shelf is likely to be low as approximately 75% of the biomass in these floes was concentrated in this "iron stressed" bottom community.

Two limitations of this method are its inability to determine the level of stress experienced by communities which were found to have a sub optimal supply of iron, and uncertainties in the significance of iron stress in communities which were found to express small amounts of ferredoxin. However, the study of ferredoxin and flavodoxin in sea ice microalgae both *in situ* and *in vitro* has provided significant guidance for further research into the role of iron in sea ice microalgal communities.

The present study has demonstrated that the availability of iron in sea ice shows substantial spatial heterogeneity over scales as small as centimetres. In order to gain an appreciation of the widespread availability of iron in sea ice a larger number of sea ice samples will need to be examined. The methods employed for such a task will need to be capable of high volume sample throughput The western blot approach is limited in this capacity, requiring several days of continuous laboratory work to process samples derived from one or two ice cores.

Development of a microplate format Enzyme Linked Immuno-Sorbant Assay (ELISA) for ferredoxin and flavodoxin would realise this high sample volume capacity. This approach has been used to develop an ELISA with polyclonal antibodies generated towards ferredoxin and flavodoxin from *Scenedesmus vacuolatus* (Inda & Peleato, 2003). The limit of detection of their method was slightly lower than that achieved with the western blot approach used in this study. Such an approach was also trialled with the antibodies generated in this study towards the proteins from *Cylindrotheca closterium.* Although a successful ELISA was developed for flavodoxin with a lower limit of detection similar to that reported by Inda & Peleato (2003) the ferredoxin antibodies proved unsuitable for ELISA development. A better approach, which would achieve high sensitivity and specificity, would be to develop ELISAs for ferredoxin and flavodoxin using monoclonal antibodies. Sandwich ELISAs developed using carefully selected pairs of monoclonal antibodies can attain limits of detection several orders of magnitude lower than that attained using western blot methodology (Harlow & Lane, 1989)

Iron replete *Fragilariopsis cylindrus* and *Fragilariopsis curta* could serve as sources for the proteins ferredoxin and flavodoxin respectively thus avoiding the need to grow large iron limited diatom cultures. Both species are relatively easy to grow in laboratory culture and readily settle out of suspension obviating the need for filtration of large volumes of culture.

Although ELISA approaches could provide rapid assessment of a large number of samples, it would be difficult to resolve the uncertainties resulting from a mixed microalgal community containing species with a constitutive flavodoxin and possibly the existence of other species in sea ice with a ferredoxin which is not suppressible. Although careful selection of monoclonal antibodies could potentially target individual species or wider taxonomic groups, RNA based methods may provide an even more suitable avenue for future studies.

Specific RNA probes could be developed for ferredoxin and flavodoxin genes from key species which dominate in this environment. Targeting individual species rather than wider taxonomic groups would overcome the problems associated with having closely related species with different patterns of expression for ferredoxin and flavodoxin (e g. *Fragilariopsis cylindrus* and *Fragilariopsis curta* which express ferredoxin only and flavodoxin only under iron replete conditions respectively). RNA probes targeted towards ferredoxin and flavodoxin genes from *Fragilariopsis cylindrus* would be a logical first choice because of this species almost ubiquitous distribution (Lizotte, 2001) and the absence of constitutive flavodoxin expression in this organism. Sequence information is currently available for ferredoxin from *Thalassiosira weissflogii* (Gueneau *et al.*, 1998) and *Odontella sinensis* (Kowallik *et al.*, 1995). More recently the entire genome has been sequenced from the diatom *Thalassiosira pseudonana* (Armbrust *et al.*, 2004). Such sequence information could be used to identify conserved regions of the ferredoxin gene enabling the construction of Polymerase Chain Reaction primers which could be used to amplify, and thus identify the relevant gene from sea ice diatoms.

An RNA assay using an approach such as Real Time Polymerase Chain Reaction (RT-PCR) would allow for quantitation of transcript abundance with a high level of sensitivity. One great advantage of this method is that it can amplify low levels of RNA. For example quantitation of RNA transcripts is possible from even single cells (Bustin, 2004). The low amount of biomass required for this type of assays could speed up ice core processing, allowing use of single cells or melted ice scrapings as samples. Thus a large number of samples could be processed rapidly. Species specific assays could also be developed for other key organisms including *Phaeocystis antarctica,* another important contributor to sea ice primary production (Lizotte, 2001). Specific probes designed for a range of organisms will help to gain a better picture of the availability of iron to the whole community. The use of such methods to identify ferredoxin and flavodoxin, in combination with other RNA probes will further elucidate the role of iron in this environment.

In terms of identifying other marker genes for iron limitation, the recent sequencing of the *Thalassiosira pseudonana* genome (Armbrust *et al.*, 2004) will provide a platform to achieve this aim through the development of RNA micro-arrays (Kohane *et al.*, 2003) The study of gene regulation in this species using this micro array technology will revolutionise our understanding of how this organism and other microalgae respond to environmental stresses by allowing the simultaneous study of the regulation of thousands of genes (Kohane *et al.*, 2003). However, studies using this approach to find new markers for iron limited growth will need to explore transcript abundance at several points upon the iron replete-iron limitation continuum. A useful approach could be to follow that taken in this study for *Fragilariopsis cylindrus* and *Fragilariopsis curta* where the onset of iron limitation was defined as occurring when growth rates fell to below 90% of maximum. The concentration of iron required to limit the growth rate to half of the maximum rate (K_m [Fe'] growth) would be an appropriate criterion to set as the physiological state representative of iron limited growth, while a growth rate of 90% maximum would

serve as a physiological state representative of the transition between iron stress and iron limited growth. Comparison of gene expression at the above two points with that which occurs during iron replete growth would be the minimum required to establish robust candidate markers for iron limited growth.

Development of reliable markers for iron limitation are still some time away and will need to be used in conjunction with other methods to gain a full appreciation of the role of iron in the sea ice microalgal community. Modulated fluorescence techniques such as fast repetition rate and pulse amplitude modulated (PAM) fluorometry may be particularly useful ancillary techniques. PAM fluorometry has already been successfully applied to the sea ice environment with studies conducted both *in situ* using fibre PAM equipment (Kuhl *et al.*, 2001; McMinn *et al.*, 2003) and on brine samples or ice scrapings taken from cores using either single cell microscopy PAM or water PAM equipment (Ralph *et al.*, 2005; Ryan *et al.*, 2004). These methods are able to provide information on the functioning of the photosynthetic apparatus which is significantly affected by iron limitation. The determination of elemental ratios using Inductively Coupled Plasma Mass Spectrometry (ICPMS) on biomass samples from sea ice may also provide useful data to assist in understanding iron availability in sea ice. This method has been successfully used to determine the trace metal ratios of cultured phytoplankton (Ho *et al.*, 2004; Quigg *et al.*, 2003).

There are currently no published analyses of dissolved iron in sea ice brines and there is little understanding of the speciation of iron in sea ice brine. These aspects will also need to be addressed to understand the role of iron in the closed or semi-closed brine channel environment. Methods for iron analysis in seawater are well developed and our understanding of iron speciation in seawater is developing through the use of techniques such as cathodic stripping voltammetry (Aldrich & van den Berg, 1998). The application of these techniques to sea ice will facilitate our understanding of the role of iron in this environment.

However, these methods used in isolation will provide only limited understanding of the role of iron in this environment. Greatest value will come from the combined application of iron stress markers, fluorescence based methods, elemental ratios and direct iron analyses. Currently, it is in the communities inhabiting the bottom of sea ice that the question of iron availability can be best addressed. In this environment seawater iron analyses, PAM fluorometry, ferredoxin and flavodoxin analyses and ICPMS can be readily applied.

References

Ainley, D.G., Tynan, C.T., & Stirling, I. (2003). Sea Ice: A Critical Habitat for Polar Marine Mammals and Birds. In *Sea ice: an introduction to its physics, chemistry, biology and geology* (eds D.N. Thomas & G. Dieckmann), pp. 240-266. Blackwell Science, Oxford.

Aldrich, A.P. & van den Berg, C.M.G. (1998) Determination of iron and its redox speciation in seawater using catalytic cathodic stripping voltammetry. *Electroanalysis*, **10**, 369-373.

Aletsee, L. & Jahnke, J. (1992) Growth and Productivity of the Psychrophilic Marine Diatoms Thalassiosira-Antarctica Comber and Nitzschia-Frigida Grunow in Batch Cultures at Temperatures Below the Freezing-Point of Sea-Water. *Polar Biology*, **11**, 643-647.

Arar, E.J.C., G.B. (1997). In vitro Determination of Chlorophyll and Pheophytin a in marine and freshwater algae by fluorescence National Exposure Research Laboratory, Office of Research and Development, U.S. Environmental Protection Agency, Cincinnati, Ohio.

Armbrust, E.V., Berges, J.A., Bowler, C., Green, B.R., Martinez, D., Putnam, N.H., Zhou, S.G., Allen, A.E., Apt, K.E., Bechner, M., Brzezinski, M.A., Chaal, B.K., Chiovitti, A., Davis, A.K., Demarest, M.S., Detter, J.C., Glavina, T., Goodstein, D., Hadi, M.Z., Hellsten, U., Hildebrand, M., Jenkins, B.D., Jurka, J., Kapitonov, V.V., Kroger, N., Lau, W.W.Y., Lane, T.W., Larimer, F.W., Lippmeier, J.C., Lucas, S., Medina, M., Montsant, A., Obornik, M., Parker, M.S., Palenik, B., Pazour, G.J., Richardson, P.M., Rynearson, T.A., Saito, M.A., Schwartz, D.C., Thamatrakoln, K., Valentin, K., Vardi, A., Wilkerson, F.P., & Rokhsar, D.S. (2004) The genome of the diatom *Thalassiosira pseudonana*: Ecology, evolution, and metabolism *Science*, **306**, 79-86.

Arrigo, K.R. (2003). Primary production in sea ice. In *Sea ice: an introduction to its physics, chemistry, biology and geology.* (eds D.N. Thomas & G. Dieckmann), pp. 143-183. Blackwell Science, Oxford.

Arrigo, K.R., Robinson, D.H., Dunbar, R.B., Leventer, A.R., & Lizotte, M.P. (2003a) Physical control of chlorophyll a, POC, and TPN distributions in the pack ice of the Ross Sea, Antarctica. *Journal of Geophysical Research-Oceans*, **108 (C10)**, Art. No. 3316.

Arrigo, K.R. & Thomas, D.N. (2004) Large scale importance of sea ice biology in the Southern Ocean. *Antarctic Science*, **16**, 471-486.

Arrigo, K.R., Worthen, D., Schnell, A., & Lizotte, M.P. (1998) Primary production in Southern Ocean waters. *Journal of Geophysical Research-Oceans*, **103**, 15587-15600.

Arrigo, K.R., Worthen, D.L., Lizotte, M.P., Dixon, P., & Dieckmann, G. (1997) Primary production in Antarctic sea ice. *Science*, **276**, 394-397.

Arrigo, K.R., Worthen, D.L., & Robinson, D.H. (2003b) A coupled ocean-ecosystem model of the Ross Sea: 2. Iron regulation of phytoplankton taxonomic variability and primary production. *Journal of Geophysical Research-Oceans*, **108 (C7)**, Art. No. 3231.

Barbeau, K., Rue, E.L., Bruland, K.W., & Butler, A. (2001) Photochemical cycling of iron in the surface ocean mediated by microbial iron (III)-binding ligands. *Nature*, **413**, 409-413.

Bates, S.S. & Cota, G.F. (1986) Fluorescence Induction and Photosynthetic Responses of Arctic Ice Algae to Sample Treatment and Salinity. *Journal of Phycology*, **22**, 421-429.

Bes, M.T., Parisini, E., Inda, L.A., Saraiva, L.M., Peleato, M.L., & Sheldrick, G.M. (1999) Crystal structure determination at 1.4 angstrom resolution of ferredoxin from the green alga Chlorella fusca. *Structure*, **7**, 1201-1211.

Bindoff, N.L., Rosenberg, M.A., & Warner, M.J. (2000) On the circulation and water masses over the Antarctic continental slope and rise between 80 and 150 degrees E. *Deep-Sea Research Part Ii-Topical Studies in Oceanography*, **47**, 2299-2326.

Bindoff, N.L., Williams, G.D., & Allison, I. (2001) Sea-ice growth and water-mass modification in the Mertz Glacier polynya, East Antarctica, during winter. *Annals of Glaciology*, **33**, 399-406.

Boyd, P., LaRoche, J., Gall, M., Frew, R., & McKay, R.M.L. (1999) Role of iron, light, and silicate in controlling algal biomass in subantarctic waters SE of New Zealand. *Journal of Geophysical Research-Oceans*, **104**, 13395-13408.

Boyd, P.W. (2002a) Environmental factors controlling phytoplankton processes in the Southern Ocean. *Journal of Phycology*, **38**, 844-861.

Boyd, P.W. (2002b) The role of iron in the biogeochemistry of the Southern Ocean and equatorial Pacific: a comparison of *in situ* iron enrichments. *Deep-Sea Research Part Ii-Topical Studies in Oceanography*, **49**, 1803-1821.

Boyd, P.W. & Abraham, E.R. (2001) Iron-mediated changes in phytoplankton photosynthetic competence during SOIREE. *Deep-Sea Research Part Ii-Topical Studies in Oceanography*, **48**, 2529-2550.

Boyd, P.W., Muggli, D.L., Varela, D.E., Goldblatt, R.H., Chretien, R., Orians, K.J., & Harrison, P.J. (1996) *In vitro* iron enrichment experiments in the NE subarctic Pacific. *Marine Ecology-Progress Series*, **136**, 179-193.

Boyd, P.W., Watson, A.J., Law, C.S., Abraham, E.R., Trull, T., Murdoch, R , Bakker, D.C.E., Bowie, A.R., Buesseler, K.O., Chang, H., Charette, M., Croot, P., Downing, K., Frew, R., Gall, M., Hadfield, M., Hall, J., Harvey, M., Jameson, G., LaRoche, J., Liddicoat, M., Ling, R , Maldonado, M T., McKay, R.M., Nodder, S., Pickmere, S., Pridmore, R., Rintoul, S., Safi, K., Sutton, P., Strzepek, R., Tanneberger, K., Turner, S., Waite, A., & Zeldis, J (2000) A mesoscale phytoplankton bloom in the polar Southern Ocean stimulated by iron fertilization. *Nature*, **407**, 695-702.

Brand, L.E. (1991) Minimum iron requirements of marine phytoplankton and the implications for the biogeochemical control of new production. *Limnology and Oceanography*, **36**, 1756-1771.

Brand, L.E., Sunda, W.G., & Guillard, R.R.L. (1983) Limitation of marine phytoplankton reproductive rates by zinc, manganese and iron. *Limnology and Oceanography*, **28**, 1182-1198.

Brierley, A.S. & Thomas, D.N. (2002). Ecology of Southern Ocean pack ice. In *Advances in Marine Biology*, Vol. 43, pp. 171-277.

Buchel, C. & Wilhelm, C. (1993) In-Vivo Analysis of Slow Chlorophyll Fluorescence Induction Kinetics in Algae - Progress, Problems and Perspectives. *Photochemistry and Photobiology*, **58**, 137-148.

Buma, A.G.J , Debaar, H.J.W., Nolting, R.F., & Vanbennekom, A.J. (1991) Metal Enrichment Experiments in the Weddell-Scotia Seas - Effects of Iron and Manganese on Various Plankton Communities. *Limnology and Oceanography*, **36**, 1865-1878.

Bustin, S.A. (2004). Quantitation of nucleic acids by PCR. In *A-Z of quantitative PCR* (ed S.A. Bustin). International University Line, La Jolla, CA.

Carmack, E.C. (1990). Large-scale physical oceanography of polar oceans. In *Polar Oeanography, Part A, Physical Science* (ed W.O. Smith), pp. 171-223. Academic Press, San Diego.

Clarke, D.B. & Ackerly, S.F. (1984) Sea ice structure and biological activity in the Antarctic marginal ice zone. *Journal of geophysical Research*, **89**, 2087-2095

Coale, K.H., Gordon, R.M., & Wang, X.J. (2005) The distribution and behavior of dissolved and particulate iron and zinc in the Ross Sea and Antarctic circumpolar current along 170 degrees W. *Deep-Sea Research Part I-Oceanographic Research Papers*, **52**, 295-318.

Coale, K.H., Johnson, K.S., Chavez, F.P., Buesseler, K.O., Barber, R.T., Brzezinski, M.A., Cochlan, W.P., Millero, F.J., Falkowski, P.G., Bauer, J.E., Wanninkhof, R.H., Kudela, R.M., Altabet, M.A., Hales, B.E., Takahashi, T., Landry, M.R., Bidigare, R.R., Wang, X.J , Chase, Z., Strutton, P.G., Friederich, G.E., Gorbunov, M.Y., Lance, V.P., Hilting, A.K., Hiscock, M.R., Demarest, M., Hiscock, W.T., Sullivan, K.F , Tanner, S.J., Gordon, R.M., Hunter, C.N., Elrod, V.A., Fitzwater, S.E., Jones, J.L., Tozzi, S., Koblizek, M , Roberts, A.E., Herndon, J., Brewster, J., Ladizinsky, N., Smith, G., Cooper, D., Timothy, D., Brown, S.L., Selph, K.E., Sheridan, C.C., Twining, B.S., & Johnson, Z.I. (2004) Southern ocean iron enrichment experiment: Carbon cycling in high- and low-Si waters. *Science*, **304**, 408-414.

Coale, K.H., Johnson, K.S., Fitzwater, S.E., Gordon, R.M., Tanner, S., Chavez, F.P., Ferioli, L., Sakamoto, C., Rogers, P., Millero, F., Steinberg, P., Nightingale, P., Cooper, D., Cochlan, W.P., Landry, M.R., Constantinou, J., Rollwagen, G., Trasvina, A., & Kudela, R. (1996) A massive phytoplankton bloom induced by an ecosystem-scale iron fertilization experiment in the equatorial Pacific Ocean. *Nature*, **383**, 495-501.

Coale, K.H., Wang, X.J., Tanner, S.J., & Johnson, K.S. (2003) Phytoplankton growth and biological response to iron and zinc addition in the Ross Sea and Antarctic Circumpolar Current along 170 degrees W. *Deep-Sea Research Part Ii-Topical Studies in Oceanography*, **50**, 635-653.

Comiso, J.C. (2003). Large-scale variability of the global sea ice cover. In *Sea ice: an introduction to its physics, chemistry, biology and geology.* (eds D.N. Thomas & G. Dieckmann), pp. 112-142. Blackwell Science, Oxford.

Cota, G.F. & Sullivan, C.W. (1990) Photoadaptation, Growth and Production of Bottom Ice Algae in the Antarctic. *Journal of Phycology*, **26**, 399-411.

Croot, P.L., Andersson, K., Ozturk, M., & Turner, D.R. (2004) The distribution and specification of iron along 6 degrees E in the Southern Ocean. *Deep-Sea Research Part Ii-Topical Studies in Oceanography*, **51**, 2857-2879.

Davey, M. & Geider, R.J. (2001) Impact of iron limitation on the photosynthetic apparatus of the diatom *Chaetoceros muelleri* (Bacillariophyceae). *Journal of Phycology*, **37**, 987-1000.

Davison, I.R. (1991) Environmental-Effects on Algal Photosynthesis - Temperature. *Journal of Phycology*, **27**, 2-8.

de Baar, H.J.W., de Jong, J.T.M., Nolting, R F , Timmermans, K.R., van Leeuwe, M.A., Bathmann, U., van der Loeff, M.R., & Sildam, J. (1999) Low dissolved Fe and the absence of diatom blooms in remote Pacific waters of the Southern Ocean. *Marine Chemistry*, **66**, 1-34.

de Baar, H.J W , Dejong, J.T.M., Bakker, D.C.E., Loscher, B.M., Veth, C., Bathmann, U., & Smetacek, V. (1995) Importance of Iron for Plankton

Blooms and Carbon-Dioxide Drawdown in the Southern-Ocean. *Nature*, **373**, 412-415.

Deacon, G.E.R. (1982) Physical and biological zonation of the Southern Ocean. *Deep-Sea Research*, **29**, 1-15.

DeBaar, H.J.W. & Boyd, P.M. (2000). The role of iron in plankton ecology and carbon dioxide transfer of the global oceans. In *The Biogeochemistry of Iron in Seawater* (eds R.B. Hanson, H.W. Ducklow & K.A. Hunter), pp. 123-253. John Wiley and Sons, Chichester.

Debaar, H.J.W., Buma, A.G.J., Nolting, R.F., Cadee, G.C., Jacques, G., & Treguer, P.J. (1990) On Iron Limitation of the Southern-Ocean - Experimental-Observations in the Weddell and Scotia Seas. *Marine Ecology-Progress Series*, **65**, 105-122.

Dieckmann, G., Eicken, H., Haas, C., Garrison, D.L., Gleitz, M., Lange, M.A., Nothig, E.M., Spindler, M., Sullivan, C.W., Thomas, D.N., & Weissenberger, J. (1998). A compilation of Data on Sea Ice algal Standing Crop from the Bellinghausen, Admunsen and Weddel Seas from 1983-1994. In *Antarctic sea ice: biological processes, interactions and variability* (eds M. Lizotte & K.R. Arrigo), Vol. 73, pp. 85-93. American Geophysical Union, Washington, D.C.

Dieckmann, G.S., Lange, M.A., Ackley, S.F., & Jennings, J.C. (1991) The Nutrient Status in Sea Ice of the Weddell Sea During Winter - Effects of Sea Ice Texture and Algae. *Polar Biology*, **11**, 449-456.

Doucette, G.J., Erdner, D.L., Peleato, M.L., Hartman, J.L., & Anderson, D.M. (1996) Quantitative analysis of iron-stress related proteins in *Thalassiosira weissflogii*: measurement of flavodoxin and ferredoxin using HPLC. *Marine Ecology Progress Series*, **130**, 269-276

Dunbar, R.B. & Leventer, A. (1992) Seasonal variation in carbon isotopic composition of antarctic sea ice and open-water plankton communities. *Antarctic Journal*, 79-81.

Edwards, R. & Sedwick, P. (2001) Iron in East Antarctic snow: Implications for atmospheric iron deposition and algal production in Antarctic waters. *Geophysical Research Letters*, **28**, 3907-3910

Eicken, H. (1992) The Role of Sea Ice in Structuring Antarctic Ecosystems *Polar Biology*, **12**, 3-13

Eicken, H. (2003). From the Microscopic, to the Macroscopic, to the Regional Scale: Growth, Microstructure and Properties of Sea Ice. In *Sea ice: an introduction to its physics, chemistry, biology and geology.* (eds D.N. Thomas & G. Dieckmann), pp. 22-81. Blackwell Science, Oxford.

Eicken, H., Bock, C., Wittig, R., Miller, H., & Poertner, H.O. (2000) Magnetic resonance imaging of sea-ice pore fluids: methods and thermal evolution of pore microstructure. *Cold Regions Science and Technology*, **31**, 207-225.

Eldridge, M.L., Trick, C.G., Alm, M.B., DiTullio, G.R., Rue, E.L., Bruland, K.W., Hutchins, D.A., & Wilhelm, S.W. (2004) Phytoplankton community response to a manipulation of bioavailable iron in HNLC waters of the subtropical Pacific Ocean. *Aquatic Microbial Ecology*, **35**, 79-91.

Emery, W.J., Fowler, C.W., & Maslanik, J.A. (1997) Satellite-derived maps of Arctic and Antarctic sea ice motion: 1988 to 1994. *Geophysical Research Letters*, **24**, 897-900.

Erdner, D.L. & Anderson, D.M. (1999) Ferredoxin and flavodoxin as biochemical indicators of iron limitation during open-ocean iron enrichment. *Limnology and Oceanography*, **44**, 1609-1615.

Erdner, D.L., Price, N.M., Doucette, G.J., Peleato, M.L., & Anderson, D.M. (1999) Characterization of ferredoxin and flavodoxin as markers of iron limitation in marine phytoplankton. *Marine Ecology-Progress Series*, **184**, 43-53.

Fiala, M. & Oriol, L. (1990) Light-Temperature Interactions on the Growth of Antarctic Diatoms. *Polar Biology*, **10**, 629-636.

Fitzgerald, M.P., Husain, A., & Rogers, L.J. (1978) A constitutive flavodoxin from a eukaryotic algae. *Biochemical and biphysical research communications*, **81**, 630-635.

Fitzwater, S.E., Johnson, K.S., Gordon, R.M., Coale, K.H., & Smith, W.O. (2000) Trace metal concentrations in the Ross Sea and their relationship with nutrients and phytoplankton growth. *Deep-Sea Research Part Ii-Topical Studies in Oceanography*, **47**, 3159-3179.

Garrison, D.L., Ackerly, S.F., & Buck, K.R. (1983) A physical mechanism for establishing algal populations in frazil ice. *Nature*, **306**, 363-365.

Garrison, D.L., Jeffries, M.O., Gibson, A., Coale, S.L., Neenan, D., Fritsen, C., Okolodkov, Y.B., & Gowing, M.M. (2003) Development of sea ice microbial communities during autumn ice formation in the Ross Sea. *Marine Ecology-Progress Series*, **259**, 1-15.

Gerringa, L.J.A., de Baar, H.J.W., & Timmermans, K.R. (2000) A comparison of iron limitation of phytoplankton in natural oceanic waters and laboratory media conditioned with EDTA. *Marine Chemistry*, **68**, 335-346.

Gervais, F., Riebesell, U., & Gorbunov, M.Y. (2002) Changes in primary productivity and chlorophyll a in response to iron fertilization in the Southern Polar Frontal Zone. *Limnology and Oceanography*, **47**, 1324-1335.

Gleitz, M. & Kirst, G.O. (1991) Photosynthesis-Irradiance Relationships and Carbon Metabolism of Different Ice Algal Assemblages Collected from Weddell Sea Pack Ice During Austral Spring (Epos-1). *Polar Biology*, **11**, 385-392.

Gleitz, M., Kukert, H., Riebesell, U., & Dieckmann, G.S. (1996) Carbon acquisition and growth of Antarctic sea ice diatoms in closed bottle incubations. *Marine Ecology-Progress Series*, **135**, 169-177.

Gleitz, M. & Thomas, D.N. (1993) Variation in phytoplankton standing stock, chemical composition and physiology during sea-ice formation in the southeastern Weddell Sea, Antarctica. *Journal of Experimental Marine Biology and Ecology*, **173**, 211-230.

Gleitz, M., Vonderloeff, M.R., Thomas, D.N , Dieckmann, G.S., & Millero, F J. (1995) Comparison of Summer and Winter Inorganic Carbon, Oxygen and Nutrient Concentrations in Antarctic Sea-Ice Brine. *Marine Chemistry*, **51**, 81-91.

Gonzalez-Davila, M., Santana-Casiano, J.M., & Millero, F.J. (2005) Oxidation of iron(II) nanomolar with H2O2 in seawater. *Geochimica Et Cosmochimica Acta*, **69**, 83-93.

Granger, J. & Price, N.M. (1999) The importance of siderophores in iron nutrition of heterotrophic marine bacteria. *Limnology and Oceanography*, **44**, 541-555.

Greene, R.M., Geider, R.J., & Falkowski, P.G (1991) Effect of Iron Limitation on Photosynthesis in a Marine Diatom. *Limnology and Oceanography*, **36**, 1772-1782.

Greene, R.M., Geider, R.J., Kolber, Z., & Falkowski, P.G. (1992) Iron-Induced Changes in Light Harvesting and Photochemical Energy-Conversion Processes in Eukaryotic Marine-Algae. *Plant Physiology*, **100**, 565-575.

Grose, M. & McMinn, A. (2003). Algal biomass in east Antarctic Pack Ice: how much is in the east? In *Antarctic Biology in a Global Context* (eds A.H.L. Huiskies, W.W.C. Gieskes, J. Rozema, R.M.L. Schorno, S.M. van der Vies & W.J. Wolff), pp. 21-25. Backhuys, Leiden, The Netherlands.

Grossmann, S. & Gleitz, M. (1993) Microbial Responses to Experimental Sea-Ice Formation - Implications for the Establishment of Antarctic Sea-Ice Communities. *Journal of Experimental Marine Biology and Ecology*, **173**, 273-289.

Gueneau, P., Morel, F., Laroche, J., & Erdner, D. (1998) The petF region of the chloroplast genome from the diatom *Thalassiosira weissflogii*: sequence, organization and phylogeny. *European Journal of Phycology*, **33**, 203-211.

Guillard, R.R.L. & Ryther, J.H. (1962) Studies on marine planktonic diatoms. 1 . *Cyclotella nana* Hustedt and *Detonula confervacae* (cleve) Gran. *Canadian Journal of Microbiology*, **8**, 229-239.

Haas, C. (2003). Dynamics versus Thermodynamics: The Sea Ice Thickness Distribution. In *Sea Ice: an introduction to its physics, chemistry, biology and geology.* (eds D.N. Thomas & G. Dieckmann), pp. 82-111. Blackwell Science, Oxford.

Harangozo, S.A. (2004) The impact of winter ice retreat on Antarctic winter sea-ice extent and links to the atmospheric meridonal circulation. *International Journal of Climatology*, **24**, 1023-1044.

Harlow, E. & Lane, D. (1989) *Antibodies : a laboratory manual* Cold Spring Harbor Laboratory, Cold Spring Harbor, NY.

Helbling, E.W., Villafane, V., & Holmhansen, O. (1991) Effect of Iron on Productivity and Size Distribution of Antarctic Phytoplankton. *Limnology and Oceanography*, **36**, 1879-1885.

Hiscock, M.R., Marra, J., Smith, W.O., Goericke, R., Measures, C., Vink, S., Olson, R.J., Sosik, H.M., & Barber, R.T. (2003) Primary productivity and its regulation in the Pacific Sector of the Southern Ocean. *Deep-Sea Research Part Ii-Topical Studies in Oceanography*, **50**, 533-558.

Ho, T.Y., Quigg, A., Finkel, Z.V., Milligan, A.J., Wyman, K., Falkowski, P.G., & Morel, F.M.M. (2004) The elemental composition of some marine phytoplankton. *Journal of Phycology*, **40**, 227-227.

Hofmann, E.E. & Lascara, C.M. (2000) Modeling the growth dynamics of Antarctic krill *Euphausia superba*. *Marine Ecology-Progress Series*, **194**, 219-231.

Hoppema, M., de Baar, H.J.W., Fahrbach, E., Hellmer, H.H., & Klein, B. (2003) Substantial advective iron loss diminishes phytoplankton production in the Antarctic Zone. *Global Biogeochemical Cycles*, **17 (1)**, Art. No. 1025.

Horner, R., Ackley, S.F , Dieckmann, G.S., Gulliksen, B., Hoshiai, T., Legendre, L., Melnikov, I.A., Reeburgh, W.S., Spindler, M., & Sullivan, C.W. (1992) Ecology of Sea Ice Biota .1. Habitat, Terminology, and Methodology. *Polar Biology*, **12**, 417-427.

Horner, R.A. (1985) *Sea Ice Biota* CRC Press, Florida.

Hudson, R.J.M. & Morel, F.M.M. (1990) Iron Transport in Marine-Phytoplankton - Kinetics of Cellular and Medium Coordination Reactions. *Limnology and Oceanography*, **35**, 1002-1020.

Hunter, K.A. (1998) SWCO2 (Freeware software available at http://neon.otago.ac.nz/chemistry/research/kah/software/swco2.htm).

Hutchins, D.A. & Bruland, K.W. (1998) Iron-limited diatom growth and Si : N uptake ratios in a coastal upwelling regime. *Nature*, **393**, 561-564.

Hutchins, D.A., DiTullio, G.R , Zhang, Y., & Bruland, K.W. (1998) An iron limitation mosaic in the California upwelling regime. *Limnology and Oceanography*, **43**, 1037-1054.

Inda, L.A & Peleato, M.L. (2003) Development of an ELISA approach for the determination of flavodoxin and ferredoxin as markers of iron deficiency in phytoplankton. *Phytochemistry*, **63**, 303-308.

Kennedy, H., Thomas, D.N., Kattner, G., Haas, C., & Dieckmann, G.S. (2002) Particulate organic matter in Antarctic summer sea ice: concentration and stable isotopic composition. *Marine Ecology-Progress Series*, **238**, 1-13.

Kirst, G O. & Wiencke, C. (1995) Ecophysiology of Polar Algae. *Journal of Phycology*, **31**, 181-199.

Kohane, I.S , Kho, A., & Butte, A.J. (2003) *Microarrays for an integrated genomics* MIT Press, Cambridge, Mass.

Kolber, Z. & Falkowski, P G. (1993) Use of Active Fluorescence to Estimate Phytoplankton Photosynthesis in-Situ. *Limnology and Oceanography*, **38**, 1646-1665.

Kowallik, K.V , Stoebe, B., Schaffran, I., KrothPancic, P., & Freier, U. (1995) The chloroplast genome of a chlorophyll a+c-containing alga, *Odontella sinensis*. *Plant Molecular Biology Reporter*, **13**, 336-342.

Krause, G.H & Weis, E. (1991) Chlorophyll Fluorescence and Photosynthesis - the Basics. *Annual Review of Plant Physiology and Plant Molecular Biology*, **42**, 313-349.

Kristiansen, S. & Farbrot, T. (1991) Nitrogen Uptake Rates in Phytoplankton and Ice Algae in the Barents Sea *Polar Research*, **10**, 187-192.

Kristiansen, S., Farbrot, T., Kuosa, H., Myklestad, S., & Quillfeldt, C.H.V. (1998) Nitrogen uptake in the infiltration community, an ice algal community in Antarctic pack-ice. *Polar Biology*, **19**, 307-315.

Kudo, I., Miyamoto, M., Noiri, Y., & Maita, Y. (2000) Combined effects of temperature and iron on the growth and physiology of the marine diatom, *Phaeodactylum tricornutum* (Bacillariophyceae). *Journal of Phycology*, **36**, 1096-1102.

Kuhl, M., Glud, R.N., Borum, J., Roberts, R., & Rysgaard, S. (2001) Photosynthetic performance of surface-associated algae below sea ice as measured with a pulse-amplitude-modulated (PAM) fluorometer and O-2 microsensors *Marine Ecology-Progress Series*, **223**, 1-14.

Kurien, B.T. & Scofield, R.H. (2003) Protein blotting: a review. *Journal of Immunological Methods*, **274**, 1-15.

La Roche, J., Boyd, P.W., McKay, R.M.L., & Geider, R.J. (1996) Flavodoxin as an *in situ* marker for iron stress in phytoplankton. *Nature*, **382**, 802-805.

La Roche, J., Geider, R.J., Graziano, L.M., Murray, H., & Lewis, K. (1993) Induction of Specific Proteins in Eukaryotic Algae Grown under Iron-Deficient, Phosphorus-Deficient, or Nitrogen-Deficient Conditions. *Journal of Phycology*, **29**, 767-777.

La Roche, J., McKay, R.M.L., & Boyd, P. (1999) Immunological and molecular probes to detect phytoplankton responses to environmental stress in nature. *Hydrobiologia*, **401**, 177-198.

La Roche, J., Murray, H., Orellana, M., & Newton, J. (1995) Flavodoxin Expression as an Indicator of Iron Limitation in Marine Diatoms. *Journal of Phycology*, **31**, 520-530.

Laemmli, U K. (1970) Cleavage of structural proteins during the assembly of the head of bacteriophage T4. *Nature*, **227**, 680-685.

Lancelot, C., Hannon, E., Becquevort, S., Veth, C., & De Baar, H.J.W. (2000) Modeling phytoplankton blooms and carbon export production in the Southern Ocean: dominant controls by light and iron in the Atlantic sector in Austral spring 1992. *Deep-Sea Research Part I-Oceanographic Research Papers*, **47**, 1621-1662.

Lange, M.A., Ackerly, S.F., Wadhams, P., Dieckmann, G., & Eicken, H. (1989) Development of sea ice in the Weddell Sea, Antarctica *Annals of Glaciology*, **12**, 92-96.

Lange, M.A. & Eicken, H. (1991) The Sea Ice Thickness Distribution in the Northwestern Weddell Sea. *Journal of Geophysical Research-Oceans*, **96**, 4821-4837.

Lange, M.A., Schlosser, P., Ackley, S.F., Wadhams, P., & Dieckmann, G.S. (1990) O-18 Concentrations in Sea Ice of the Weddell Sea, Antarctica. *Journal of Glaciology*, **36**, 315-323.

Legendre, L., Ackley, S.F., Dieckmann, G.S., Gulliksen, B., Horner, R., Hoshiai, T., Melnikov, I.A., Reeburgh, W.S., Spindler, M., & Sullivan, C.W. (1992) Ecology of Sea Ice Biota .2. Global Significance. *Polar Biology*, **12**, 429-444.

Liu, X.W. & Millero, F.J. (1999) The solubility of iron hydroxide in sodium chloride solutions. *Geochimica Et Cosmochimica Acta*, **63**, 3487-3497.

Liu, X.W. & Millero, F.J. (2002) The solubility of iron in seawater. *Marine Chemistry*, **77**, 43-54.

Lizotte, M. (2003). The Microbiology of Sea Ice. In *Sea ice: an introduction to its physics, chemistry, biology and geology.* (eds D.N. Thomas & G. Dieckmann), pp. 184-210. Blackwell Science Ltd, Oxford.

Lizotte, M.P. (2001) The contributions of sea ice algae to Antarctic marine primary production. *American Zoologist*, **41**, 57-73.

Lizotte, M.P. & Sullivan, C.W. (1992a) Biochemical-Composition and Photosynthate Distribution in Sea Ice Microalgae of Mcmurdo-Sound, Antarctica - Evidence for Nutrient Stress During the Spring Bloom. *Antarctic Science*, **4**, 23-30.

Lizotte, M.P. & Sullivan, C.W. (1992b) Photosynthetic Capacity in Microalgae Associated with Antarctic Pack Ice. *Polar Biology*, **12**, 497-502.

Loscher, B.M., DeBaar, H.J.W., DeJong, J.T.M., Veth, C., & Dehairs, F. (1997) The distribution of Fe in the Antarctic Circumpolar Current. *Deep-Sea Research Part Ii-Topical Studies in Oceanography*, **44**, 143-187.

Lytle, V.I., Worby, A.P., Massom, R., Paget, M.J., Allison, I., Wu, X., & Roberts, A. (2001) Ice formation in the Mertz Glacier polynya, East Antarctica, during winter. *Annals of Glaciology*, **33**, 368-372.

Macrellis, H.M., Trick, C.G., Rue, E.L., Smith, G., & Bruland, K.W. (2001) Collection and detection of natural iron-binding ligands from seawater. *Marine Chemistry*, **76**, 175-187.

Maldonado, M.T. & Price, N.M. (1996) Influence of N substrate on Fe requirements of marine centric diatoms. *Marine Ecology-Progress Series*, **141**, 161-172.

Maldonado, M.T. & Price, N.M. (2001) Reduction and transport of organically bound iron by *Thalassiosira oceanica* (Bacillariophyceae). *Journal of Phycology*, **37**, 298-309.

Martin, J.H. & Fitzwater, S.E. (1988) Iron-Deficiency Limits Phytoplankton Growth in the Northeast Pacific Subarctic. *Nature*, **331**, 341-343.

Martin, J.H., Fitzwater, S.E., & Gordon, R.M. (1990a) Iron defficiency limits phytoplanton growth in Antarctic waters. *Global Biogeochemical Cycles*, **4**, 5-12.

Martin, J.H., Gordon, R.M., & Fitzwater, S.E. (1990b) Iron in Antarctic Waters. *Nature*, **345**, 156-158.

Matsubara, H. (1968) Purification and some properties of *Scenedesmus* Ferredoxin. *The Jounal of Biological Chemistry*, **243**, 370-375.

McKay, R.M.L., Geider, R.J., & LaRoche, J (1997) Physiological and biochemical response of the photosynthetic apparatus of two marine diatoms to Fe stress. *Plant Physiology*, **114**, 615-622.

McKay, R.M.L., La Roche, J., Yakunin, A.F., Durnford, D.G., & Geider, R.J. (1999) Accumulation of ferredoxin and flavodoxin in a marine diatom in response to Fe. *Journal of Phycology*, **35**, 510-519.

McKay, R.M.L., Villareal, T.A., & La Roche, J. (2000) Vertical migration by *Rhizosolenia sp.* (Bacillariophyceae): Implications for Fe acquisition. *Journal of Phycology*, **36**, 669-674.

McMinn, A. & Ashworth, C. (1998) The use of oxygen microelectrodes to determine the net production by an Antarctic sea ice algal community. *Antarctic Science*, **10**, 39-44.

McMinn, A., Ashworth, C., & Ryan, K.G. (2000) *In situ* net primary productivity of an Antarctic fast ice bottom algal community. *Aquatic Microbial Ecology*, **21**, 177-185.

McMinn, A., Ryan, K., & Gademann, R. (2003) Diurnal changes in photosynthesis of Antarctic fast ice algal communities determined by pulse amplitude modulation fluorometry. *Marine Biology*, **143**, 359-367.

McMinn, A., Skerratt, J., Trull, T., Ashworth, C., & Lizotte, M. (1999) Nutrient stress gradient in the bottom 5 cm of fast ice, McMurdo Sound, Antarctica. *Polar Biology*, **21**, 220-227.

Measures, C.I. & Vink, S. (2001) Dissolved Fe in the upper waters of the Pacific sector of the Southern Ocean. *Deep-Sea Research Part Ii-Topical Studies in Oceanography*, **48**, 3913-3941.

Melnikov, I.A. (1998) Winter production of sea ice algae in the western Weddell Sea. *Journal of Marine Systems*, **17**, 195-205.

Millero, F.J. (1998) Solubility of Fe(III) in seawater. *Earth and Planetary Science Letters*, **154**, 323-329.

Milligan, A.J. & Harrison, P.J. (2000) Effects of non-steady-state iron limitation on nitrogen assimilatory enzymes in the marine diatom *Thalassiosira weissflogii* (Bacillariophyceae). *Journal of Phycology*, **36**, 78-86

Mitchell, C & Beardall, J. (1996) Inorganic carbon uptake by an Antarctic sea-ice diatom, *Nitzschia frigida*. *Polar Biology*, **16**, 95-99.

Mock, T. (2002) *In situ* primary production in young Antarctic sea ice. *Hydrobiologia*, **470**, 127-132.

Mock, T. & Gradinger, R. (1999) Determination of Arctic ice algal production with a new *in situ* incubation technique. *Marine Ecology-Progress Series*, **177**, 15-26.

Mock, T. & Thomas, D.N. (2005) Recent advances in sea-ice microbiology. *Environmental Microbiology*, 7, 605-619.

Mock, T. & Valentin, K. (2004) Photosyntheis and cold acclimation. Molecular evidece from a polar diatom. *Journal of Phycology*, **40**, 732-741.

Moore, J.K. & Abbott, M.R. (2002) Surface chlorophyll concentrations in relation to the Antarctic Polar Front. seasonal and spatial patterns from satellite observations *Journal of Marine Systems*, **37**, 69-86.

Morel, F., Rueter, J.G., Anderson, D.M., & Guillard, R.R.L. (1979) Aquil: A Chemically defined phytoplankton culture medium for trace metal studies. *Journal of Phycology*, **15**, 135-141.

Morel, F.M.M. & Hering, J.G. (1993) *Principles and Applications of Aquatic Chemistry* John Wiley & Sons, Inc., New York.

Morel, F.M.M., Hudson, R.J.M., & Price, N.M. (1991) Limitation of Productivity by Trace-Metals in the Sea. *Limnology and Oceanography*, **36**, 1742-1755.

Orsi, A.H , Whitworth, T., & Nowlin, W.D. (1995) On the Meridional Extent and Fronts of the Antarctic Circumpolar Current. *Deep-Sea Research Part I-Oceanographic Research Papers*, **42**, 641-673.

Palmisano, A.C., Soohoo, J.B., & Sullivan, C.W. (1987) Effects of 4 Environmental Variables on Photosynthesis-Irradiance Relationships in Antarctic Sea-Ice Microalgae. *Marine Biology*, **94**, 299-306.

Peleato, M.L., Ayora, S., Inda, L.A., & Gomezmoreno, C. (1994) Isolation and Characterization of 2 Different Flavodoxins from the Eukaryote Chlorella-Fusca. *Biochemical Journal*, **302**, 807-811.

Platt, T., Gallegos, C.L., & Harrison, W.G. (1980) Photoinhibition of photosynthesis in nautural assemblages of marine phytoplankton. *Journal of Marine Research*, **38**, 687-701.

Porra, R.J., Thompson, W.A., & Kriedemann, P.E. (1989) Determination of accurate extinction coefficients and simultaneous equations for assaying chlorophylls a and b extracted with four different solvents: verification of the concentration of chlorophyll standards by atomic absorbtion spectroscopy. *Biochim.Biophys. Acta*, **975**, 384-394.

Price, N.M., Harrison, G.I., Hering, J.G., Hudson, R.J.M., Nirel, P.M.V., Palenik, B., & Morel, F.M.M. (1989) Preparation and chemistry of the artificial algal culture medium Aquil. *Biological Oceanography*, **6**, 443-461.

Priddle, J., Leakey, R.J.G., Archer, D.E , & Murphey, E.J. (1996) Eukaryotic microbiolta in surface waters and sea ice of the Southern Ocean: aspects of physiology, ecology and biodiversity in a "two phase" ecosystem. *Biodiversity and Conservation*, **5**, 1437-1504.

Quigg, A., Finkel, Z.V., Irwin, A.J., Rosenthal, Y., Ho, T.Y., Reinfelder, J.R., Schofield, O., Morel, F.M.M , & Falkowski, P.G. (2003) The evolutionary inheritance of elemental stoichiometry in marine phytoplankton. *Nature*, **425**, 291-294

Ralph, P.J. & Gademann, R. (2004) Rapid light curves: a powerfull tool for the assessment of photosynthetic activity. *Aquatic Botany*, **82**, I222-237.

Ralph, P.J., McMinn, A., Ryan, K.G., & Ashworth, C. (2005) Short-term effect of temperature on the photokinetics of microalgae from the surface layers of Antarctic pack ice. *Journal of Phycology*, **41**, 763-769.

Raven, J.A. (1990) Predictions of Mn and Fe Use Efficiencies of Phototrophic Growth as a Function of Light Availability for Growth and of C Assimilation Pathway. *New Phytologist*, **116**, 1-18.

Raven, J.A., Evans, M.C.W., & Korb, R.E. (1999) The role of trace metals in photosynthetic electron transport in O-2-evolving organisms. *Photosynthesis Research*, **60**, 111-149.

Robinson, D.H., Kolber, Z., & Sullivan, C.W. (1997) Photophysiology and photoacclimation in surface sea ice algae from McMurdo Sound, Antarctica. *Marine Ecology-Progress Series*, **147**, 243-256

Rose, A.L., Salmon, T.P., Lukondeh, T., Neilan, B.A., & Waite, T.D. (2005) Use of superoxide as an electron shuttle for iron acquisition by the marine cyanobacterium *Lyngbya majuscula*. *Environmental Science & Technology*, **39**, 3708-3715.

Rose, A.L. & Waite, T.D. (2002) Kinetic model for Fe(II) oxidation in seawater in the absence and presence of natural organic matter. *Environmental Science & Technology*, **36**, 433-444.

Roy, R.N., Roy, L.N., Vogel, K.M., Portermoore, C., Pearson, T., Good, C.E., Millero, F.J., & Campbell, D.M. (1993) The Dissociation-Constants of Carbonic-Acid in Seawater at Salinities 5 to 45 and Temperatures 0-Degrees-C to 45-Degrees-C. *Marine Chemistry*, **44**, 249-267.

Ryan, K.G., Ralph, P., & McMinn, A. (2004) Acclimation of Antarctic bottom-ice algal communities to lowered salinities during melting. *Polar Biology*, **27**, 679-686.

Sakshaug, E. & Slagstad, D. (1991) Light and Productivity of Phytoplankton in Polar Marine Ecosystems - a Physiological View. *Polar Research*, **10**, 69-85.

Sambrotto, R.N., Matsuda, A., Vaillancourt, R., Brown, M., Langdon, C., Jacobs, S.S., & Measures, C. (2003) Summer plankton production and nutrient consumption patterns in the Mertz Glacier Region of East Antarctica. *Deep-Sea Research Part Ii-Topical Studies in Oceanography*, **50**, 1393-1414.

Schecher, W.D. & McAvoy, D.C. (1992) Mineql+ - a Software Environment for Chemical-Equilibrium Modeling. *Computers Environment and Urban Systems*, **16**, 65-76.

Schnack-Schiel, S.B. (2003). The Macrobiology of Sea Ice. In *Sea ice: an introduction to its physics, chemistry, biology and geology.* (eds D.N. Thomas & G. Dieckmann), pp. 211-239. Blackwell Science Ltd, Oxford.

Schreiber, U. (2004). Pulse-Amplitude-Modulation (PAM) Fluorometry and Saturation Pulse Method: An Overview. In *Chlorophyll fluorescence: A signature of Photosynthesis* (eds G.C. Papageorgiou & G. Govindjee), pp. 279-319. Kluwer Academic Publishers, Dordrecht, The Netherlands.

Sedwick, P.N. & DiTullio, G.R. (1997) Regulation of algal blooms in Antarctic shelf waters by the release of iron from melting sea ice. *Geophysical Research Letters*, **24**, 2515-2518.

Sedwick, P.N., DiTullio, G.R., & Mackey, D.J. (2000) Iron and manganese in the Ross Sea, Antarctica: Seasonal iron limitation in Antarctic shelf waters. *Journal of Geophysical Research-Oceans*, **105**, 11321-11336.

Shaked, Y., Kustka, A.B., & Morel, F.M.M. (2005) A general kinetic model for iron acquisition by eukaryotic phytoplankton. *Limnology and Oceanography*, **50**, 872-882.

Sohrin, Y., Iwamoto, S., Matsui, M., Obata, H., Nakayama, E., Suzuki, K., Handa, N., & Ishii, M. (2000) The distribution of Fe in the Australian sector of the Southern Ocean. *Deep-Sea Research Part I-Oceanographic Research Papers*, **47**, 55-84.

Soria-Dengg, S., Reissbrodt, R., & Horstmann, U. (2001) Siderophores in marine, coastal waters and their relevance for iron uptake by phytoplankton: experiments with the diatom *Phaeodactylum tricornutum*. *Marine Ecology-Progress Series*, **220**, 73-82

Sournia, A. (1978) *Phytoplankton manual* UNESCO, Paris.

Stoecker, D.K., Gustafson, D.E., Baier, C.T., & Black, M.M.D. (2000) Primary production in the upper sea ice. *Aquatic Microbial Ecology*, **21**, 275-287.

Strzepek, R. & Harrison, P.J. (2004) Photosynthetic architecture differs in coastal and oceanic diatoms. *Nature*, **431**, 689-692.

Strzepek, R.F. & Price, N.M. (2000) Influence of irradiance and temperature on the iron content of the marine diatom *Thalassiosira weissflogii* (Bacillariophyceae). *Marine Ecology-Progress Series*, **206**, 107-117.

Sunda, W. & Huntsman, S. (2003) Effect of pH, light, and temperature on Fe-EDTA chelation and Fe hydrolysis in seawater. *Marine Chemistry*, **84**, 35-47.

Sunda, W.G. & Huntsman, S.A. (1995) Iron uptake and growth limitation in oceanic and coastal phytoplankton. *Marine Chemistry*, **50**, 189-206.

Sunda, W.G. & Huntsman, S.A. (1997) Interrelated influence of iron, light and cell size on marine phytoplankton growth. *Nature*, **390**, 389-392.

Sunda, W.G., Swift, D.G., & Huntsman, S.A. (1991) Low Iron Requirement for Growth in Oceanic Phytoplankton. *Nature*, **351**, 55-57.

Syvertsen, E.E. & Kristiansen, S. (1993) Ice Algae During Epos, Leg-1 - Assemblages, Biomass, Origin and Nutrients. *Polar Biology*, **13**, 61-65.

Takeda, S. (1998) Influence of iron availability on nutrient consumption ratio of diatoms in oceanic waters. *Nature*, **393**, 774-777.

Thomas, D.N. (2003) Iron limitation in the Southern Ocean. *Science*, **302**, 565-565.

Thomas, D.N. & Dieckmann, G.S. (2002) Biogeochemistry of Antarctic sea ice. *Oceanography and Marine Biology*, **40**, 143-169.

Thomas, D.N. & Papadimitriou, S. (2003) Biogeochemistry of Sea Ice. In *Sea Ice: an Introduction to its physics, chemistry, biology and geology.* (eds D.N. Thomas & G. Dieckmann), pp. 267-302. Blacwell Science, Oxford.

Timmermans, K.R., Davey, M.S., van der Wagt, B., Snoek, J., Geider, R.J., Veldhuis, M.J.W., Gerringa, L.J.A., & de Baar, H.J.W. (2001a) Co-limitation by iron and light of *Chaetoceros brevis*, *C. dichaeta* and *C. calcitrans* (Bacillariophyceae). *Marine Ecology-Progress Series*, **217**, 287-297.

Timmermans, K.R., Gerringa, L.J.A., de Baar, H J.W., van der Wagt, B., Veldhuis, M.J.W., de Jong, J.T.M., Croot, P.L., & Boye, M. (2001b) Growth rates of large and small Southern Ocean diatoms in relation to availability of iron in natural seawater. *Limnology and Oceanography*, **46**, 260-266.

Timmermans, K.R., Stolte, W., & Debaar, H.J.W. (1994) Iron-Mediated Effects on Nitrate Reductase in Marine-Phytoplankton. *Marine Biology*, **121**, 389-396.

Timmermans, K.R., van der Wagt, B., & de Baar, H.J.W. (2004) Growth rates, half saturation constants and silicate, phosphate and nitrate depletion in relation to iron availability of four large open ocean diatoms fro the Southern Ocean. *Limnology and Oceanography*, **49**, 2141-2151.

Timmermans, K.R., van Leeuwe, M.A., de Jong, J T.M., McKay, R.M.L., Nolting, R.F., Witte, H.J., van Ooyen, J., Swagerman, M.J W., Kloosterhuis, H., & de Baar, H.J.W. (1998) Iron stress in the Pacific region of the Southern Ocean: evidence from enrichment bioassays. *Marine Ecology-Progress Series*, **166**, 27-41.

Treguer, P. & Jacques, G. (1992) Dynamic of nutrients and phytoplankton, and fluxes of carbon, nitrogen and silicon in the Antarctic Ocean. *Polar Biology*, **12**, 149-162.

Trenerry, L.J., McMinn, A., & Ryan, K.G. (2002) *In situ* oxygen microelectrode measurements of bottom-ice algal production in McMurdo Sound, Antarctica. *Polar Biology*, **25**, 72-80.

Trevena, A.J., Jones, G.B., Wright, S.W., & van den Enden, R.L. (2000) Profiles of DMSP, algal pigments, nutrients and salinity in pack ice from eastern Antarctica. *Journal of Sea Research*, **43**, 265-273.

Trull, T., Rintoul, S.R., Hadfield, M., & Abraham, E.R. (2001) Circulation and seasonal evolution of polar waters south of Australia: Implications for iron fertilization of the Southern Ocean. *Deep-Sea Research Part Ii-Topical Studies in Oceanography*, **48**, 2439-2466.

Ussher, S.J., Achterberg, E.P., & P.J., W (2004) Marine Biogeochemistry of Iron. *Environmental Chemistry*, **1**, 67-80.

van Leeuwe, M.A. & De Baar, H.J.W. (2000) Photoacclimation by the Antarctic flagellate *Pyramimonas sp* (Prasinophyceae) in response to iron limitation. *European Journal of Phycology*, **35**, 295-303.

van Leeuwe, M.A., Scharek, R., DeBaar, H.J.W., DeJong, J.T.M., & Goeyens, L. (1997) Iron enrichment experiments in the Southern Ocean: Physiological responses of plankton communities. *Deep-Sea Research Part Ii-Topical Studies in Oceanography*, **44**, 189-207.

van Oijen, T., van Leeuwe, M.A., Gieskes, W.W.C., & de Baar, H.J.W. (2004a) Effects of iron on photosynthesis and carbohydrate metabolism in the Antarctic diatom *Chaetoceros brevis* (Bacillariophyceae). *European Journal of Phycology*, **39**, 161-171.

van Oijen, T , van Leeuwe, M.A., Granum, E., Weissing, F.J., Bellerby, R.G.J., Gieskes, W.W.C., & de Baar, H.J.W. (2004b) Light rather than iron controls photosynthate production and allocation in Southern Ocean phytoplankton populations during austral autumn. *Journal of Plankton Research*, **26**, 885-900.

Vassiliev, I.R., Kolber, Z., Wyman, K.D., Mauzerall, D., Shukla, V.K., & Falkowski, P.G. (1995) Effects of Iron Limitation on Photosystem-II Composition and Light Utilization in *Dunaliella tertiolecta*. *Plant Physiology*, **109**, 963-972.

Veldhuis, M. & de Baar, H.J.W. (2005) Iron resources and oceanic nutrients: advancement of global environment simulations. *Journal of Sea Research*, **53**, 1-6.

Wadhams, P., Lange, M.A., & Ackley, S.F. (1987) The Ice Thickness Distribution across the Atlantic Sector of the Antarctic Ocean in Midwinter. *Journal of Geophysical Research-Oceans*, **92**, 14535-14552.

Watson, A.J., Law, C.S., Vanscoy, K.A., Millero, F.J., Yao, W., Friederich, G.E., Liddicoat, M.I., Wanninkhof, R.H., Barber, R.T., & Coale, K.H. (1994)

Minimal Effect of Iron Fertilization on Sea-Surface Carbon-Dioxide Concentrations. *Nature*, **371**, 143-145.

Weeks, W.F. (1998). Growth conditions and the structure and properties of sea ice. In *Physics of ice covered seas* (ed M. Lepparanta), Vol. 1, pp. 25-104. University of Helsinki Press, Helsinki, Finland.

Weeks, W.F. & Ackerly, S.F. (1986). The Growth structure and properties of sea ice. In *The geophysics of sea ice* (ed N. Untersteiner), Vol. 146, pp. 9-164. Plenum Press, New York.

Wells, M.L., Price, N.M., & Bruland, K.W. (1995) Iron Chemistry in Seawater and Its Relationship to Phytoplankton - a Workshop Report. *Marine Chemistry*, **48**, 157-182.

Whitworth III, T., Orsi, A.H., Kim, S.J., & Nowlin Jr, W.D. (1998). Water masses and mixing near the Antarctic Slope Front. In *Ocean, Ice and Atmosphere: Interactions at the Antarctic Continental Margin.* (eds S.S. Jacobs & R.F. Weiss), pp. 1-27. Americal Geophysical Union, Washington D.C.

Wilhelm, S.W. & Trick, C.G. (1994) Iron-Limited Growth of Cyanobacteria - Multiple Siderophore Production Is a Common Response. *Limnology and Oceanography*, **39**, 1979-1984.

Witter, A.E., Hutchins, D.A., Butler, A., & Luther, G.W. (2000) Determination of conditional stability constants and kinetic constants for strong model Fe-binding ligands in seawater. *Marine Chemistry*, **69**, 1-17.

Wong, A.P.S., Bindoff, N.L., & Forbes, A. (1998). Ocean-ice shelf interactions and possible bottom water formation in the vacinity of Prydz bay, Antarctica. In *Ocean, Ice and Atmosphere: Interactions at the Antarctic Continental Margin* (eds S.S. Jacobs & R.F. Weiss), pp. 173-188. American Geophysical Union, Washington D.C.

Worby, A.P., Massom, R., Allison, I., Lytle, V.I., & Heil, P. (1998). East antarctic sea ice: a review of its structure, properties and drift. In *Antarctic sea ice : physical processes, interactions, and variability* (ed M.O. Jeffries), Vol. 74, pp. 41-67. American Geophysical Union, Washington D.C.

Appendix A : Metal speciation calculations

A.1 Introduction

The procedure used to calculate metal speciation was based on the method described by Gerringa *et al.* (2000).

The total concentration of a dissolved metal in solution can represented by a mass balance equation which partitions the metal amongst "free" ion, various inorganic complexes with the dominant anions in seawater and complexes with EDTA, in the case where this chelator is the dominant organic ligand in solution.

For iron it is assumed that it is distributed amongst free Fe^{+3}, two iron hydrolysis species $Fe(OH)^{+2}$ and $Fe(OH)_2^{+}$ and three EDTA complexes $FeEDTA^{-}$, $Fe(OH)EDTA^{-2}$ and $Fe(OH)_2EDTA^{-4}$ deriving the following mass balance.

$$[Fe_T]_{diss} = [Fe^{+3}] + [Fe(OH)^{+2}] + [Fe(OH)_2^{+}] + [FeEDTA] + [Fe(OH)EDTA^{-2}] + [Fe(OH)_2EDTA^{-4}]$$

For each complex the conditional stability constant K′ can be written as

$$K' = \frac{[FeL_n]^{3-nx}}{[Fe^{+3}][L^{-x}]^n} \text{ or}$$

$$[FeL_n]^{3-nx} = K' [Fe^{+3}] [L^{-x}]^n$$

By defining α (the side reaction coefficient) as the product of the free ligand concentration and the stability constant

$[FeL_n]^{3-nx} = \alpha\,[Fe^{+3}]$

The mass balance can be rewritten in terms of free ion concentrations and alpha values alone.

$$[Fe_T]_{diss} = [Fe^{+3}] + \alpha_{i1}[Fe^{+3}] + \alpha_{i2}[Fe^{+3}] + \alpha_{EDTA1}[Fe^{+3}] + \alpha_{EDTA2}[Fe^{+3}] + \alpha_{EDTA3}[Fe^{+3}]$$

$$[Fe_T]_{diss} = [Fe^{3+}] + \alpha_{inorganic}[Fe^{3+}] + \alpha_{EDTA}[Fe^{3+}]$$

which becomes

$$[Fe_T]_{diss} = [Fe^{3+}](1 + \alpha_{inorganic} + \alpha_{EDTA})$$

For complexes involving the hydroxide ion (e.g. $Fe(OH)^{+2}$) the formation of such species is represented by the reaction:

$$Fe^{3+} + H_2O = Fe(OH)^{+2} + H^+$$

Hence for this species the alpha value is defined as

$$\alpha = K'[H^+]$$

For the other trace metals in solution a similar approach can be taken where the total metal concentrations is described by a mass balance equation which partitions the dissolved metal into "free", inorganic and EDTA bound fractions on the basis of alpha values.

A.2 Calculation of alpha values

The inorganic complexes considered for the five trace metals (including iron) added to the media are shown in Table A.1 with their corresponding stability constants

which were obtained using the equilibrium modelling program MINEQL+ for S=35 and 2° C except for those for the two iron hydrolysis species which were from Millero (1998).

Table A.1 Inorganic metal complexes considered in metal speciation calculations.

Metal	Complex	Log K′	Alpha
Cobalt	$CoCl^+$	-0.07	0.48
	$CoSO_4$	1.36	0.31
		Total $\alpha_{inorganic}$	0.48
Copper	$Cu(OH)_2$ aq	-14.0	100
	$CuCO_3$ aq	5.59	37.0
	$Cu(CO3)_2^{-2}$	8.69	4.42
		Total $\alpha_{inorganic}$	141
Manganese	$MnCl^+$	0.04	0.61
	$MnCl^{-3}$	-1.16	0.01
	$MnCl_2$ aq	-0.82	0.05
	$MnSO_4$	0.98	0.13
		Total $\alpha_{inorganic}$	0.80
Zinc	ZnOHCl Aq	-8.05	0.50
	$Zn(OH)_2$ Aq	-17.2	0.06
	$ZnCl_3$-	-0.94	0.02
	$ZnCl^+$	-0.62	0.13
	$ZnCl_2$ Aq	-0.93	0.04
	Zn CO_3 Aq	4.16	1.37
	$Zn(CO3)_2^{-2}$	8.49	2.79
	$ZnSO_4$	1.14	0.19
		Total $\alpha_{inorganic}$	5.10
Iron	$FeOH^{+2}$	-2.6	$2.51x\ 10^5$
	$Fe(OH)_2^+$	-6	10^{10}
		Total $\alpha_{inorganic}$	10^{10}

The alpha values for these species are listed in the second last column of Table A.1 and total $\alpha_{inorganic}$ for each metal are tabulated in the final column of the table. These alpha values were calculated from the stability constant for the complex and the "free" concentrations of the appropriate inorganic ligand.

For sulphate and chloride "free" concentrations were calculated using MINEQL+ (Schecher & McAvoy, 1992) using the components listed in Table A.2. The concentrations used for these components were for representative seawater of S=35 and were the same as used by Gerringa *et al.* (2000) except for sodium which was included at 0.48 M (Morel & Hering, 1993) and CO_3^{-2} which was entered into MINEQL+ at a concentration equal to that of total carbonate (H_2CO_3 + HCO_3^- + CO_3^{-2}) which was calculated using the program SWCO2 (Hunter, 1998) for seawater at 2° C, pH 8.0 and a salinity of 35 with total alkalinity estimated from salinity by the program. The constants of Roy *et al.* (1993) were used for the carbonate calculations. The concentration of CO_3^{-2} used to calculate the inorganic side reaction coefficients for the trace metals was that of free CO_3^{-2} calculated with the program SWCO2. Free Ca^{+2} and Mg^{+2} (used in the final iron speciation calculations to gain an estimate for free $EDTA^{-4}$) were calculated from the same run of MINEQL+ and are also shown in Table A.2.

Table A.2 Components used in the calculation of free inorganic ligand concentrations using MINEQL+

Component	Total Concentration	Free Concentration
pH	Fixed solid at 8.0	H+ = $1x\ 10^{-8}$
Na+	0.48 M	0.474 M
Ca+2	1.00×10^{-2} M	8.51×10^{-3}
Mg+2	5.50×10^{-2} M	4.79×10^{-2} M
SO4-2	2.90×10^{-2} M	1.35×10^{-2} M
CO3-2	2.21×10^{-3} M	9.5×10^{-5} M
Cl-	0.56 M	0.56 M

Species considered during these calculations were $CaHCO_3^+$, $CaCO_3$ aq, $CaSO_4$ aq $MgSO_4$ aq, $MgCO_3$ aq, $MgHCO_3^+$, H_2CO_3 aq, HCO_3^-, $NaHCO_3$, $NaSO_4^-$

A.3 Calculation of metal speciation in EDTA buffered media

Metal speciation was calculated by an iterative process similar to that described by Gerringa *et al.* (2000). The calculations for media containing 100 nM of iron are outlined in Table A.3. Firstly, the free metal concentrations for each of five trace metals were calculated based only on the inorganic side reaction coefficients, i.e. using the $\alpha_{inorganic}$ values presented in Table A.1, the added concentration of each metal and based on the mass balance:

$$[M_{diss}]_{TOTAL} = M_{FREE}\,(1+\alpha_{inorganic})$$

The concentrations of free Ca^{+2} and Mg^{+2} shown in Table A.2 were calculated with MINEQL+ and remain fixed during subsequent calculations as their concentrations are several orders of magnitude greater than that of EDTA and hence are not significantly altered by complexation with this ligand.

These first estimates of free metal concentrations were then used to calculate the α_{EDTA} for each metal from the stability constants listed in Table A.4 and the calculated free metal concentration. For the divalent metals the calculation is simply:

$$\alpha_{MEDTA} = K'[M^{+2}]$$

However iron forms three EDTA complexes and the calculation takes the form:

$$\alpha_{FeEDTA} = [Fe^{+3}]\left(K_{FeEDTA} + \frac{K_{FeOHEDTA}}{[H^+]} + \frac{K_{Fe(OH)_2EDTA}}{[H^+]^2}\right)$$

Similarly EDTA forms mono, di, tri and tetra protonated species and the total side reaction coefficient for reaction of EDTA with the hydrogen ion is given by:

$\alpha_{pHEDTA} = K_{HEDTA}[H^+] + K_{H2EDTA}[H^+]^2 + K_{H3EDTA}[H^+]^3 + K_{H4EDTA}[H^+]^4$

The first estimates of the side reaction coefficients of cations with EDTA are then used to calculate free $EDTA^{-4}$ by solving the equation:

$[EDTA]_{TOTAL} = EDTA^{-4}(1 + \alpha_{CoEDTA} + \alpha_{CuEDTA} + \alpha_{MnEDTA} + \alpha_{ZnEDTA} + \alpha_{FeEDTA} + \alpha_{CaEDTA} + \alpha_{MgEDTA} + \alpha_{pHEDTA})$

The calculated $EDTA^{-4}$ concentration was then used to re-calculate an EDTA side reaction coefficient for the formation of the metal EDTA complexes. The free metal concentrations were then recalculated incorporating this side reaction coefficient into the mass balance The mass balance becomes:

$[Mdiss]_{TOTAL} = M_{FREE}(1 + \alpha_{inorganic} + \alpha_{EDTA})$

where $\alpha_{EDTA} = K'[EDTA^{-4}]$

These second estimates of free metal concentrations are then used to recalculate α_{EDTA} for each metal for a second time, which in turn can be used to recalculate the concentration of $EDTA^{-4}$ and hence refine the free metal concentration once again. The procedure was repeated for four iterations where the values converge.

Table A.3 Metal speciation calculations for media containing 100 nM iron

Cation	Concentration (M)	$\alpha_{inorganic}$	Free metal 1st estimate	α_{EDTA} 1st estimate	Free metal 2nd estimate
Co	$5.00x10^{-8}$	0.48	$3.39x10^{-8}$	$1.70x10^{8}$	$1.32x10^{-10}$
Cu	$2.00x10^{-8}$	141	$1.40x10^{-10}$	$3.53x10^{6}$	$9.84x10^{-12}$
Mn	$1.20x10^{-7}$	0.80	$6\ 66x10^{-8}$	$1.67x10^{6}$	$3.25x10^{-8}$
Zn	$5.00x10^{-7}$	5.10	$8.19x10^{-8}$	$1.03x10^{7}$	$3.21x10^{-8}$
Fe	$1.00x10^{-7}$	10^{10}	$1\ 00x10^{-17}$	$1.03x10^{9}$	$1.29x10^{-20}$
Ca	$8.51x10^{-3}$	-	$8.51x10^{-3}$	$1.07x10^{8}$	$8.51x10^{-3}$
Mg	$4.79x10^{-2}$	-	$4.79x10^{-2}$	$6.61x10^{6}$	$4.79x10^{-2}$
H	$1x10^{-8}$		$1x10^{-8}$	6.04	$1x10^{-8}$

Cation	α_{EDTA} 2nd estimate	Free metal 3rd estimate	α_{EDTA} 3rd estimate	Free metal 3rd estimate	α_{EDTA} 4th estimate
Co	$6\ 62x10^{5}$	$1.20x10^{-11}$	$6.03\ x10^{4}$	$1.14x10^{-11}$	$5.73\ x10^{4}$
Cu	$2.47x10^{5}$	$9.55\ x10^{-11}$	$2\ 40\ x10^{4}$	$9.06\ x10^{-11}$	$2.28\ x10^{4}$
Mn	$8.16x10^{5}$	$5.31\ x10^{-11}$	$1.33x10^{5}$	$5.06\ x10^{-11}$	$1.27\ x10^{5}$
Zn	$4.0x10^{6}$	$4.53x10^{-9}$	$5.70x10^{5}$	$4.31\ x10^{-9}$	$5.43\ x10^{5}$
Fe	$1.33x10^{6}$	$1.17x10^{-21}$	$1.21x10^{5}$	$1.11\ x10^{-21}$	$1.15\ x10^{5}$
Ca	$1.07x10^{8}$	$8.51x10^{-3}$	$1.07x10^{8}$	$8.51x10^{-3}$	$1.07\ x10^{8}$
Mg	$6.61x10^{6}$	$4.79x10^{-2}$	$6.61x10^{6}$	$4.79x10^{-2}$	$6.61\ x10^{6}$
H	6.04	$1x10^{-8}$	6.04	$1x10^{-8}$	

Cation	Free metal Final estimate
Co	$1.14x10^{-11}$
Cu	$9\ 06\ x10^{-11}$
Mn	$5.05\ x10^{-11}$
Zn	$4.31\ x10^{-9}$
Fe	$1.11\ x10^{-21}$
Ca	$8.51x10^{-3}$
Mg	$4.79x10^{-2}$
H	$1x10^{-8}$

Table A.4 Metal EDTA complexes and their stability constants used in calculations

Cation	Species	Log K′	Cation	Species	Log K′
Co	$CoEDTA^{-2}$	15.8	Fe	$FeEDTA^{-}$	24.4
Cu	$CuEDTA^{-2}$	16.5		$Fe(OH)EDTA^{-2}$	18
Mn	$MnEDTA^{-2}$	13.5		$Fe(OH)2EDTA^{-3}$	8.1
Zn	$ZnEDTA^{-2}$	14.2			
Ca	$CaEDTA^{-2}$	10.2	H	$HEDTA^{-3}$	8.82
Mg	$MgEDTA^{-2}$	8.21		$H2EDTA^{-2}$	14.2
				$H3EDTA^{-}$	16.3
				H4EDTA	18.1